

DETECTING AND PROCESSING THE FOETAL ELECTROCARDIOGRAM  
OBTAINED USING ABDOMINAL ELECTRODES

A thesis presented to the University of Aston in  
Birmingham for the degree of Doctor of Philosophy.

by

R.G.J.BUTLER, B.Sc., A.Inst.P., M.Sc., C.Eng., M.I.E.E.

OCTOBER 1969

THE UNIVERSITY  
OF ASTON IN  
BIRMINGHAM.  
LIBRARY

19 DEC 1969

Sheep 124817

621.30352

BUT

SUMMARY

The signal detected from electrodes placed on the abdomen of an expectant mother consists of the foetal electro-cardiogram, estimated between 5 and 60 microvolts, a larger maternal complex, potentials originating from breathing and abdominal muscles and electronic noise. In this thesis the development of an amplifier to improve the quality of the foetal signal to facilitate its interpretation is described.

The basic amplifier, of the balanced input type, is designed with complementary dual field effect transistors and is temperature compensated. The input impedance is about  $10^{10}$  ohms and the bandwidth extends from d.c. to  $10^5$  Hz. For electrocardiographic purposes these were limited to  $10^7$  ohms for each input and 1Hz to 130Hz respectively. The use of negative common mode feedback gives a rejection ratio estimated to be 120 db. The electronic noise is less than 1 microvolt peak to peak. The output is single ended and the overall gain is  $10^4$ .

Spurious signals due to interaction between metallic electrode materials and body electrolytes are reduced by the use of graphite electrodes in the form of blocks and cloth drastically cleaned initially to remove other metals with which it had come into contact during manufacture.

F.M. tape recording and averaging using a PDP8/I computer was undertaken to produce noise-free foetal electro-cardiograms for diagnostic purposes. The various shapes of the averaged electro-cardiograms obtained are discussed.

The effect of bandwidth on the averaged waveform and on the diagnosis of foetal presentation is demonstrated.

The system has also been used for detecting foetal life, multiple pregnancies, presentation and for measuring heart rate.

Recent methods for improving the computer processing techniques are also discussed.

It is concluded that foetal electro-cardiography using abdominal electrodes can provide a single and safe method for obtaining invaluable information for the obstetrician.

The basic amplifier with its high input impedance, wide bandwidth and low noise level and additional processing techniques so developed may have applications in general electrophysiology.

ACKNOWLEDGMENTS

The investigations reported were undertaken as a result of consultation between Mr. R. F. Farr and Dr. J. A. Newell of the Medical Physics Department of the Queen Elizabeth Hospital, Birmingham, and Dr. C. S. Bull of the University of Aston in Birmingham.

Professor H. C. McLaren provided excellent facilities, including a laboratory, a computer and expectant women in the New Birmingham Maternity Hospital.

I am indebted to Professor McLaren for continuous encouragement and to all his colleagues in the Professorial Unit and in the Medical Physics Department at the Hospital, and in particular, Dr. A. Webster and Sister J. Stancer for arranging conditions in which the expectant women were always very co-operative during recordings.

I would like to thank Dr.C.S.Bull for supervising the research for the University of Aston.

I would like to thank the Ghana Academy of Sciences for granting study leave and the Association of Commonwealth Universities for a scholarship which enabled me to stay in Britain to complete my studies.

Finally, I thank Mrs. Valerie Hathaway, the wife of my colleague, Dr. D.E.G. Hathaway, who sewed the graphite cloth electrodes.

LIST OF CONTENTS

SUMMARY	1
ACKNOWLEDGMENTS	3
INTRODUCTION	4
Direct Electrode System	7
Indirect Electrode System	8
<u>CHAPTER I</u>	
DETECTING SYSTEM	10
Importance of effect of Circuit Unbalances	17
THE PRESENT CIRCUIT	20
The pre-amplifier stage	21
Description of the circuit used in the present experiment	35
Temperature Compensation	41
The main amplifier	46
Noise Level of detecting System	
Thermal Noise	50
Shot Noise	51
Flicker Noise	55
Excess Noise	60
Other Sources of noise	61
DETECTING ELECTRODES	64
Input impedance of detecting system	72
<u>CHAPTER II</u>	
PROCESSING THE FOETAL ELECTROCARDIOGRAM OBTAINED WITH ABDOMINAL ELECTRODES	
A Foetal heart rate	74
B Waveform of Foetal Electrocardiogram	
a) Testing for foetal life	80
b) Presentation of foetus (Effect of low frequency cut-off)	81
Effect of low frequency cut-off point on waveform	82
c) Diagnosis of Multiple Pregnancy	87

The use of Computer to obtain the waveform of the foetal electrocardiogram	98
Description of auxiliary circuits designed for maternal blanking and triggering computer	104
Averaging of Signals immersed in Noise	116
The averaged foetal complex	122
Results of Averaging using the system	125
Samples of Averaged foetal QRS Complexes	128
Effect of High Cut-off frequency on averaged waveform	140
Effects of changes in foetal heart rate on averaged complex	141
Time Measurements on Averaged Foetal QRS complexes	142
 <u>CHAPTER III</u>	
USE OF THE DIGITAL COMPUTER FOR ELIMINATING THE MATERNAL COMPLEX	146
Scheme for eliminating the Maternal Complex	152
 REFERENCES	 155
 APPENDIX I	 160
Continuation of Calculations from page 30	
 APPENDIX II	 164
GRAPHITE CLOTH	
 APPENDIX III	 165
FOA'S RECORD	
 APPENDIX IV	 166
Specifications of F.M. Tape Recorder	

DETECTING AND PROCESSING THE FOETAL ELECTROCARDIOGRAM  
OBTAINED USING ABDOMINAL ELECTRODES

INTRODUCTION

During the period that the human foetus spends in the uterus, obstetricians try to obtain information about its health.

The avenues of contact take the form of palpation or feeling the foetus with their trained hands, osculation or listening to the heart beats with foetal stethoscopes, phonocardiograms, doppler tone generators, and through the use of ultrasound and X-radiation.

Another method of reaching the foetus is through the use of electrocardiography which is the recording and study of the electrical activity of the heart.

The subject of electro-cardiography has been developed to a great extent in the adult and foetal electro-cardiography is an attempt to extend this wealth of knowledge to the unborn baby.

Among the claims on information obtainable through the use of foetal electro-cardiography are the diagnosing of:

- a) Foetal life.
- b) Foetal presentation or the direction of orientation of the foetus in the uterus.
- c) Multiple pregnancy.
- d) Foetal heart disease.

This thesis describes the technical difficulties encountered in obtaining this information through the use of simple and safe electrodes placed on the maternal abdomen and attempts to overcome these difficulties.

In 1906, Cremer,<sup>(1)</sup> a physicist, recorded the first foetal electro-cardiogram. He used a string galvanometer and his electrode system consisted of one rectal and one abdominal gold electrode.

Fig.1 shows his record.

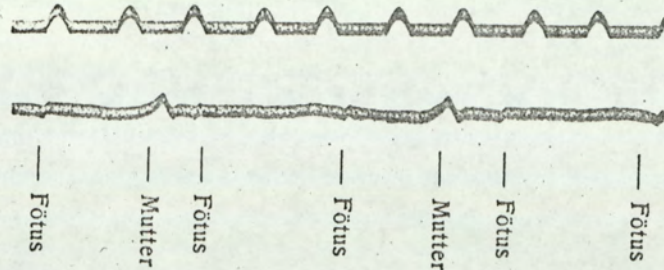


Fig. 1.

Cremer's Electrocardiographic Record showing the Foetal and Maternal Complexes.

The top trace represents time markers occurring at 0.2 second intervals.

In 1911 Foa<sup>(2)</sup> disagreed with the electrode system used by Cremer and insisted that to avoid errors in interpretation only rigorously non-polarizable electrodes should be used. His electrode system consisted of gauze in physiological saline introduced into the vagina with long forceps and another piece of gauze placed on the maternal fundus. The other ends of the pieces of gauze were dipped in a saturated solution of zinc sulphate and the solution was connected to a string galvanometer with a zinc wire. This produced a better trace. [It was very difficult to reproduce his result from his paper - the attempt is shown in the appendix]. He was also the first to state that

the orientation of the foetal R-wave gave the diagnosis of presentation.

Their efforts were greeted with ridicule; some obstetricians said they could produce such recordings from men!

Since then there have been reports of attempts at recording a reliable foetal electro-cardiogram to assist the obstetrician in the management of pregnancy. Notable among these are those of Krumbahr<sup>(3)</sup> (1916), Maekawa and Toyoshima<sup>(4)</sup> (1930) who used the vacuum tube as a pre-amplifier for a string galvanometer to produce superior results. Bell<sup>(5)</sup> (1938) was the first to record the electro-cardiograph of twins. They made use of improvements in instrumentation for general electrophysiology. Obstetricians still regarded their efforts as technical feats of no practical significance.

There was a rebirth of interest around 1953 through the work of Smyth<sup>(6)</sup>, Southern<sup>(7)</sup> (1957) G. Shömig and P. Nimmer. Its popularity was enhanced by international conferences [Mount Sinai Hospital, New York 1956, International Federation of Medical Electronics since 1958]. Monographs such as those by Larks<sup>(8)</sup> and Bernstein<sup>(9)</sup> have also been written about the subject.

Throughout the world, publications on the subject have multiplied and various reviews have been written. Among these are those by Caughery<sup>(10)</sup> (1961), Shubeck<sup>(11)</sup> (1964), Sureau<sup>(12)</sup> (1965), Shenker<sup>(13)</sup> (1966). Almost all of these have reported on the achievements and limitations of this method of detecting foetal distress.

It can be said in general that improvement in the quality of the detected signal as a diagnostic tool has followed in the wake of general improvements in detecting techniques in Electrophysiology.

The first part of the thesis will therefore take a look at the detecting systems used and highlight what might have been the main difficulties.

The main objective is to improve the signal-to-noise ratio to such an extent that all extraneous potentials except that emanating from the foetal heart are eliminated.

In the realisation of this objective two main techniques have been used. They can be categorised under DIRECT and INDIRECT electrode systems.

#### DIRECT ELECTRODE SYSTEMS

The signal picked up from the foetus with electrodes directly in contact with or passed through the foetal skin, has higher amplitude than with electrodes placed far away from it. Caldeyro-Barcia<sup>(14)</sup> (1959) used needle electrodes passed into the body of the foetus through a trans-abdominal (maternal) puncture. Drew-Smythe also pierced with a catheter to lie in the liquor well above the presenting part. There is, however, the danger of damaging the placenta. Other workers like Hon<sup>(15)</sup> have used electrodes applied directly to the scalp - graffe clip - after rupture of the membrane of the womb. The signals thus picked up are quite free of the maternal complex and can be used to trigger a rate meter directly. The method however has the following disadvantages:-

- a) It can only be used in the terminal stages of pregnancy when the membrane is ruptured.
- b) As Sureau noted there is always the danger of ascending infection.
- c) Shelley<sup>(16)</sup> pointed out "People had distaste for the idea of piercing the foetal scalp".
- d) No one can be certain not to pierce an important organ such as the eye. Also it cannot be used in multiple pregnancy on all the foetuses.

In many of the attempts the method has been justified by saying that the foetus was clearly already distressed and the need to keep a close watch on the foetal heart rate outweighed any inconvenience in the method.

However, Hon and others have extensively dealt with the interpretation of foetal heart rate changes during labour and delivery using the method. One point which has to be cleared is whether with the needle in place any pain felt, especially during contraction when more pressure is put on the needle site, can result in heart rate changes which might affect the interpretation.

Other forms of electrode systems in this category are those in which electrodes are passed into the vagina and made to touch but not pierce the foetal skin. They can be suction types in which the electrode element is placed in a cup which is attached to the presenting part by suction. The indifferent electrode is placed in the amniotic fluid. Shelley<sup>(16)</sup> describes some of these.

#### INDIRECT OR ABDOMINAL ELECTRODE SYSTEM

In this system electrodes are attached to the maternal abdomen usually along the midline. One electrode is placed on the symphysis pubis and the other on the top of the fundus.

The foetal signal detected with this system is, however, small due to attenuation caused by the maternal tissues between the foetus and detecting electrodes. The signal is of the order of 5 - 50 microvolts and is accompanied by larger maternal complexes and other potentials originating from the maternal musculature. The detection of the signal demands more stringent instrumentation standards. It is the technical difficulty of detecting this signal that has driven workers to the use of the direct electrode systems of measurements with all their disadvantages.

If these technical problems could be solved this would appear to be the method of choice.

The main difficulty lies in the elimination of the maternal complex and in this Sureau and Trocellier<sup>(17)</sup> <sup>(18)</sup> pioneered efforts to eliminate maternal signal from abdominal leads.

By trial and error a maternal electro-cardiogram with no foetal signal was obtained from another part of the body and used to cancel the maternal complex. This method is laborious and not always successful. Other workers like Walden and Birnbaum<sup>(19)</sup> have used similar techniques.

Another method for getting rid of the maternal complex is to use the higher amplitude of the maternal R-wave to gate out a delayed form of the detected signal whenever a maternal complex occurs. This is known as "Maternal Blanking". It has been used by Goddard, Newell et al.<sup>(20)</sup> It was as a result of their work that the present project was arranged between the Queen Elizabeth Hospital, Birmingham and the University of Aston.

The thesis therefore describes the design of a system for detection and analysis of the foetal electro-cardiogram using abdominal electrodes. It introduces the use of graphite as a suitable electrode material for foetal electro-cardiography. It also reports on computer "averaging" to obtain cleaner foetal complexes for diagnosis.

It ends by proposing a method of using a computer for eliminating the maternal complexes.

The project was undertaken in an effort to clarify and remedy some of the problems involved in the use of the much simpler and safer abdominal electrode system for foetal electro-cardiography.

CHAPTER I

DETECTING SYSTEM

CHAPTER IDETECTING SYSTEM

Prior to the discovery of the string galvanometer by Einthoven workers in electrophysiology like Burdon-Sanderson (1879) and Waller (1887, 1889)<sup>(21)</sup> had used the Lippman Capillary electrometer for the measurement of "action current" of the heart.

The time constant of the electrometer was very long. Einthoven corrected this by calculating the time derivative of the record and in 1894 used it to derive the electro-cardiogram. The components of the electro-cardiogram he denoted as P.Q.R.S.T. and this nomenclature has existed up to the present. He developed the string galvanometer in 1903 to avoid the laborious calculations needed for correcting the recordings obtained with the capillary electrometer.

The problem with the string galvanometer was that it was not robust. It was basically a current measuring device with low input impedance. The moving part was a string which could not have had a very high gain-bandwidth product. Its power sensitivity was therefore too low for measuring potentials in the microvolt region. With the invention of the radio-valve the problem of power sensitivity was overcome.

Electrophysiologists like Adrian used a valve as an input stage followed by the capillary electrometer but due to the inertia of the mercury, the records had to be analysed with a machine, invented by Keith Lucas, in which cross-wires had to be set tangentially to the record. This was very laborious. The valve and the string-galvanometer did not form a very good combination even when the string galvanometer was used at high frequencies.<sup>(22)</sup> This was due to the fragility of the string to any artifacts in the pre-amplifier stage. However, in 1930 Maekawa and Toyoshima<sup>(4)</sup> used this combination to obtain better records.

Adrian and Matthews (1934)<sup>(23)</sup> expressed dissatisfaction with the use of single input amplifiers for simultaneously recording action potentials from three regions in the cortex of a cat.

They were not sure whether when they earthed one side of each single input amplifier in the mouth, the outputs were a reflection of the activities at these regions or were originating from intervening tissues (cortex to mouth). To illustrate this problem Matthews<sup>(24)</sup> writes:- "If a pair of electrodes is placed on a frog's heart and a second on the liver, when these are connected to two recording systems having grid-earth input amplifiers, the pair on the liver yield an electro-cardiogram only slightly smaller than that recorded from the pair on the heart and of opposite sign : such potential changes in the liver being improbable, on further reflection it is clear that the effect is due to the interaction of the two electrodes via the earth".

Their solution was to use a floating input - floating output amplifier or an amplifier which would only measure the difference between two signals of interest.

Fig.2 shows a diagram of their circuit.

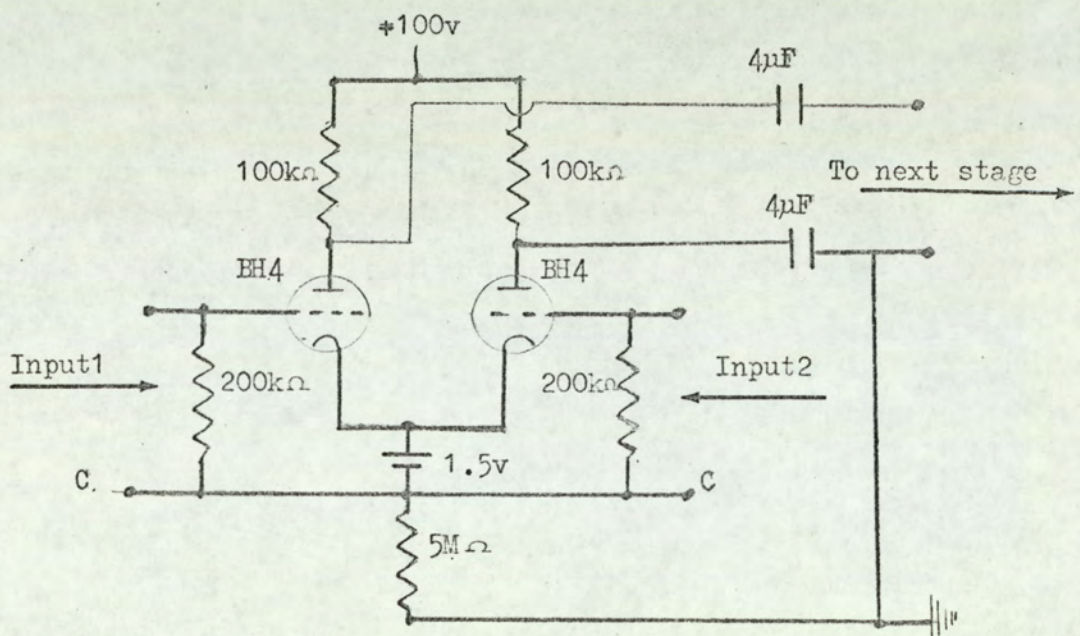


Fig.2. Difference amplifier by Matthews and Adrian.  
Common electrodes connected to C.

It is important to note that the input was applied between I/1 or I/2 and common (C). This means that the  $5M\Omega$  resistor did not provide degenerative feedback.

Fig.3 in a general way illustrates how the unwanted signal is injected when a single input system is used.

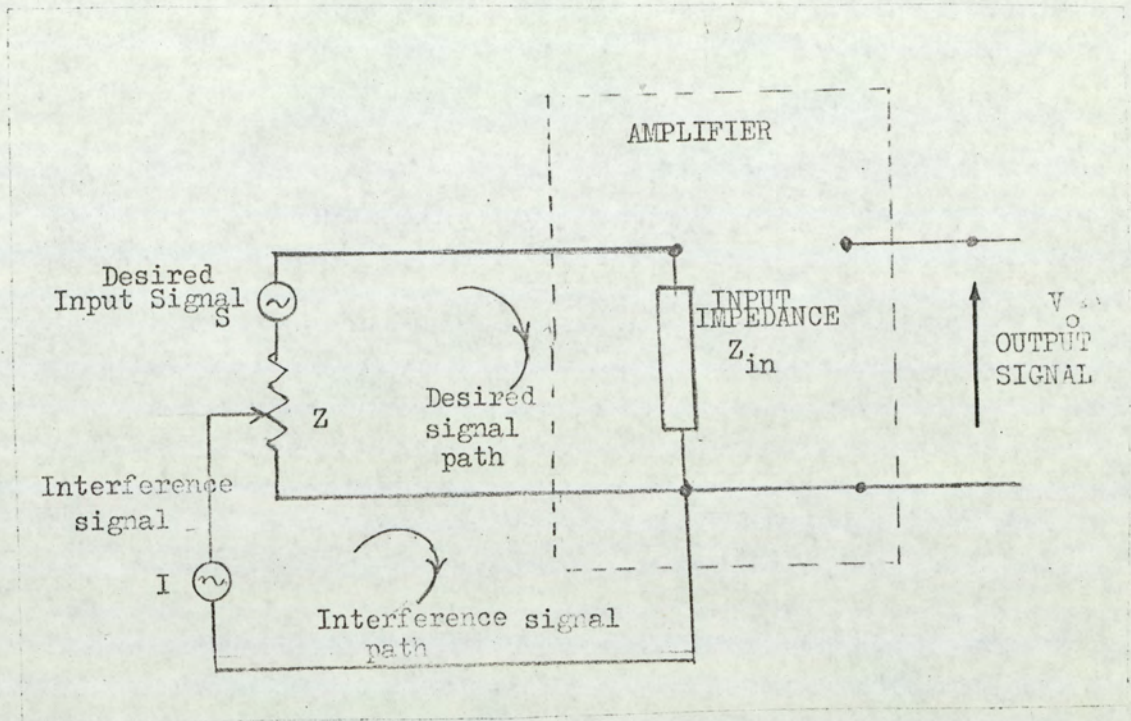


Fig.3. Demonstration of how unwanted signal is injected in a single input amplifier.

Here the impedance  $Z$  represents the physiological resistance between electrodes and the contact resistance of each electrode (Middlebrook) (25).

Despite the high input impedance ( $Z_{in}$ ) of the device, spurious interference voltages originating from biological sources and from external surroundings (mains supply) are injected.

Fig.4. illustrates the situation with amplifiers having floating inputs.

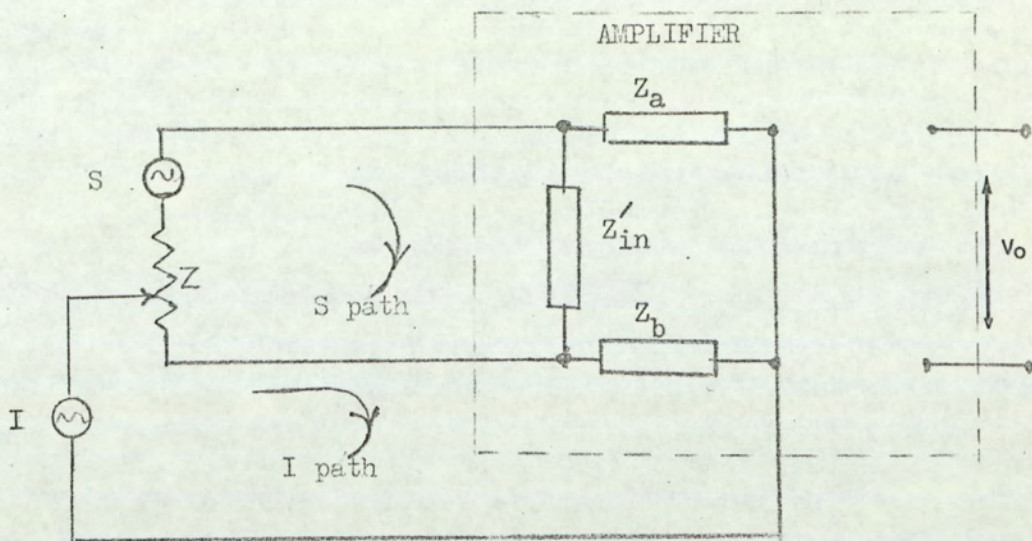


Fig.4. Injection of Interference Signals in the case of an amplifier having Floating Inputs.

In this case the effect of interference signal is reduced because each input electrode experiences the same common mode or inphase signal appearing at both terminals and thus the difference which is measured at the floating output is small.

With the need for further amplification, and therefore necessity for cascading of stages, came the problem of overloading the subsequent stages with ever increasing common-mode signals especially when using d-c coupling between stages.

Offner<sup>(26)</sup> suggested negative feedback from a common point in a later stage to a common input point. He also thought that "motor boating" due to coupling through a common plate supply was overcome with this technique.

Meanwhile, Blumlein<sup>(7)</sup> took a British patent for a circuit

called a "Long tail pair" which seemed to have been the answer to most of the major problems. He applied a degenerative common cathode resistor to the floating input - floating output amplifier.

Fig.5 shows the circuit diagram.

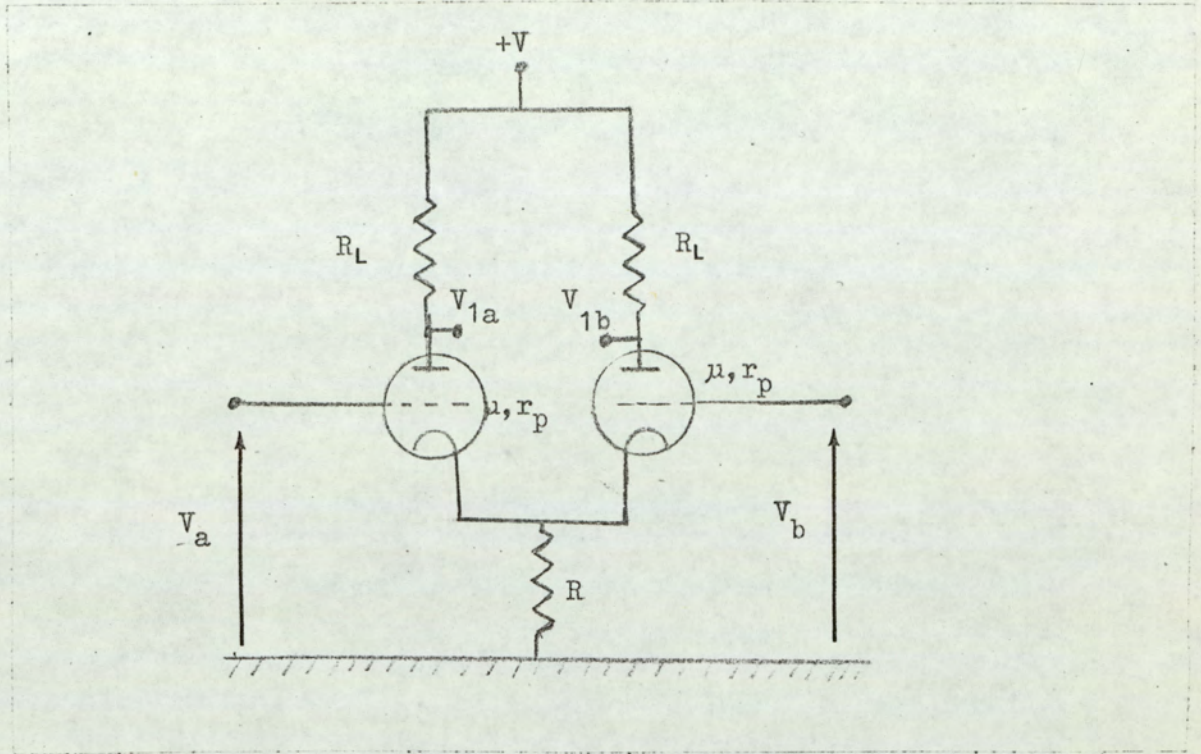


Fig.5. Blumlein's circuit.

The nature of this circuit is now discussed. Straightforward circuit analysis leads to

$$\left(\frac{V_{1a} + V_{1b}}{2}\right) = -\frac{\mu R_L}{R_L + r_p + 2R(1 + \mu)} \left(\frac{V_a + V_b}{2}\right) \dots\dots\dots (1)$$

$$\left(\frac{V_{1a} - V_{1b}}{2}\right) = -\frac{\mu R_L}{R_L + r_p} \left(\frac{V_a - V_b}{2}\right) \dots\dots\dots (2)$$

Equation (1) gives the gain (Acc) for common-mode or inphase signals as:-

$$\text{Acc} = - \frac{\mu R_L}{R_L + r_p + 2R(1 + \mu)}$$

Acc is inversely dependent on the value of the degenerate<sup>ing</sup> resistor R.

Equation 2 gives the gain (Add) for differential mode or out-of-phase signals as the familiar:-

$$\text{Add} = - \frac{\mu R_L}{R_L + r_p}$$

which is unaffected by the introduction of the degenerate<sup>ing</sup> resistor R.

If the desired output is to be connected to a single input amplifier, addition and subtraction of equations (1) and (2) give:-

$$V_{1a} = - \text{Acc} \left( \frac{V_a + V_b}{2} \right) - \text{Add} \left( \frac{V_a - V_b}{2} \right) \dots \dots \dots (3)$$

$$V_{1b} = - \text{Acc} \left( \frac{V_a + V_b}{2} \right) + \text{Add} \left( \frac{V_a - V_b}{2} \right) \dots \dots \dots (4)$$

Variations of this circuit (by shorting one of the load resistors) were used by Matthews<sup>(28)</sup> and Tönnies<sup>(29)</sup> (1938) under the name of the "compressor" input stage to provide single ended outputs from floating inputs.

It can be inferred from equation (1) that one way of reducing the value of Acc is to make R as large as possible. This however means increasing the supply voltage accordingly to maintain the working points of the valves.

Goldberg<sup>(30)</sup> solved this problem by using the so-called "constant current source" properties of the pentode whilst keeping the supply

voltage within a manageable range. Fig. 6 shows a diagram of his circuit.

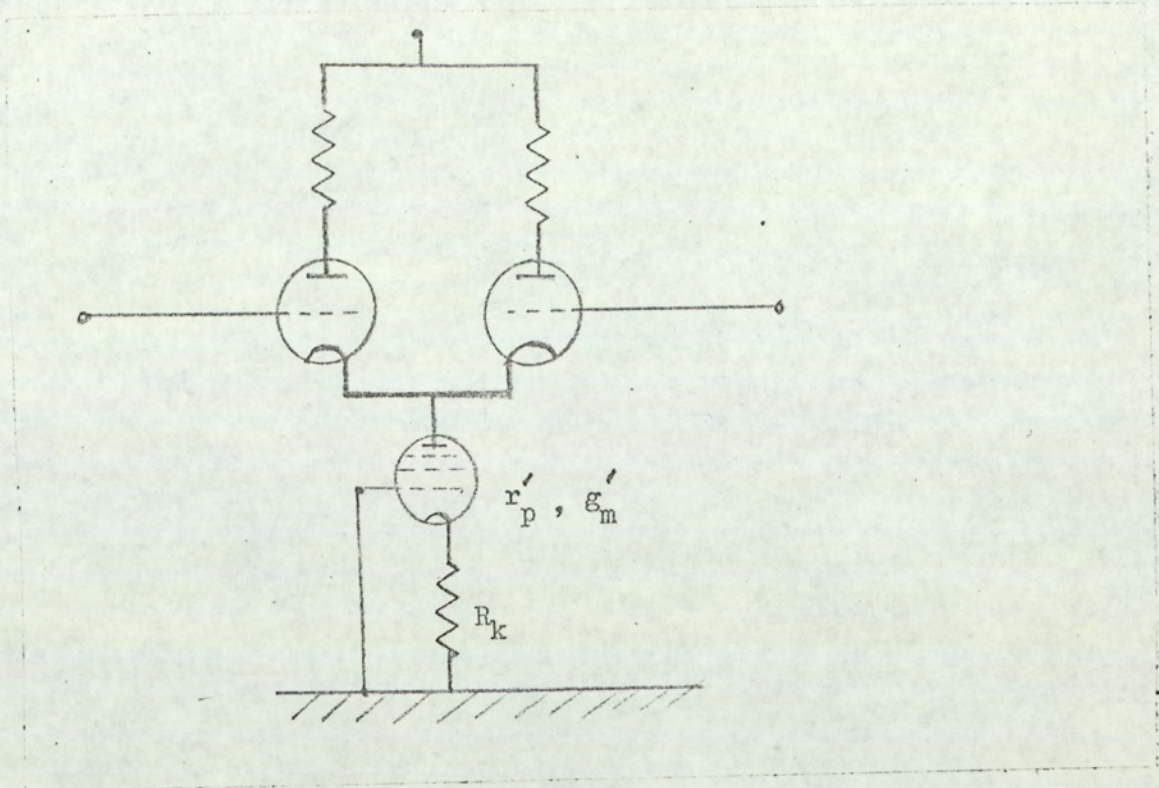


Fig.6. Pentode Constant current source.  
The high plate resistance  $r'_p$  effectively becomes  $r'_p(1 + g'_m R_k)$  without affecting the bias point of the differential pair.

Typical example in improvement of performance taken from Middlebrook<sup>(25)</sup> with values from regular valve data gives:

	DEGENERATE CATHODE RESISTOR	CONSTANT CURRENT SOURCE
Acc	0.455	0.0016
Add	10	10

Further reduction of the value of Acc was called for in work where lower potentials required to be measured as Goldberg<sup>(30)</sup> wrote "Probably all metabolic and katabolic processes of living matter

produce electric phenomena ....". Among the qualities of a good bio-electric amplifier, he included:-

Differential gain	- 120 db (because the output was connected directly to oscilloscope deflecting plates).
Frequency response	- 0 → 10 k Hz
Input impedance	- not less than 1 M Ω
Amplifier noise voltage	- less than 1 microvolt.

To offset the effect of interference from mains supply Goldberg used a battery operated pre-amplifier stage.

#### IMPORTANCE OF EFFECT OF CIRCUIT UNBALANCES

In the foregoing analysis it has been assumed that the two halves of the differential amplifier have the same characteristics. Middlebrook shows by assuming all parameters of the pair stay the same except the amplification factors, giving them values  $(\mu + \delta\mu)$  and  $(\mu - \delta\mu)$  where  $\delta\mu/\mu \approx 1/10$  that equations (1) and (2) are modified to:-

$$\left(\frac{V_{1a} + V_{1b}}{2}\right) = - \frac{\mu R_L}{r_p + R_L + 2R(1+\mu)} \left[ \left(\frac{V_a + V_b}{2}\right) + \frac{\delta\mu}{\mu} \left(\frac{V_a - V_b}{2}\right) \right] \dots (5)$$

$$\begin{aligned} \left(\frac{V_{1a} - V_{1b}}{2}\right) = & - \frac{\mu R_L}{r_p + R_L} \left[ \left(1 - \frac{\left(\frac{\delta\mu}{\mu}\right)^2 \cdot 2R\mu}{r_p + R_L + 2R(1+\mu)}\right) \left(\frac{V_a - V_b}{2}\right) \right. \\ & \left. + \frac{\delta\mu}{\mu} \left(1 - \frac{2R\mu}{r_p + R_L + 2R(1+\mu)}\right) \left(\frac{V_a + V_b}{2}\right) \right] \dots (6) \end{aligned}$$

In other words a differential, (subscript d), input gives a common-mode, (subscript c), output, and vice versa defining new cross-parameters:-

$$A_{cd} \equiv \frac{\delta\mu}{\mu} \cdot \frac{\mu R_L}{r_p + R_L + 2R(1+\mu)} \dots (7)$$

$$A_{dc} = \frac{\delta\mu}{\mu} \cdot \frac{\mu R_L}{r_p + R_L} \left( 1 - \frac{2 R \mu}{r_p + R_L + 2R(1+\mu)} \right) \dots\dots\dots (8)$$

Note  $A_{cd} \neq A_{dc}$

$$\text{now } A_{cc} = \frac{\mu R_L}{r_p + R_L + 2R(1+\mu)} \dots\dots\dots (9)$$

$$A_{dd} = \frac{\mu R_L}{r_p + R_L} \left[ 1 - \frac{\left(\frac{\delta\mu}{\mu}\right)^2 \cdot 2 R \mu}{r_p + R_L + 2R(1+\mu)} \right] \dots\dots\dots (10)$$

and substituting in equations (5) and (6)

$$\left( \frac{V_{1a} + V_{1b}}{2} \right) = - A_{cc} \left( \frac{V_a + V_b}{2} \right) - A_{cd} \left( \frac{V_a - V_b}{2} \right) \dots\dots\dots (11)$$

$$\left( \frac{V_{1a} + V_{1b}}{2} \right) = - A_{dd} \left( \frac{V_a - V_b}{2} \right) - A_{dc} \left( \frac{V_a + V_b}{2} \right) \dots\dots\dots (12)$$

from (11) and (12)

$$V_{1a} = - (A_{dd} + A_{cd}) \left( \frac{V_a - V_b}{2} \right) - (A_{cc} + A_{dc}) \left( \frac{V_a + V_b}{2} \right) \dots\dots\dots (13)$$

$$V_{1b} = - (A_{dd} + A_{cd}) \left( \frac{V_a - V_b}{2} \right) - (A_{cc} - A_{dc}) \left( \frac{V_a + V_b}{2} \right) \dots\dots\dots (14)$$

If the voltage of interest is the difference is the difference voltage the form equation (12), the common mode rejection ratio is  $A_{dd}/A_{dc}$  in contradistinction from the  $A_{dd}/A_{cc}$  obtained in (1) and (2) assuming balanced circuits.

It can be seen from equation 10 that

$$\begin{aligned} A_{dd} &\rightarrow \frac{\mu R_L}{r_p + R_L} \left[ 1 - \frac{\left(\frac{\delta\mu}{\mu}\right)^2}{1+\mu} \right] \\ &\approx \frac{\mu R_L}{r_p + R_L} \quad \text{for } R \gg r_p + R_L \dots\dots\dots (15) \end{aligned}$$

$$A_{dc} \rightarrow \frac{\delta\mu}{\mu} \frac{\mu R_L}{r_p + R_L} \cdot \frac{1}{\mu + 1} \quad \text{for } R \gg r_p + R_L \dots\dots\dots (16)$$

Hence from (15) and (16) the common mode rejection factor:

$$H_c = \frac{A_{dd}}{A_{dc}} \text{ tends to a limiting value - } \mu (1 + \mu) / \delta\mu$$

as the degenerate resistor becomes far larger than  $R_L + r_p$  even though discrimination factor  $\frac{A_{dd}}{A_{cc}}$  becomes very high. This conclusion was pointed out by Parnum<sup>(32)</sup> and also arrived at by Klein<sup>(33)</sup> although in their conclusions they allowed  $R$  to go to infinity and  $\frac{A_{dd}}{A_{cc}}$  to also reach the same infinite limit.

Such cross-coupling properties are therefore the result of unbalances (not only in the amplification factors) in components of the two halves of the "long tail" pair. Attempts were therefore made to equalise the characteristics in the pair, Goldberg<sup>(30)</sup> varied the heater currents to decrease the unbalance in the valves and thus improved the value of the common-mode rejection ratio.

It can be seen from the foregoing that the differential amplifier is a much more complex system than the single input amplifier and that impetus for its development has been given by needs in electro-physiology.

Later workers like Birt,<sup>(35)</sup> although working at audio frequencies showed that the use of 'common-mode negative feedback from a second differential stage helped to increase the value of common-mode rejection ratio. His circuit is schematically shown in Fig.7. The a.c. common-mode negative feedback was applied from  $R_1, C_1$  in the second stage to the first stage.

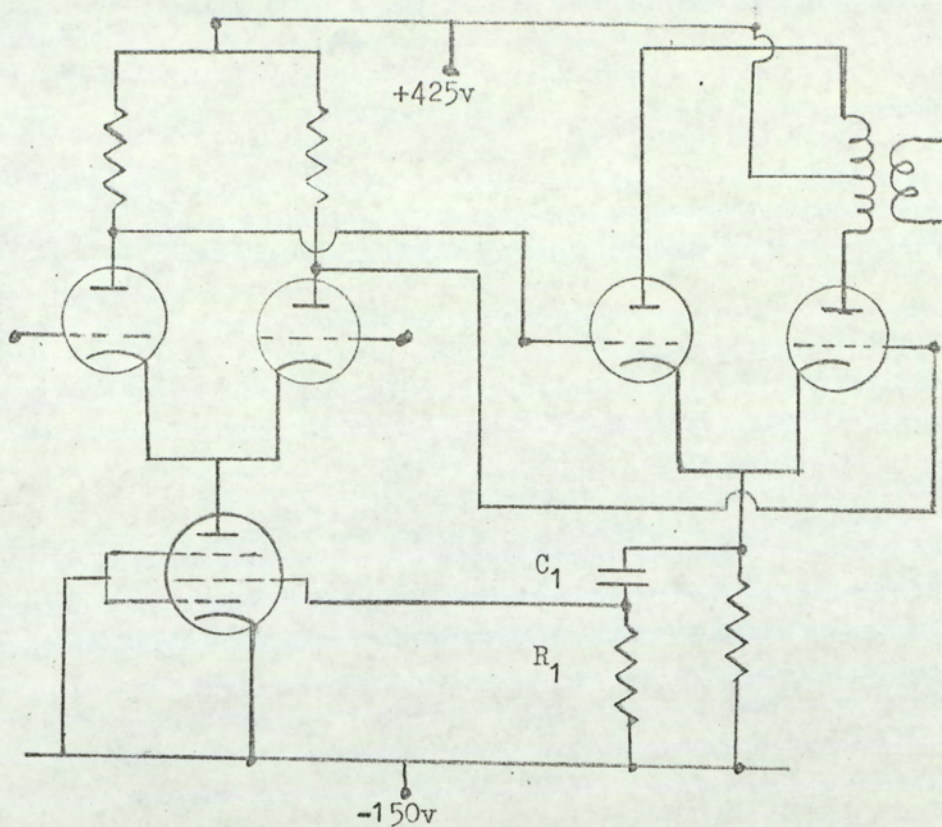


Fig.7. Birt's Common-mode negative feedback circuit (Schematic).

Addition of this "second stage" meant that the calculation of the performance from the variation of the circuit parameters involves very cumbersome algebra, especially when other sources of unbalance like the effects of temperature and supply voltage changes are to be studied.

Middlebrook<sup>(25)</sup> using transistors has developed a sequential method of analysis of unbalanced symmetrical circuits with a view to simplifying the unwieldy algebra needed for stages of differential amplifiers beyond the first stage.

#### THE PRESENT CIRCUIT

The design of the system used in this research for the detection of foetal electro-cardiogram has made use of the information on valves and bipolar transistors.

Many forms of circuits have been designed for low frequency amplification using monolithic circuits in the form of operational amplifiers.

The signal, namely the foetal electro-cardiogram, from the abdominal wall has been estimated at between 5 → 50 microvolts. The presence of other bio-electric signals in the form of myopotentials originating from the muscles of the maternal abdomen makes it imperative that amplifiers for such measurements should have very high rejection factors.

Secondly, due to tissue and electrode resistances which form the signal source impedance, the input impedance of such an amplifier should be high.

The third important property is that the amplifier must have a low level of intrinsic noise compared with the minimum expected, of a few microvolts.

#### The Pre-amplifier stage:

The first stage of the present circuit is built around a field effect transistor having high input impedance and low noise. Common-mode negative feedback is accomplished by an arrangement similar to that shown in Fig.7. using a complementary pair in the second stage.

Fig.8(a) shows the schematic diagram of the pre-amplifier circuit and Fig.8(b) shows a simplification of the circuit for analysis.

The circuit is mainly a two stage differential amplifier with common-mode negative feedback. The first stage has a degenerate cathode coupling provided by field effect transistors  $T_3$ .  $T_1$  and  $T_2$  are dual field effect transistors,  $T_1$  being an n-channel,  $T_2$  a P-channel device, forming a complementary circuit.

The sequential method of analysis as outlined by Middlebrook<sup>(25)</sup> is used. This is an extension of the bisection theorem<sup>(35)</sup> to cater for small unbalances in the two halves of a symmetrical circuit.

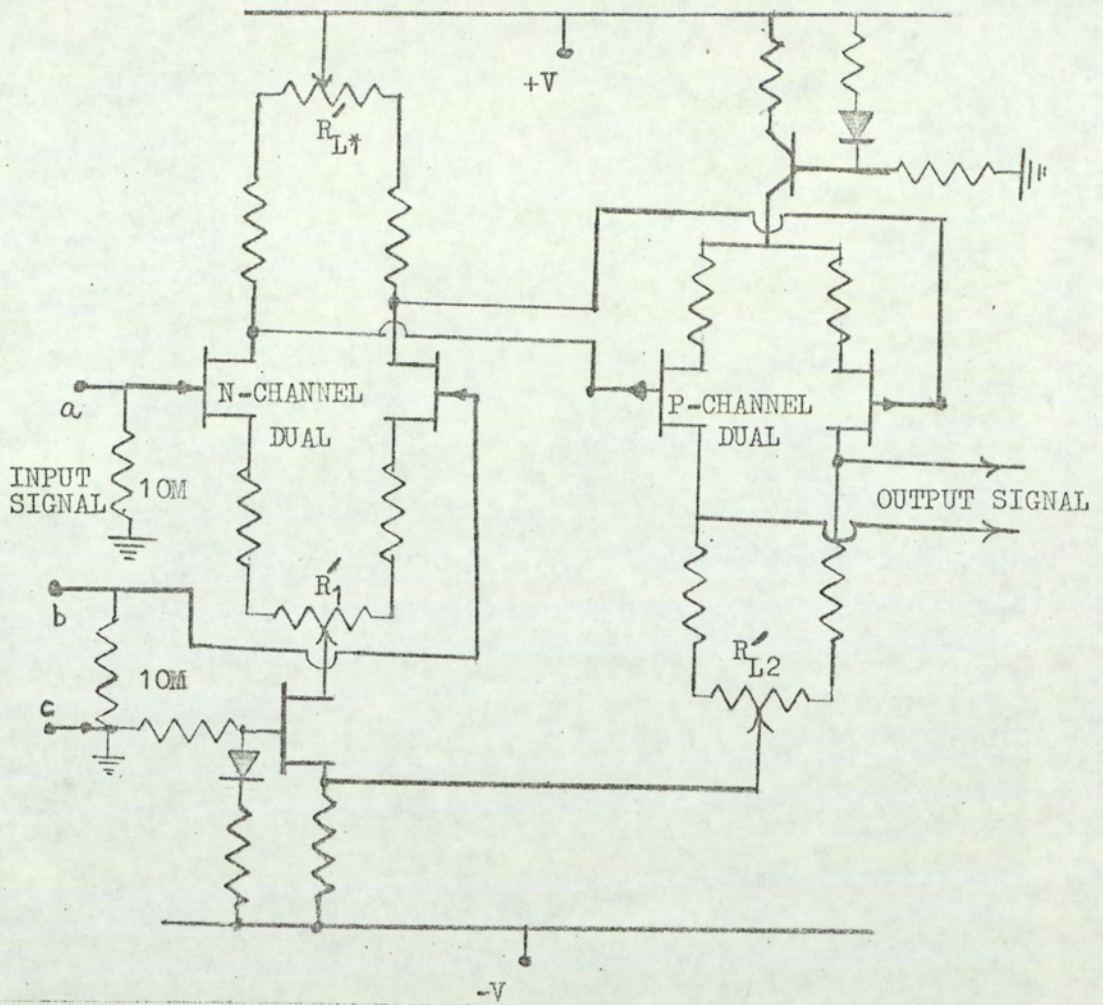


Fig.8a

Schematic Diagram of the Pre-amplifier Circuit

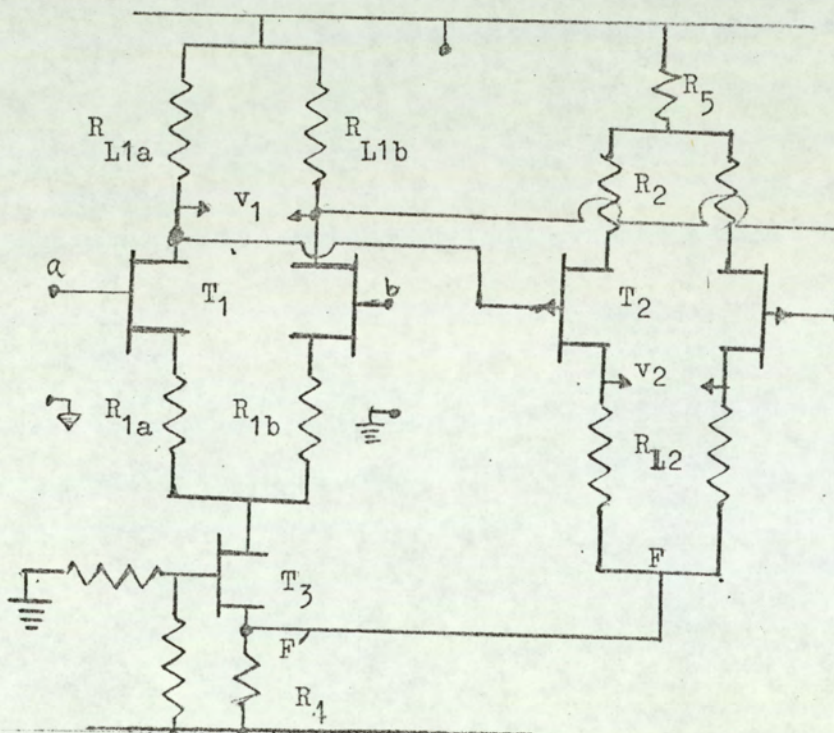


Fig.8b

Simplified form of the circuit shown in Fig.8a

Fig.9. can be used to explain the bisection theory.

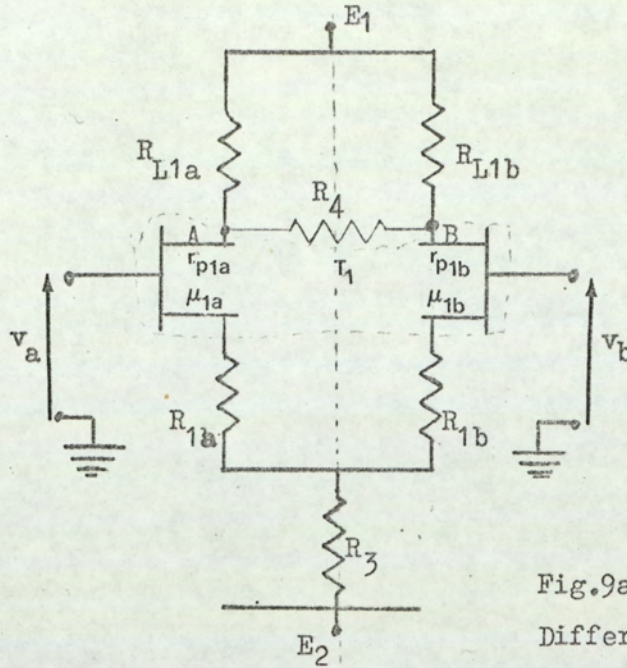


Fig.9a  
Differential Amplifier  
Circuit.

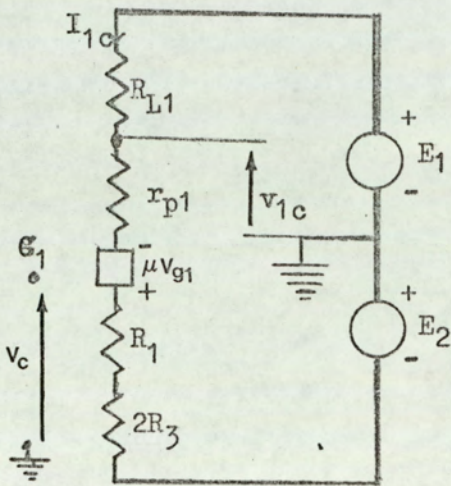


Fig.9b  
Common-mode Equivalent  
Half-Circuit.

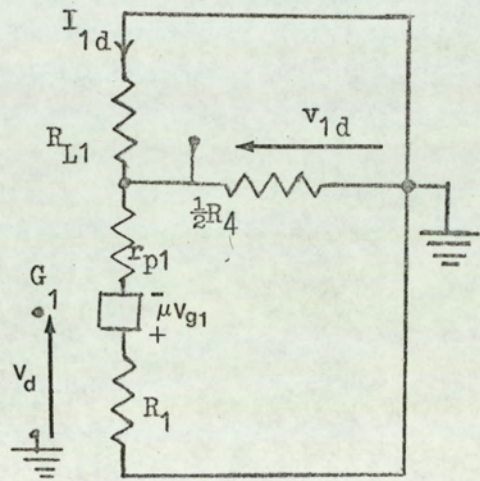


Fig.9c  
Differential-mode Equivalent  
Half-Circuit.

If the two halves of the first stage  $T_1$ , are identical and if  $R_{L1a} = R_{L1b}$ ,  $R_{1a} = R_{1b}$ , the circuit is said to be balanced and the bisection theory can be applied.

The circuit is divided along the line of symmetry and two half circuits are drawn, one for common-mode signals, Fig.9b, and the other for differential mode signals, Fig.9c.

The following observations are made:-

1. For a common-mode signal, where  $V_a = V_b$ , voltages occurring at similar points (homologous) in the two halves of the circuit are equal since the circuit is balanced. There is therefore no current flowing into components joining these points such as  $R_4$  joining A and B. Components such as  $R_3$  that lie along the line of symmetry carry twice the current in either side and are represented by twice their values in
2. For the differential mode input signal  $V_a = -V_b$ . The corresponding change in signal at homologous points is equal but opposite in sign, therefore a virtual ground exists at the meeting points of these elements. This is because there is no change in current in elements such as  $R_3$  as a result of the input signal. In the differential mode half circuit therefore, elements such as  $R_3$  are shorted to ground.
3. To identify the signals in the two modes subscripts, C for common-mode and d for differential mode signals are attached to the circuit parameters. The following are defined for input voltages:

$$\text{Common-mode signal (C.M)} \quad V_c = \frac{V_a + V_b}{2}$$

$$\text{Differential mode signal (D.M)} \quad V_d = \frac{V_a - V_b}{2}$$

Circuit properties such as currents are given the same subscripts depending on the mode.

A composite circuit, Fig.10. can be drawn from Figs. 9b and 9c and used for the algebraic analyses for I and V.

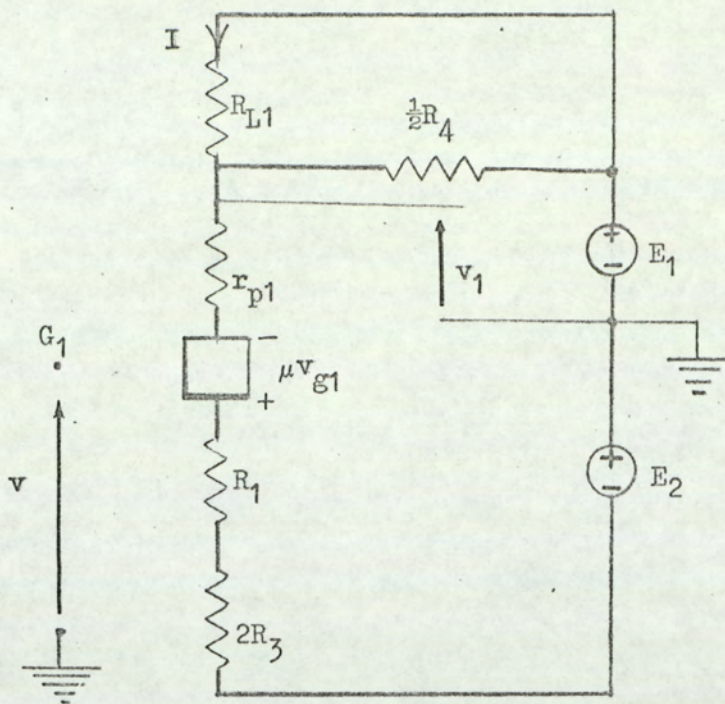


Fig.10. Composite Equivalent Half-circuit of the equivalent circuits shown in Figs.9b. & 9c.

To obtain the common-mode properties, Fig.9b, put  $R_4/2 \rightarrow \infty$  and append the c subscripts to the values of  $I$  and  $V$  calculated.

To obtain the differential mode properties, Fig.9c, put  $R_3 = 0$ ,  $E_1 = 0$ ,  $E_2 = 0$  and append subscripts d to the values of  $I$  and  $V$  calculated from the composite circuit.

This method of analysis was extended to circuits with small unbalances or slight departure from symmetry by Middlebrook.

Here if there is unbalance in any of the homologous elements such as  $R_{L1a}$  and  $R_{L1b}$  [ Fig.9a ], they are represented by  $R_{L1}$ , in series with an 'interaction' generator such that

$$R_{L1a} = R_{L1} + \delta R_{L1}$$

$$R_{L1b} = R_{L1} - \delta R_{L1}$$

where  $\delta R_{L1} = \frac{1}{2} (R_{L1a} - R_{L1b})$ , and the 'interaction' generator to be placed in the common-mode and differential mode circuits would be

$\delta R_{L1}$   $i_{1d}$  and  $\delta R_{L1}$   $i_{1c}$  respectively. This process is carried out on all circuit parameters of interest.

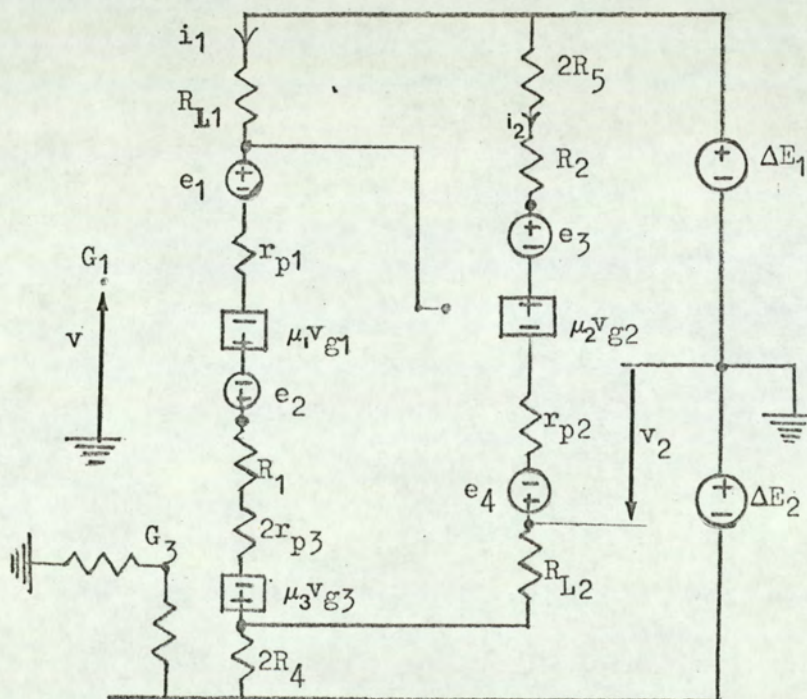
In the present work the theory in this form is applied to the field effect transistor circuit,  $R_4$  (see Fig.9a) is assumed to be high compared to  $R_{L1}$  as this stage is followed by one with high input impedance.

The circuit to be analysed is Fig.8b.  $R_3$  in Fig.9a is replaced by the field effect transistor ( $T_3$ ) circuit which constitutes a 'constant current' source. Feedback from a common point, F, in the second stage is applied through the degenerate resistance  $R_4$ , of  $T_3$ .

$R_5$  represents the "constant current" source of the second stage.

The unbalance in the amplification factor,  $\mu$ , and drain resistance ( $r_p$ ) are considered. Unbalance in the components external to the transistors are not discussed as these can be balanced by potentiometers  $R_L'$  and  $R'$ , shown in Fig.8a. [Changing  $R_L'$  and  $R'$  can, however, lead to changes in  $\mu$  and  $r_p$  as well but this will have second order effect].

Fig.11 shows the composite equivalent half-circuit of circuit of Fig.8b,



$e_1, e_2, e_3, e_4$  are the interaction generators.  $\Delta E_1$  and  $\Delta E_2$  represent changes in the power supply such as mains hum. In the present circuit batteries were used to supply this pre-amplifier circuit and the effects of  $\Delta E_1$  and  $\Delta E_2$  will be left out in the analysis.

Considering the input stage in Fig.11.

$$i_1(R_{L1} + r_{p1} + R_1 + 2r_{p3} + 2R_4) + i_2 \cdot 2R_4 = \mu_1 V_{g1} + \mu_3 V_{g3} + e_2 - e_1 \dots (17)$$

$$V_{g1} = V - \left[ i_1(R_1 + 2r_{p3} + 2R_4) + i_2 \cdot 2R_4 - \mu_3 V_{g3} \right] \dots (18)$$

$$V_{g3} = -2R_4(i_1 + i_2) \dots (19)$$

substituting (18) and (19) in (17) and re-arranging,

$$\begin{aligned} i_1 \left[ R_{L1} + r_{p1} + R_1(1 + \mu_1) + 2r_{p3}(1 + \mu_1) + 2R_4(1 + \mu_1)(-1 + \mu_3) \right] + i_2 2R_4(1 + \mu_1)(1 + \mu_3) \\ = \mu_1 V + e_2 - e_1 \dots (20) \end{aligned}$$

Considering the second stage,

$$i_1 2R_4 + i_2 (R_{L2} + r_{p2} + R_2 + 2R_5 + 2R_4) = e_4 - e_3 - \mu_2 V_{g2} \dots (21)$$

$$V_{g2} = -i_1 R_{L1} + i_2 (2R_5 + R_2) \dots (22)$$

substituting (22) in (21), and re-arranging,

$$i_1 (2R_4 - \mu_2 R_{L1}) + i_2 \left[ R_{L2} + r_{p2} + R_2(1 + \mu_2) + 2R_5(1 + \mu_2) + 2R_4 \right] = e_4 - e_3 \dots (23)$$

$$\text{Write } \alpha = R_{L1} + r_{p1} + R_1(1+\mu_1) + 2r_{p3}(1+\mu_1) + 2R_4(1+\mu_1)(1+\mu_3) \dots (24)$$

$$\beta = 2R_4(1+\mu_1)(1+\mu_3) \dots (25)$$

$$\alpha' = 2R_4 - \mu_2 R_{L1} \dots (26)$$

$$\beta' = R_{L2} + r_{p2} + (1+\mu_3)(2R_5 + R_2) + R_4 \dots (27)$$

Substituting (24), (25), (26), (27) in (20) and (23)

$$\alpha i_1 + \beta i_2 = \mu_1 V + e_2 - e_1 \dots (28)$$

$$\alpha' i_1 + \beta' i_2 = e_4 - e_3 \dots (29)$$

From (28) and (29)

$$i_1 = \frac{\beta'(\mu_1 V + e_2 - e_1) - \beta(e_4 - e_3)}{\beta'\alpha - \beta\alpha'} \dots (30)$$

$$i_2 = \frac{\alpha(e_4 - e_3) - \alpha'(\mu_1 V + e_2 - e_1)}{\beta'\alpha - \beta\alpha'} \dots (31)$$

$$\text{The composite output voltage } V_2 = i_2(R_{L2} + 2R_4) + i_1 2R_4 \dots (32)$$

The output voltage of interest is the differential one,  $V_{2d}$ . To obtain  $V_{2d}$  from the composite circuit all elements along the line of symmetry should be shorted to ground so put  $r_{p3} = 0$ ,  $R_4 = 0$ ,  $R_5 = 0$ , and append the subscript d to all circuit components.

Applying this for equations from (24) to (32)

$$\alpha_d = R_{L1} + r_{p1} + R_1(1 + \mu_1)$$

$$\beta_d = 0$$

$$\alpha'_d = -\mu_2 R_{L1}$$

$$\beta'd = R_{L2} + r_{p2} + R_2 (1 + \mu_2)$$

$$i_{2d} = \frac{-\alpha'd(\mu_1 V_d + e_2 - e_1)}{\beta'd \alpha_d} + \frac{1}{\beta'd} (e_4 - e_3)$$

$$V_{2d} = i_{2d} \cdot R_{L2}$$

$$\therefore V_{2d} = \frac{\mu_2 R_{L2} \cdot R_{L1} (\mu_1 r_d + e_2 - e_1)}{[R_{L2} + r_{p2} + R_2(1 + \mu_2)][R_{L1} + r_{p1} + R_1(1 + \mu_1)]} + \frac{R_{L2}}{R_{L2} + r_{p2} + R_2(1 + \mu_2)} (e_4 - e_3) \quad (33)$$

re-arranging equation (33)

$$V_{2d} = \frac{\mu_2 R_{L2}}{R_{L2} + r_{p2} + R_2(1 + \mu_2)} \cdot \frac{\mu_1 R_{L1}}{R_{L1} + r_{p1} + R_1(1 + \mu_1)} \cdot V_d + \frac{\mu_2 R_{L2}}{R_{L2} + r_{p2} + R_2(1 + \mu_2)} \times \frac{R_{L1}}{R_{L1} + r_{p1} + R_1(1 + \mu_1)} (e_2 - e_1) + \frac{R_{L2}}{R_{L2} + r_{p2} + R_2(1 + \mu_2)} (e_4 - e_3) \dots (34)$$

It can be seen from Figs. 9a and 9c that

$$\frac{\mu_1 R_{L1}}{R_{L1} + r_{p1} + R_1(1 + \mu_1)} \text{ is the differential gain of a balanced differential}$$

amplifier with degenerate resistance  $R_1$

$$\text{write this as } A_{d10} = - \frac{\mu_1 R_{L1}}{R_{L1} + r_{p1} + R_1(1 + \mu_1)} \dots (35)$$

$$\text{similarly write } A_{d10} = - \frac{\mu_2 R_{L2}}{R_{L2} + r_{p2} + R_2(1 + \mu_2)} \dots (36)$$

substituting (35) and (36) in (34)

$$V_{2d} = A_{d10} \times A_{d20} V_d + \frac{A_{d10} \times A_{d20}}{\mu_1} (e_2 - e_1) - \frac{A_{d20}}{\mu_2} (e_4 - e_3) \\ = A_{d10} \times A_{d20} \left[ V_d + \frac{(e_2 - e_1)}{\mu_1} - \frac{(e_4 - e_3)}{\mu_2 \cdot A_{d10}} \right] \dots (37)$$

$e_1, e_2, e_3$  and  $e_4$  are the interaction voltage generators defined as follows:-

$$\begin{aligned} e_1 &= \delta r_{p1} i_{lco} & e_3 &= \delta \mu_2 V_{g2co} \\ e_2 &= \delta \mu_1 V_{glco} & e_4 &= \delta r_{p2} i_{2co} \end{aligned}$$

The subscript o denotes the values when there is no unbalance, the values of  $i_{lco}, i_{2co}, V_{glco}, V_{g2co}$  are obtained from equations (30), (31), (18) and (22) respectively by putting  $e_1 = 0, e_2 = 0$  and writing  $V = V_c$  the common mode input signal.

All these values are dependent on  $V_c$  and when they are calculated and substituted equation (37) can be re-written as

$$V_{2d} = Ad_{10} \times Ad_{20} \left[ V_d + \frac{1}{H_{cf}} V_c \right] \dots \dots \dots (38)$$

In equation (38),  $H_{cf}$  is the common mode rejection ratio with feedback. The rather long expression for this has been derived in Appendix 1, equations A-15 and A-17

By substituting typical values for the resistances as follows:-

$$\begin{aligned} R_{L1} = R_{L2} &= 2 \times 10^4, r_{p1} = r_{p2} = r_{p3} = 10^5 \\ R_{L1} &= 10^3, 2R_4 = 10^4, R_2 = 3 \times 10^3, 2R_5 = 10^5, \end{aligned}$$

$$\frac{1}{H_{cf}} \approx \frac{1}{100} \left[ \frac{\delta \mu_1}{\mu_1} - \frac{1}{13} \frac{\delta r_{p1}}{r_{p1}} + \frac{1}{600} \frac{\delta \mu_2}{\mu_2} + \frac{1}{1500} \frac{\delta r_{p2}}{r_{p2}} \right] \dots \dots (39)$$

From equation (39) it can be deduced that the contribution to the common mode rejection action by unbalances in the second stage (subscript 2) is small compared to that contributed by unbalance in the first stage, except when the first stage unbalances are very small.

For the attainment of very high common mode rejection ratios therefore, the unbalances in the second stage should be comparably small.

$\frac{1}{H_c}$  in the first stage only is given from equation A-17 by

$$\frac{1}{H_c} = \frac{R_{L1} + r_{p1} + R_1 + 2r_{p3} + 2R_4(1 + \mu_3)}{R_{L1} + r_{p1} + R_1(1 + \mu_1) + 2r_{p3}(1 + \mu_1) + 2R_4(1 + \mu_1)(1 + \mu_3)} \left[ \frac{\delta\mu_1}{\mu_1} - \frac{r_{p1}}{R_{L1} + r_{p1} + 2r_{p3} + R_1 + 2R_4(1 + \mu_2)} \cdot \frac{\delta r_{p1}}{r_{p1}} \right] \dots\dots\dots (40)$$

$r_{p3} + R_4(1 + \mu_3)$  can be written as R the "tail" resistance of the differential amplifier.

substituting in equation 40

$$\frac{1}{H_c} = \frac{R_{L1} + r_{p1} + R_1 + 2R}{R_{L1} + r_{p1} + R_1(1 + \mu_1) + 2R(1 + \mu_1)} \left[ \frac{\delta\mu_1}{\mu_1} - \frac{r_{p1}}{R_{L1} + r_{p1} + R_1 + 2R} \cdot \frac{\delta r_{p1}}{r_{p1}} \right] \dots\dots\dots (41)$$

It can be seen that when the value of the  $2R \gg R_{L1} + r_{p1} + R_1$  equation 41 reduces to:-

$$\frac{1}{H_c} \rightarrow \frac{1}{(1 + \mu_1)} \cdot \frac{\delta\mu_1}{\mu} \dots\dots\dots (42)$$

Parnum<sup>(34)</sup> Andrew<sup>(37)</sup> Klein<sup>(33)</sup> reached the conclusion that when R is made infinitely large the common mode rejection ratio tends to the limiting value given in equation (42). On page 86 of his book, Middlebrook further observes that by using pentodes to make  $r_p$  tend to infinity  $\frac{1}{H_c}$  can be made to tend to zero even in the presence of unbalances. His method of approach was first to recast equation (41)

$$\mu = gm r_p \dots\dots\dots (43)$$

$$\therefore \frac{\delta\mu}{\mu} = \frac{\delta gm}{gm} + \frac{\delta r_p}{r_p} \dots\dots\dots (44)$$

and substituting in equation (41) without the individual degenerating resistors  $R_L$  to get:-

$$\frac{1}{H_c} = \frac{1+k}{1+k+2gmR} \left( \frac{\delta gm}{gm} + \frac{k}{1+k} \frac{\delta r_p}{r_p} \right) \dots\dots\dots (45)$$

$$\text{where } k \equiv \frac{R_L + 2R}{r_p} \dots\dots\dots (46)$$

if now  $r_p \rightarrow$  infinity,  $k \rightarrow$  zero

$$\text{and } \left. \frac{1}{H_c} \right|_{r_p \rightarrow \infty} = \frac{1}{1+2gmR} \frac{\delta gm}{gm} \dots\dots\dots (47)$$

He concludes from now that if  $R$  tends to infinity in (47)

$\frac{1}{H_c} \rightarrow$  zero even in the presence of unbalance in the transconductances  $gm$ .

This procedure to the zero limit is not correct because in obtaining equation (47) it has been assumed that  $R$  remains finite at a value far less than  $r_p$  and therefore cannot in the next instance be made to tend to infinity.

In obtaining the limiting case in equation (42) from equation (41)  $R$  must be made bigger than  $r_p$ . This is realised in practice by using another device whose  $r'_p$  is comparable to, and may be greater than,  $r_p$ . Therefore  $k$  cannot be made to tend to zero in practice.

One can, however, envisage a situation where both  $r_p$  and  $R$  are very large compared with the other components in the circuit. This can be illustrated using equations (41) and (42) and remembering that we are dealing with one circuit at a time.

Suppose we desire a common mode rejection ratio of  $10^4$   
(which is not infinite)

$$\text{when } g_m = 2000 \text{ micro mho}$$

$$\delta g_m / g_m = 0.1$$

Then using Middlebrook's equation (47)

$$10^4 = \{1 + 2 \times 2 \times 10^{-3} \times R\} \times 10$$

$$\therefore R = 0.25 \times 10^6 \Omega$$

since  $k = \frac{R_L + 2R}{r_p}$ , to make it tend to a moderate value of say 0.001, not zero, one needs

$$\begin{aligned} r_p &= \frac{2R}{k} = \frac{0.5 \times 10^6}{0.001} \\ &= 500 \text{ M}\Omega \end{aligned}$$

This requires a device with an amplification factor

$$\mu = g_m r_p = 10^6$$

According to this approach, therefore, to obtain a common mode rejection ratio which tends to infinity one should use a device which has an amplification factor which tends to infinity. It can be seen that this conclusion could have been reached from equation (42) in any case and nothing has been added by using equation (47). With a device having a  $\mu = 10^6$  and even the maximum possible fractional unbalance of  $\frac{\delta \mu}{\mu} = 1/2$  using equation (42) would have resulted in  $H_C = 2 \times 10^6$  which is far better than the  $10^4$  we used

in equation (47) to obtain R. This discrepancy lies in the approach used to obtain equation (47). Middlebrook

$$\begin{aligned} &\text{writes } \mu = g_m r_p \\ &\text{and defines } \frac{\delta \mu}{\mu} = \frac{\delta g_m}{g_m} + \frac{\delta r_p}{r_p} \text{ by differentiation.} \end{aligned}$$

In the analysis, however,  $\delta \mu$  represent only the unbalance between the

two halves constituting the differential pair, say  $\mu_a$  and  $\mu_b$ . It is not a mathematical necessity that the differential should hold. Consider a case in which even,  $\mu_a = \mu_b$ , therefore it is quite possible that

$$g_{ma} > g_{mb}$$

$$r_{pa} < r_{pb}$$

In this instance

$$\delta\mu = \frac{\mu_a - \mu_b}{2} = 0$$

$$\text{but } \delta g_m = \frac{g_{ma} - g_{mb}}{2} \neq 0$$

$$\text{and } \delta r_p = \frac{r_{pa} - r_{pb}}{2} \neq 0$$

and the common mode rejection ratio will not be infinite.

It is concluded that to obtain a high value for the common mode rejection ratio,  $H_c$ , equation (41) must be upheld and means found to reduce the values of the terms in brackets or the unbalances in the devices made or made to cancel out.

The parameters of field effect transistors and transistors in general are dependent on the current flowing in them and in a circuit such as is shown in Fig.8(a) the potentiometers  $R'_1$  and  $R'_2$  can be used to bias the two halves so as to make the gains equal. However, this balance can only be attained at one operating point. The use of the negative common mode feedback is to force the circuit to work at this balance point and to make it possible to obtain a high value of the tail resistance or in equation (41) to make  $2R$  high.

The use of individual degenerate resistors  $R_{1a}$  and  $R_{1b}$

See Fig.8(b) makes the differential gain  $\frac{\mu R_L}{R_L + r_p + (1 + \mu_1) R_1}$  It can be

seen that the higher the value of  $R_1$  is the more this gain tends to  $\frac{\mu}{1 + \mu_1} \frac{R_L}{R_1}$ . for devices with high amplification factors,  $\mu$ , the differential gain tends to  $R_L/R_1$  this is why the use of  $R'_1$  and  $R'_2$  can

lead to very close balance of the amplification of the two halves constituting the differential pair.

The preceding analysis of the common mode rejection ratio has been undertaken because of its importance when measuring low level signal like the foetal electro-cardiogram in the presence of other unwanted signals. It was also an attempt to find out the effect of common mode negative feedback on the common mode rejection factor.

#### DESCRIPTION OF THE CIRCUIT USED IN THE PRESENT EXPERIMENT

Fig.(12) shows a diagram of the circuit.

The first stage consists of low-noise N-channel f.e.t. dual T1S 25 for the differential pair and an N-channel mos.f.e.t 3N138 for the constant current source.

The outputs go into a second stage consisting of PNP dual BFX\* 36 which is also a low noise device. It is complementary to T1S 25 to facilitate direct coupling. Source and emitter degeneration has been employed for the first and second stages respectively to make the circuit less dependent on the transmitter parameters. The degeneration in the second stage also increases the input impedance of the second stage so as not to load the output of the second stage. Originally a P-channel mos.f.e.t. was used in the second stage until it was found that the intrinsic noise could be reduced by the use of the PNP bipolar dual transistor. There is a feedback from the common point P in the second stage (mid point of  $R_{L2}'$ ) to the source of the first stage constant current generator.

The diode chains  $D_1$  and  $D_2$  have been used to compensate for temperature variations and also to offset changes in the power supply. The voltage drop across the diode decreases with the current flowing through it less rapidly than if a resistor had been used.

The circuit incorporating the BFX 37 was added to compensate for changes in the positive power supply voltage and also to provide

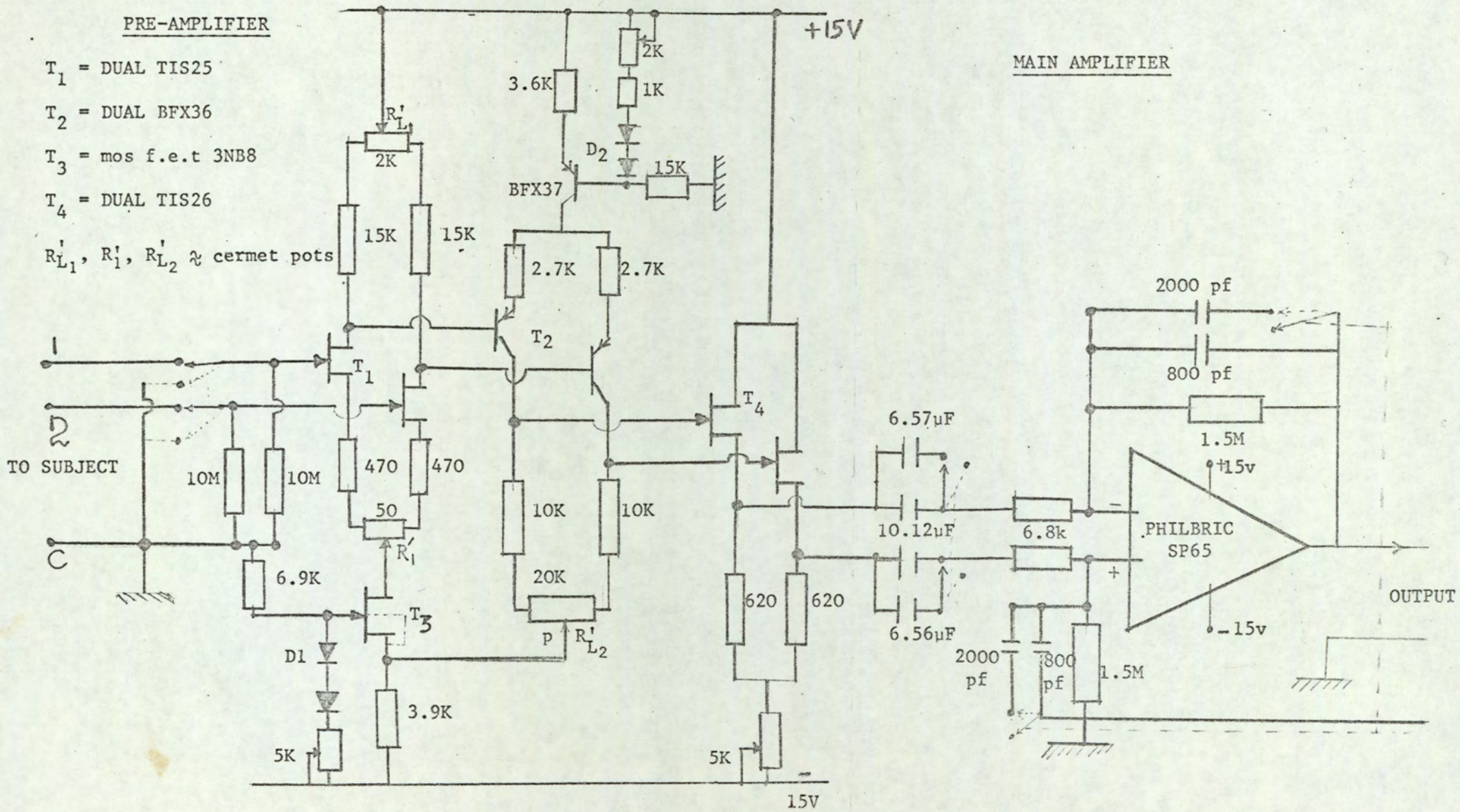


FIG.12. CIRCUIT DIAGRAM OF THE DETECTING AMPLIFIER.

similar current drains in the positive and negative supply batteries.

Batteries have been used to improve the safety in regard to the patient, since the input terminals are attached directly to the maternal abdominal wall.

Although the input impedance of the f.e.t. is high of the order of  $10^{11}\Omega$ ,  $10^7\Omega$  resistors of close tolerance were used to shunt them to make the input impedances of the two halves nearly the same. This means that the differential input impedance was  $20M\Omega$  and this was found to be adequate for this study.

The output of the second stage is directly coupled to a source follower circuit consisting of an N-channel f.e.t., T1S 26 which is complementary to BFX36. This stage was used to present high impedance to the output of the second stage and a low output impedance ( $\approx 1.2k\Omega$  differential) to the main amplifier.

The following are some properties of the circuit obtained using the original configuration when the input stage was a P-channel mos f.e.t. (BSX86). The two sources are joined together internally and so it was not possible to include the degenerating resistors  $R_{1a}$ ,  $R_{1b}$  and the balancing resistor  $R'_1$  (see Fig.8). Because of this the common-mode rejection ratio was low even with negative feedback from the second stage.

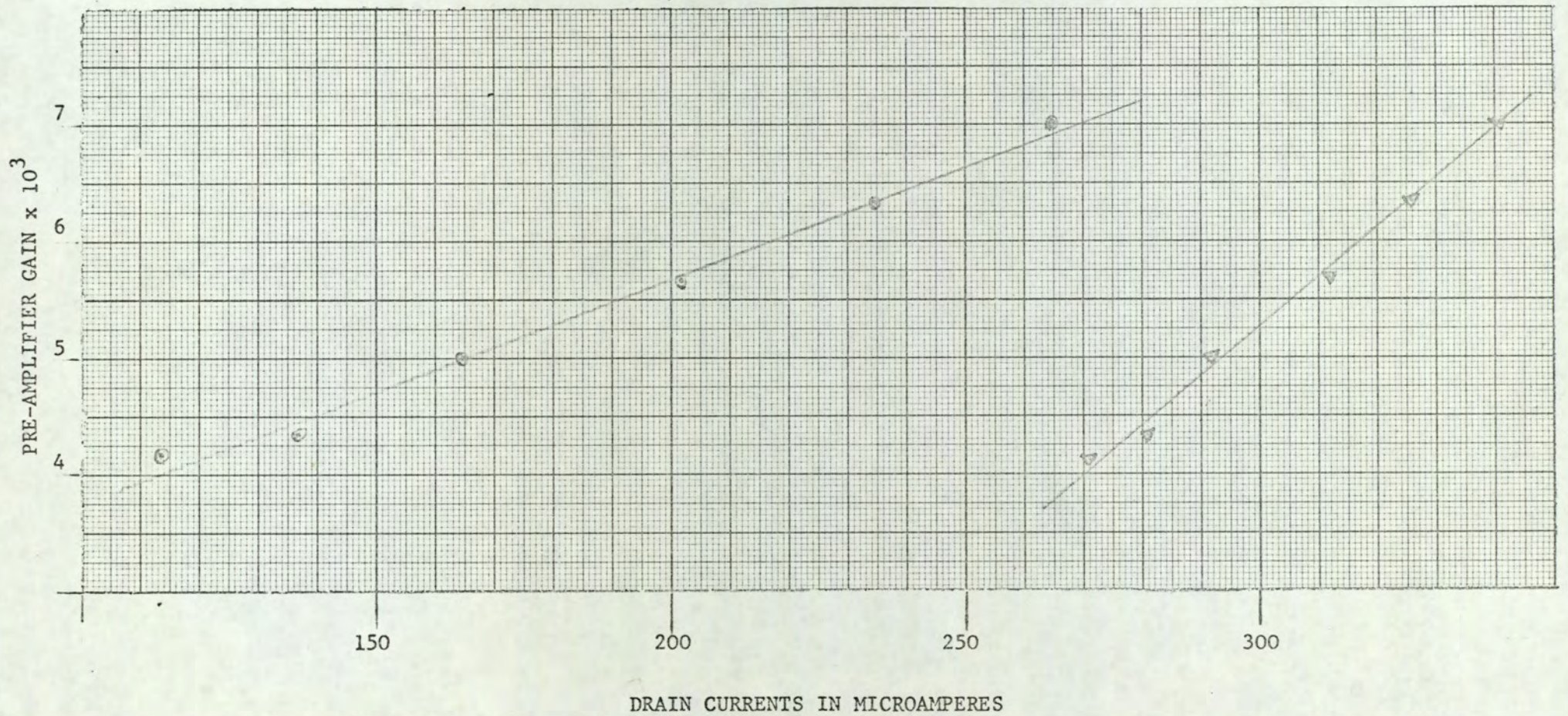
Table I and Fig.13 show how the total gain varies with the drain currents flowing in the two stages of the pre-amplifier:-

$I_1, \mu A$	185	216	248	285	313	336
$\delta I_1, \mu A$	9	15	17	19	19	19
$I_2, \mu A$	109	124	138	158	169	179
$\delta I_2, \mu A$	4	3	0.3	5	6	7
GAIN $10^3$	4.00	4.66	5.34	6.00	6.67	6.83

TABLE 1.

Variation of total pre-amplifier gain with drain currents

FIG.13. VARIATION OF TOTAL PRE-AMPLIFIER GAIN WITH DRAIN CURRENTS.



Here  $I$  is the mean of the currents flowing in the two halves and  $\delta I$  is the mean difference.

The total gain goes up, effectively linearly with the current. This is usually the case. The difference between the currents  $\delta I_1$  is greater than  $\delta I_2$ . The difference in  $\delta I_2$  however shows a minimum but this stage had separate sources and balancing resistors had been incorporated. Secondly, the second stage biasing is controlled by unbalance in the first stage. Because of higher unbalance coupled with higher level of intrinsic noise in the BSX86 the second configuration in which the BSX86 was made the second stage.

Fig.14a. shows the variation of gain with changes in power supply voltage:

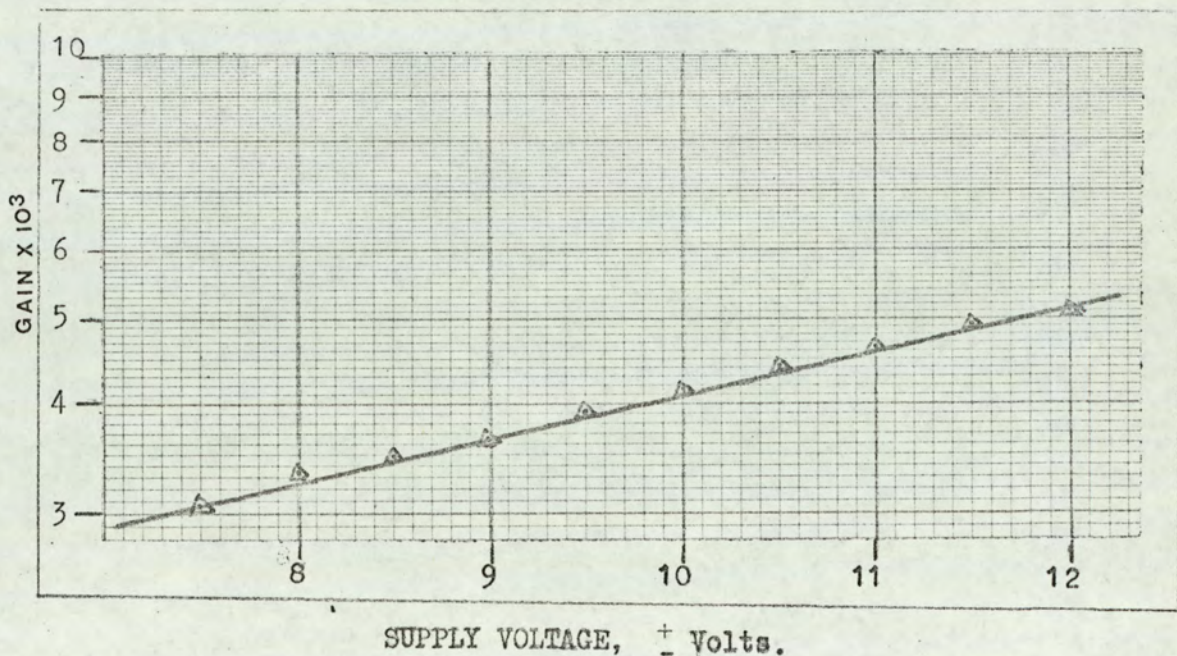


Fig.14a. Variation of Pre-amplifier Gain with Supply Voltage.

These readings were taken because the pre-amplifier stage was to be supplied with batteries and inevitable effect of the battery voltage falling with time was considered likely to be important. The gain decreases steadily and linearly with decrease in supply voltage from a value 5100 at +12, -12v at a rate of 9%/volt down to 2800 @ +7v, -7v.

The common mode rejection ratio does not, however, follow a

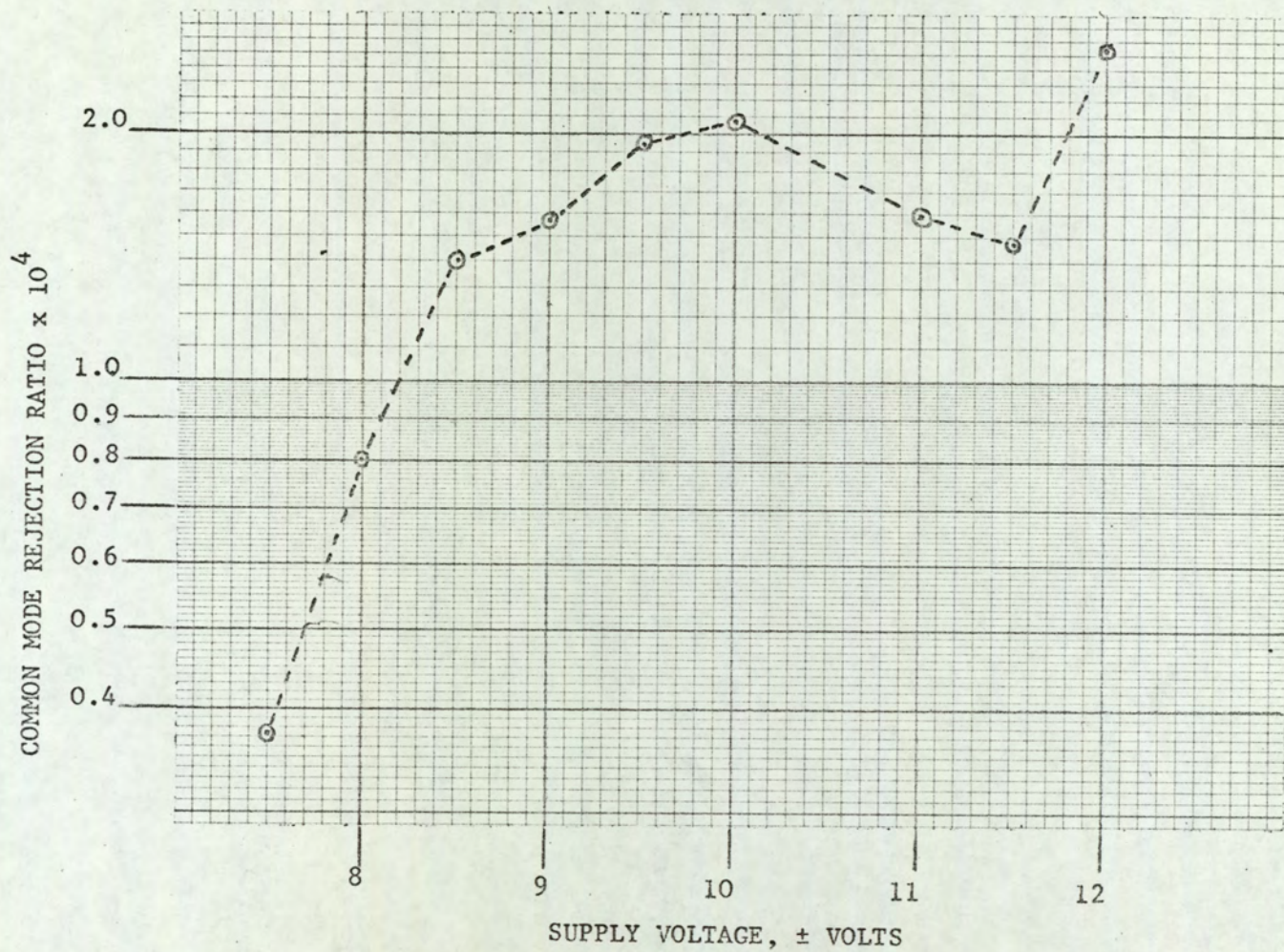


FIG.14b. Variation of Common Mode Rejection Ratio with Supply Voltage.

linear curve once set for a maximum of about -86 db at +12v - 12v supply, as shown in Fig.14b.

What can be inferred from these graphs of readings are:

1. The gain goes up with supply voltage or increase in current flowing in the device. This is quite to be expected.
2. The common mode rejection ratio depends solely on the unbalance in the branches forming the differential pair and this unbalance changes with different operating currents.

In actual operation, however, the battery voltage remains quite constant as the drain on it is not high at all, being less than a milliamp<sup>e</sup>.

The final circuit in this experiment consisted of the circuit shown in Fig.(12). The common mode rejection ratio is estimated to be of the order of -120 db. This has been obtained by:-

- (a) Choosing a first stage f.e.t. (T1S 25) which is a dual with nominal amplification factor  $\approx 160$  and  $\delta\mu \approx 2\frac{1}{2}\%$  max. (manufacturer's statement).
- (b) Using  $R_1$  and  $R_2$  degenerating source resistors to make the characteristics less dependent on the transistor parameters.
- (c) Use of  $R'$  and  $RL'$  to set balance and reduce the unbalance in the differential pair even further.

#### TEMPERATURE COMPENSATION

Transistors are better than vacuum tubes with respect to drift due to temperature. One major source of drift in d-c vacuum tubes, namely changes in heater properties, is eliminated by the use of transistors. In addition to this, since dual transistors are monolithic i.e. made from the same semiconductor chip, temperature variations in the characteristics of the two halves forming a dual,

tend to be of the same order. Silicon transistors have lower temperature coefficients than germanium transistors. The transistors  $T_1, T_2, T_3$  are all duals and made from silicon chips and each surrounded by a metal case which keeps the temperature distribution uniform.

Shea<sup>(38)</sup> has reviewed various methods for temperature compensation of differential d-c amplifiers. The general scheme is as shown in Fig.(15).

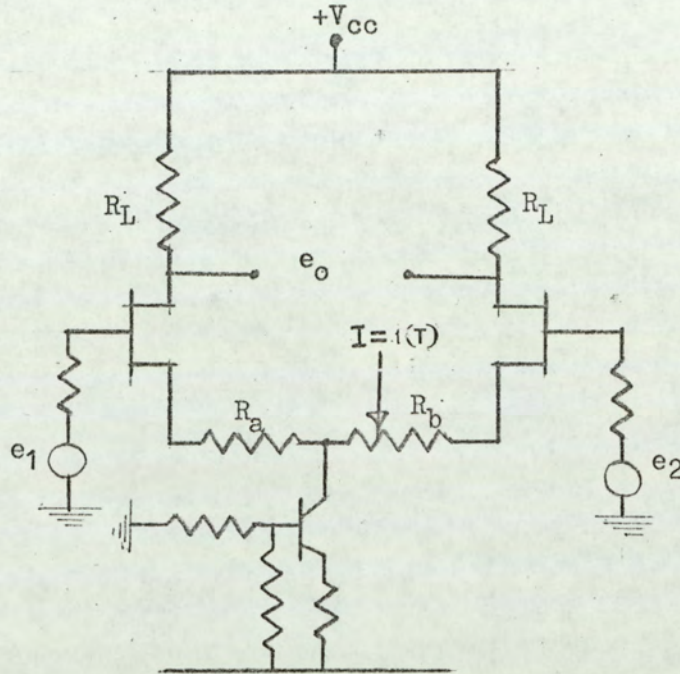


Fig.15. Scheme for Temperature Compensation. Current  $I=f(T)$ , is fed to  $R_b$ .

The compensation is applied on the differential pair. A current  $I$  which is a function of temperature is fed at the highest temperature of interest more to one branch than the other, and the amplifier is set for balance at this temperature. As the temperature changes the amount of current fed to it changes and tracking over a temperature range is obtained.

Middlebrook and Taylor<sup>(39)</sup> used such a scheme in addition to the use of negative common mode feedback to obtain equivalent input drift of  $\approx \pm 100\mu V$  for eight hours over a temperature range from  $25^\circ C$  to  $100^\circ C$ .

What must be remembered in using such schemes is that the

source of  $I = f(T)$  must be of very high resistance so as not to reduce the value of the tail resistance ( $R$  in equation 41). Otherwise the differential compensation will be achieved at the cost of the common mode rejection ratio.

It has already been stated that the use of monolithic duals in which characteristics track with temperature is a better method. However, if the characteristics should change in one direction it means that the common mode compensation is needed. The circuit of constant current source requires to be stabilised to keep the quiescent currents nearly constant. In constant current sources employing n-p-n transistors, the variation of the base to emitter voltage,  $V_{BE}$ , with temperature can be offset by the use of thermistors or diodes in the base circuits. In fig.(16) is shown a current stabilising circuit.

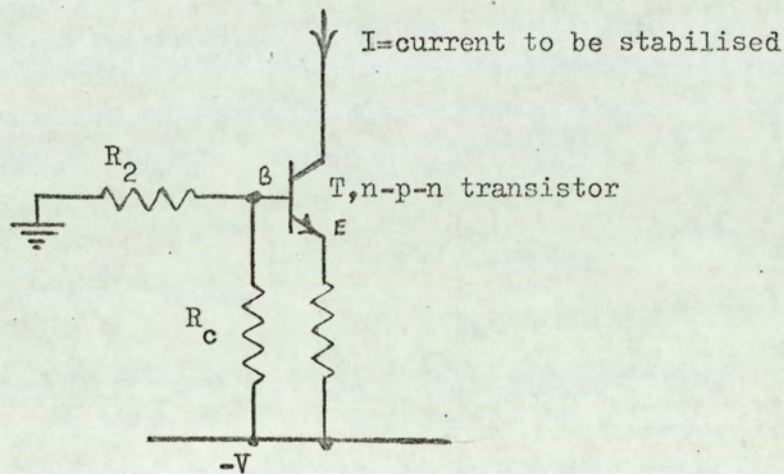


Fig.16. Current Stabilising Circuit.

The effect of increase in temperature is to increase the collector current. If at the same time,  $R_C$  is reduced so that the point B becomes negative, then the expected increase in  $I$  will be arrested. A device, therefore, which will drop less voltage with increase in temperature, for example, a diode whose characteristic can

be represented by  $I_d = I_s (e^{qV/mkT} - 1)$  may be used in  $R_c$ . Also a thermistor, the resistance of which falls with temperature could have been used. The temperature characteristics of the controlling device must be similar to those of the controlled device to ensure good tracking. Hence a germanium diode should be used for controlling a germanium device and a silicon diode for a silicon transistor. In the present circuit constant current source in the first stage consists of an N-channel mos.f.e.t. which has good temperature properties. The Diodes  $D_1$  and  $D_2$  Fig.(12) were used both to compensate for changes in the supply voltage and temperature.

In arrangements to give temperature compensation only the most temperature dependent devices are considered, since changes in components like resistors are taken to be of second order.

In recent years the use of integrated circuit technology has given what might be the best method of counteracting drift resulting from temperature variation in d-c amplifiers. This technique is known as temperature stabilised substrates. The original concept was put forward by Evans, formerly of Texas Instruments, Inc. Dallas. Emmons and Spence<sup>(40)</sup> have discussed it exhaustively.

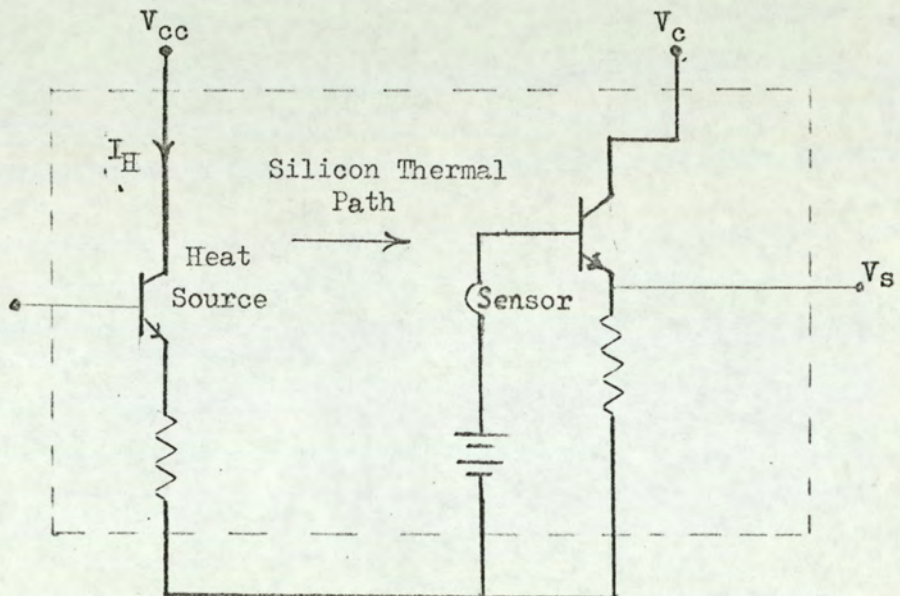


Fig.17. Basic Thermal-Electric Element.

$V_S$  is used to control the heater current,  $I_H$ .

Incorporated in the same monolithic chip is a system shown in Fig.(17). A heat source consisting of the transistor on the left carrying current  $I_H$  heats the whole substrate. Another amplifier is used as a heat sensor. The output of the sensor is used to control the heater current. Thus a thermal-electric feedback system is obtained which keeps the substrate at a fixed temperature normally slightly above ambient temperature. In such same controlled substrate one could have the differential amplifiers. Emmons and Spence used a differential amplifier circuit not structurally unlike the present system but only in monolithic form to produce drifts of 0.1 to 0.2 $\mu$ V/°c.

It must be said that chopper stabilisation of drift, that is where the signal is first turned to a-c and fed into a-c amplifiers and then synchronously demodulated, have been used quite extensively.

Here both mechanical and semiconductor switches have been used. Short life, low frequency chopping rate, sources of transients, bulk and power requirements are the main disadvantages of mechanical switches. The semiconductor switches have residual resistance and suffer from temperature variations themselves.

There have been other methods of chopping only the drift voltage, smothering it and feeding it back (Goldberg) into the input. These chopper stabilised amplifiers have been used in electro-encephalography and been found quite satisfactory. With the advent of methods for temperature stabilisation such as have been outlined above in connection with Fig.(17), chopper stabilised amplifier techniques will have great competition and will probably be rendered obsolete.

THE MAIN AMPLIFIER

The main amplifier was built around a Philbrick operational amplifier and used to provide a single ended output from the differential output of the pre-amplifier stage.

It was also used as the only stage for controlling the bandwidth and to determine at which frequency the low frequency half power point should be. The signal from the maternal abdominal wall contains very large low frequency signals arising from changes in resting muscle potentials accompanying maternal breathing. It was intended that the best compromise on frequency characteristics which would filter off "breathing" potentials and least affect the foetal signal should be found experimentally. Also, the nature of the effect of filtering and bandwidth of the detecting system on the characteristics of the foetal waveform are not properly understood and this was intended to be studied. It was therefore thought that it would be best to have the frequency determining components in one stage.

Basically, this stage consists of the circuit shown in Fig.(18)

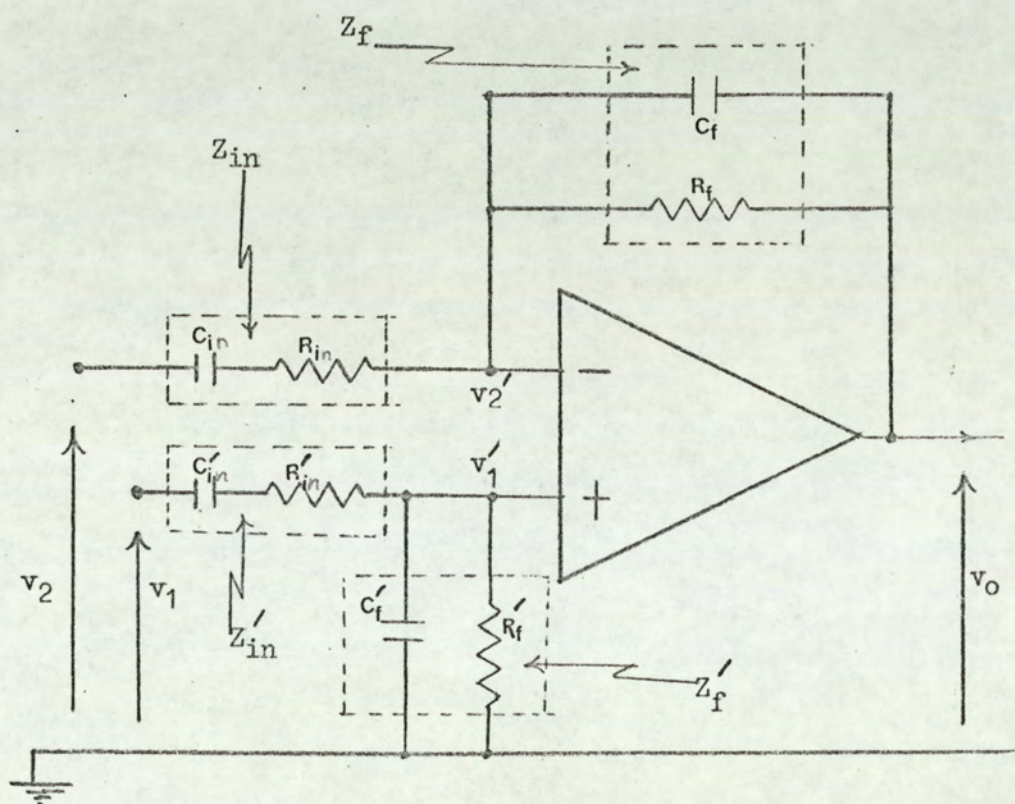


Fig.18. CIRCUIT DIAGRAM OF THE MAIN AMPLIFIER.

Using the superposition theorem,

$$v_2' = v_o \frac{Z_{in}}{Z_{in} + Z_f} + v_2 \frac{Z_f}{Z_{in} + Z_f} \dots\dots\dots (48)$$

$$v_1' = v_1 \frac{Z_{f'}}{Z_{f'} + Z_{in'}} \dots\dots\dots (49)$$

$$v_2' - v_1' = -\frac{V_o}{G} \dots\dots\dots (50)$$

from (48), (49) and (50)

$$v_o \frac{Z_{in}}{Z_{in} + Z_f} + v_2 \frac{Z_f}{Z_{in} + Z_f} - v_1 \frac{Z_{f'}}{Z_{f'} + Z_{in'}} = -\frac{V_o}{G}$$

$$v_o \left( \frac{1}{G} + \frac{Z_{in}}{Z_{in} + Z_f} \right) = -v_2 \frac{Z_f}{Z_{in} + Z_f} - v_1 \frac{Z_{f'}}{Z_{f'} + Z_{in'}} \quad (51)$$

for  $G \gg 1$  and  $Z_f = Z_{f'}$ ,  $Z_{in} = Z_{in'}$

equation (51) becomes

$$v_o = -\frac{Z_f}{Z_{in}} \cdot (v_2 - v_1) \dots\dots\dots (52)$$

The differential gain,  $A_v = -\frac{Z_f}{Z_{in}}$

In the present system

$$Z_{in} = R_{in} + \frac{1}{\omega c_{in}} = R_{in} \left( 1 + \frac{1}{\omega c_{in} R_{in}} \right)$$

$$Z_f = \frac{R_f \times \frac{1}{\omega c_{in}}}{R_f + \frac{1}{\omega c_f}} = R_f / (1 + \omega c_f R_f)$$

$$\therefore \text{the stage gain, } A_v = -\frac{R_f}{R_{in}} \cdot \frac{1}{1 + \omega c_f R_f} \cdot \frac{1}{1 + \frac{1}{\omega c_{in} R_{in}}} \dots\dots (53)$$

The low frequency half power point occurs at

$$\omega_L = \frac{1}{C_{in} R_{in}} \dots\dots\dots (54)$$

The high frequency half point occurs at

$$\omega_H = \frac{1}{C_f R_f} \dots\dots\dots (55)$$

The analysis assumes that the input impedance of the operational amplifier is higher than valves used for  $Z_{in}$  and  $Z_f$ .

After trials which will be discussed later, the values obtained for  $Z_{in}$  and  $Z_f$ , shown in Fig.(12) were obtained. Two cut off points each for high and low frequencies were found adequate for measurement of the foetal electro-cardiogram using abdominal electrodes.

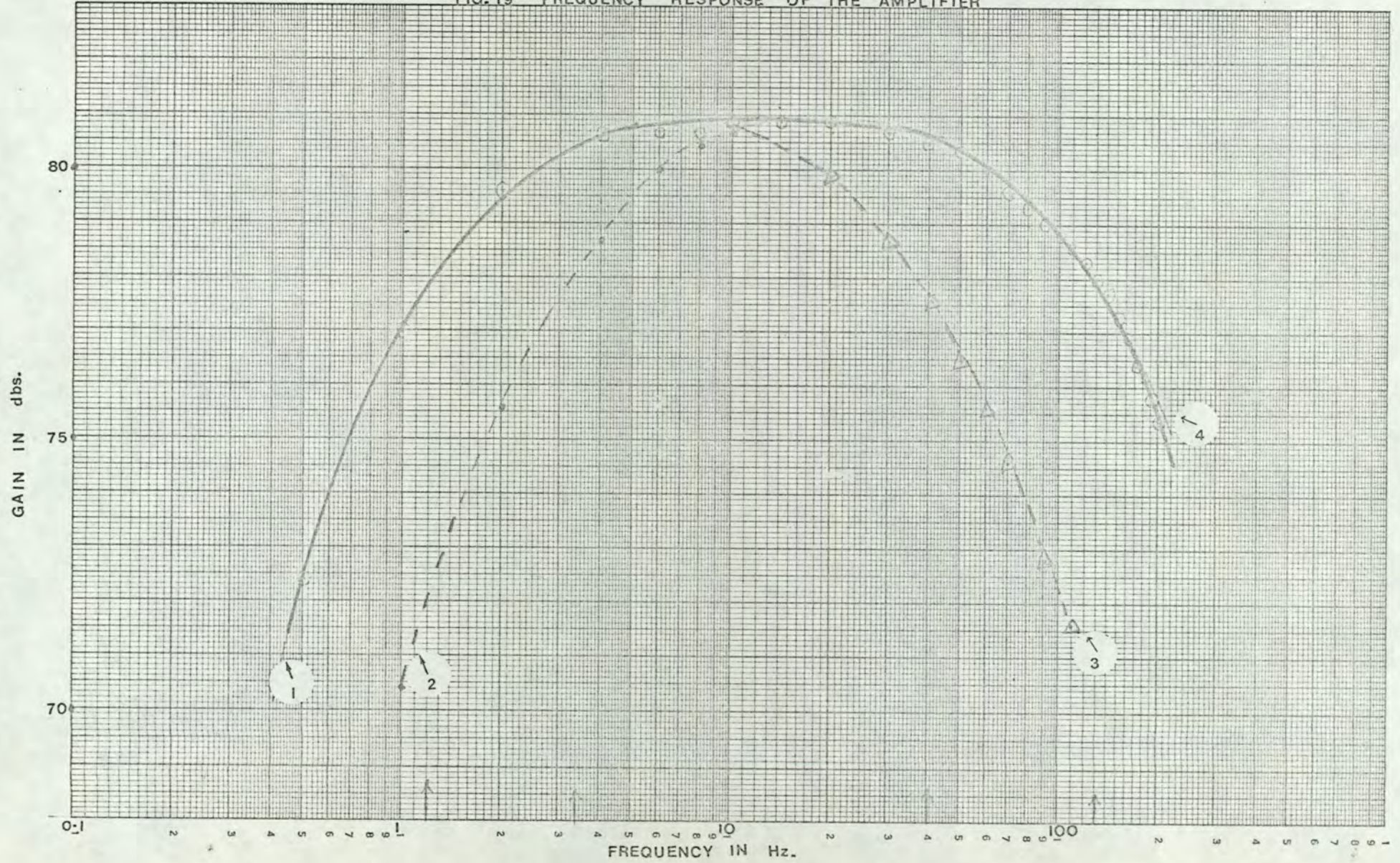
The amplitude of the foetal signal lies between  $5\mu V$  and  $50\mu V$  and the maternal R-wave about  $100\mu V$ . Since the maternal wave was to be used for triggering during maternal blanking a gain of  $10^4$  was chosen to give a trigger voltage of about a volt.

Fig.(19) shows a graph of the frequency response of the amplifier which was finally used.

With  $C_{in} = 16.69\mu F$ ,  $R_{in} = 6.8k\Omega$ ,  $R_f = 1.5M\Omega$  and  $C_f = 800pf$ , expected low frequency  $f_L$ , and high frequency  $f_H$  cut-off points were  $f_L = 1.38Hz$ ,  $f_H = 133Hz$ , from the frequency response curve (1-4) these points (-3db) points occur at  $1.2Hz$  and  $133Hz$  respectively.

Under circumstances where there is too much low frequency signal components, such as caused by heavy breathing by the mother there were switches to change the (-3db) point to  $3.4Hz$  curve 3-4. Similarly, there was provision for lowering the high frequency cut-off point. There was, however, no occasion to use this later provision.

FIG. 19 FREQUENCY RESPONSE OF THE AMPLIFIER



NOISE LEVEL OF DETECTING SYSTEM

This section deals with the inherent noises of the detecting system which are classified as follows:

1. Thermal Noise
2. Shot Noise
3. Flicker Noise
4. Noise due to signals may be of the shot type.

The signal to noise ratio of a detecting system is dependent to a greater extent on the noise level of the first stage if this stage is amplifying.

The contribution to the total noise of the later  $n^{\text{th}}$  stage is a fraction  $\frac{1}{G_{n-1}}$  of the total noise where  $G_{n-1}$  is the amplification of the signal up to the input of the  $n^{\text{th}}$  stage.

The first amplifier stage noise therefore is the crucial stage as far as noise is concerned.

In the present system the active input device is a dual f.e.t. (T1S25) and being a semiconductor it will suffer from the types of noise outlined.

Thermal or Johnson Noise.

By the use of the principle of the equipartition of energy the fluctuation voltage arising from an electrical circuit or component which in thermal equilibrium with its surroundings can be adequately explained.

Nyquist in 1928 first expressed the thermal noise in terms of a voltage generator in series with a resistance  $R$  as

$$\overline{v_{\text{th}}^2} = 4 KTR/\text{unit bandwidth} \dots\dots\dots (56)$$

where  $K$  is Boltzmann's constant =  $1.37 \times 10^{-23}$  joules  $^{\circ}\text{K}^{-1}$

$T$  is the absolute equilibrium temperature in  $^{\circ}\text{K}$

$R$  is the resistance

The total thermal noise voltage developed across the terminals A and B in circuit such as shown in Fig.(20) is given by

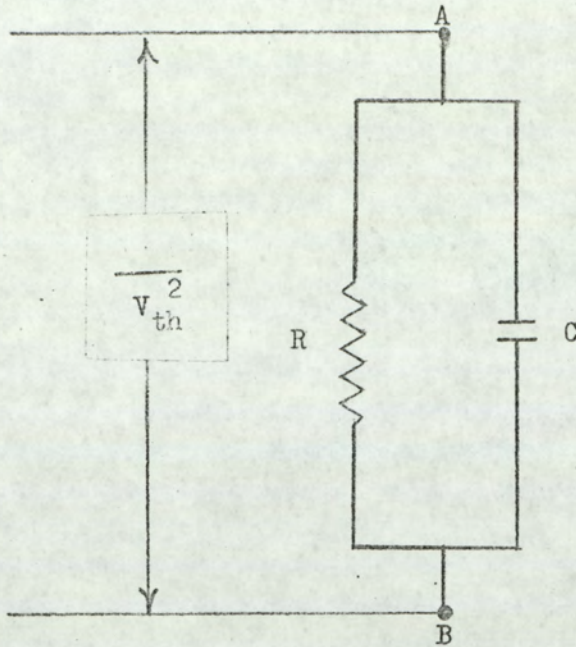


Fig.20. Resistance-Capacitance Noise Network.

$$\overline{V_{th}^2} = \frac{kT}{C} \dots\dots\dots (57)$$

and is therefore independent of the resistance R and does not favour any part of the frequency band.

Equation (56) is obtained from equation (57) when one wants to express noise in terms of elements of any frequency band.

In the field effect transistor therefore, the thermal agitation of carriers in the channel resistance can be regarded as a source of thermal noise. One can also think of the thermal agitation in the input circuit giving rise to thermal noise.

### Shot Noise.

Considering the electron or charge carrier as discrete, the current which depends on the number passing a barrier per unit time will be subjected to fluctuation as a result of inevitable instant to instant changes in the number of charge carriers. This effect will

not be confined to anode current in a valve as Schottky first observed, but wherever current flows in any device.

A derivation of shot noise voltage which explains the mechanism satisfactorily is given by Bull (42).

This derivation is, however, modelled on the controversial field-line theory. A derivation which makes the mechanism easily understood without recourse to field lines given by Bull in a post-graduate lecture course is presented:-

Consider the circuit shown in Fig.(21) in which electrons are flowing:-

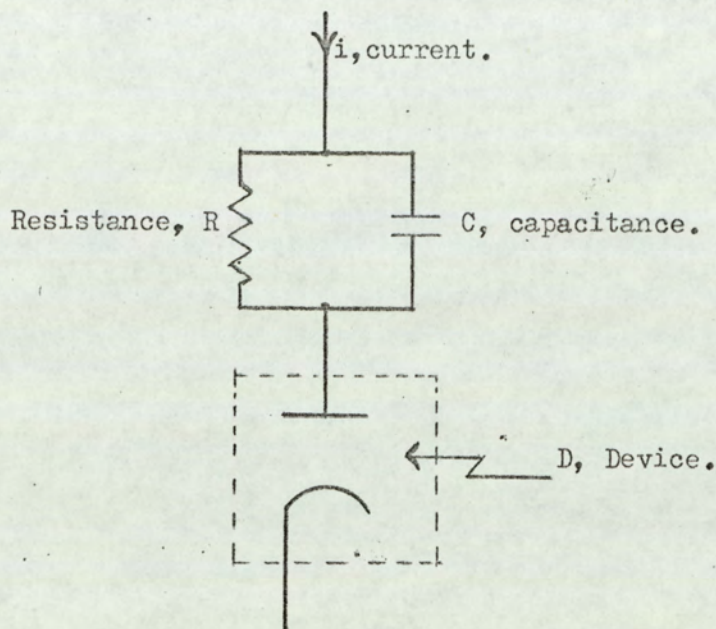


Fig.21. Circuit for derivation of Shot Noise  
In a charge-carrying device, D.

Let  $p$  electron charges be on the capacitor on the average.

If there is a residue number  $r$  due to fluctuation, the energy of the capacitor is given by

$$\frac{(p + r)^2 e^2}{2c} = \frac{p^2 e^2}{2c} + \frac{pre^2}{c} + \frac{r^2 e^2}{2c} \dots\dots\dots (58)$$

where  $e$  is the electronic charge

$r$  can have a positive or negative value and will

therefore have a mean of zero.

$$\text{i.e. } \bar{r} = 0 \dots\dots\dots (59)$$

The Average Energy  $\bar{E}$  of the capacitor is given by:-

$$\bar{E} = \frac{p^2 e^2}{2c} + \frac{e^2 \bar{r}^2}{2c} + \frac{pe^2 \bar{r}}{c} \dots\dots\dots (60)$$

substituting (59) in (60)

$$\bar{E} = \frac{p^2 e^2}{2c} + \frac{e^2 \bar{r}^2}{2c}$$

and the variance in  $r$ ,  $\sigma_r^2 = \overline{(r - \bar{r})^2} = \overline{r^2}$  for  $\bar{r} = 0$

$$\begin{aligned} \therefore \bar{E} &= \frac{p^2 e^2}{2c} + \frac{e^2 \sigma_r^2}{2c} \\ &= E_{av} + \delta E_{av} \dots\dots\dots (61) \end{aligned}$$

$\delta E_{av}$  is the average increase in energy per time constant  $\delta t$  say. This extra energy is dissipated in the resistor,  $R$ , by the noise voltage defined as  $V_{sh}$ .

$$\begin{aligned} \text{The average noise power } \frac{\delta E_a}{\delta t} &= \frac{V_{sh}^2}{R} \\ &= \frac{e^2 \sigma_r^2}{2c \delta t} \text{ from equation (61)} \end{aligned}$$

$$\text{total } \overline{V_{sh}^2} = \frac{e^2 \sigma_r^2}{2c \delta t} \dots\dots\dots (62)$$

Assuming a Poisson Distribution for  $n$  the number of charge carriers it can be shown that the variance

$$\sigma_r^2 = \bar{n} \dots\dots\dots (63)$$

substituting in (62)

$$\text{total } \overline{V_{sh}^2} = \frac{e^2 \bar{n} R}{\delta t \times 2c} \dots\dots\dots (64)$$

$$\text{the average current } i = \frac{\bar{n} e}{\delta t}$$

∴ equation (64) becomes

$$\text{total } \overline{V_{sh}^2} = e \frac{i R}{2c} \dots\dots\dots (65)$$

Equation (65) is the total mean square shot noise voltage given by Schottky (43).

Assuming that there is a mean square shot noise current,  $\overline{i_{sh}^2}$ , independent of frequency

$$\text{then } \overline{i_{sh}^2} = \overline{i_{sh}^2} \int_0^{\infty} |Z|^2 \delta f \dots\dots\dots (66)$$

where Z is the impedance of the R-C circuit (see Fig.21) at a frequency f.

$$\text{total } \overline{V_{sh}^2} = \frac{\overline{i_{sh}^2}}{2\pi} \int_0^{\infty} \frac{R^2}{1+\omega^2 c^2 R^2} \delta\omega = \frac{1}{4cR} \overline{i_{sh}^2} \dots (67)$$

from equations (65) and (67)

$$\overline{i_{sh}^2} = 2 e i / \text{unit bandwidth} \dots\dots\dots (68)$$

Equation (68) has been arrived at by assuming that the variance  $\sigma_r^2$  in equation (62) is that for a distribution with small probabilities, namely, the Poisson distribution. In actual measurement it is found that equation (68) is not strictly true, especially when there is space <sup>charge in</sup> ~~change~~ the system. This means that the variance  $\sigma_r^2$  is not strictly equal to  $\bar{n}$ .

This gives rise to a smoothing effect and equation (68) is modified to

$$i_{sh}^2 = \sqrt{}^2 2 e i / \text{unit bandwidth} \dots\dots\dots (69)$$

where  $\sqrt{}^2$  is the 'smoothing factor'

In his book Bull<sup>(42)</sup> using the theory of field lines and probability generating functions accounts for the smoothing factor from first principles without making assumptions of any special probability distributions.

It can be seen from equations (56) and (68) that the wider the bandwidth, the higher the value of the mean square noise. In the present system the bandwidth is narrow (<1KHz) and the current  $i \approx 300$  microamperes. The contribution of the frequency independent noise:, "white noise", to the total noise at the input stage is small.

#### Flicker Noise.

Johnson<sup>(44)</sup> reported that valves display a noise considerably greater than "shot noise" at low frequencies. Shottky<sup>(45)</sup> has explained this by saying that ions remain on the cathode for varying periods of time and thus the emission becomes erratic. Bull<sup>(42)(46)</sup> has stated that such effects have been observed in Resistors and semi-conductors as well and at frequencies hitherto considered to be too high for the effect to take place. He shows in<sup>(46)</sup> that space charge can be a source of the excess noise attributed to the flicker effect.

In semiconductors, however, the effect called "modulation noise" is said to originate from imperfections in crystal structure. It looks as if the phenomenon is not properly understood. This might not be due to the fact that the statistical theory for say "shot noise" derivation is wrong. It might be due to the experimental methods with which the theory is tested.

Equation (62) states that

$$\text{total } \overline{V_{sh}^2} = \frac{e^2 \sigma_r^2 R}{2c \delta t}$$

There does not seem to be anything wrong with this equation. Secondly, we can only measure the variation in number of charges flowing in unit time irrespective of the mechanism causing the variation

or fluctuation. The difficulties arise in the determination of the variance  $\sigma_r^2$ . It is possible that  $\sigma_r^2$  is quite complex and made up of components which depend on say temperature,  $\sigma_{rt}^2$ ; frequency,  $\sigma_{rf}^2$ ; current,  $\sigma_{ri}^2$ , etc.

$$\text{i.e. } \sigma_r^2 = \sigma_{rt}^2 + \sigma_{rf}^2 + \sigma_{ri}^2 + \dots \quad (70)$$

Since the statistics are only interested in the fluctuation from the mean and not how fast or slowly this takes place, the idea of temperature dependence or independence derived from it must only be to make it possible to make measurements which employ amplifiers of finite or limited bandwidth. The aim being to answer the question "How much noise theoretically can one have when working between frequencies  $F_1$  and  $F_2$ ?"

One then postulates a frequency independent current  $\overline{i_{sh}^2}$  and writes correctly

$$\text{total } \overline{V_{sh}^2} = \overline{i_{sh}^2} \int_0^{\infty} |Z|^2 \delta f$$

which is the same as for equation (67).

In trying to realise this equation in practice, what we do is

$$\overline{V_{sh}^2} = \overline{i_{sh}^2} \sum_{F_1}^{F_2} |Z|^2 \Delta f \dots \quad (71)$$

as we cannot have an infinitesimal  $\delta f$ .

It is as though we are sampling between  $F_1$  and  $F_2$  in a frequency domain with each data point separated from the next by  $\Delta f$ .  $\Delta f$  must therefore be quite small compared to the bandwidth,  $(F_2 - F_1)$  if an equation like (71) is to be used.

We therefore start with say a  $\Delta f$  of say 200Hz and draw part of the spectrum from mean frequency of say 5kHz and work our way down. We get to a mean frequency 200Hz and then cannot go further down because we cannot have a mean frequency of say 50Hz and use the same  $\Delta f$  which

we hope is our unit bandwidth.

It can be seen that we are not giving equal weighting to each point in the frequency spectrum because with the fixed "unit bandwidth" the  $Q$  of the measuring circuit, namely  $f_0/\Delta f$  is changing all the time as we move down the frequency spectrum. Secondly, if we were to have connected inductances directly to the output circuit of the device under test, as earlier workers like Johnson did, then in trying to get down to lower resonant frequencies by increasing capacitance we are altering the dynamic impedance of the circuit. Johnson's results would have been different if he had approached the lower frequency by keeping  $\frac{L}{C}$  of the detecting resonant circuit constant.

Bull (42-pp 158 of his book) states that "It is perfectly clear, but has never been remarked upon, that in order to reduce the mean frequency at which measurements are made it is essential to reduce the bandwidth".

The other problem facing one who wants to find out about noise at low frequencies ( $<500\text{Hz}$ ) is that observation time gets longer the lower in frequency one gets.

In view of these the following method of measurement is proposed:-

1. One should work with fixed percentage bandwidth in scanning the spectrum. This will make the  $Q$  of the measuring system constant and the effect of "ringing" in lightly damped circuits will be eliminated.
2. At any mean frequency with the constant  $Q$  a number,  $N$ , of samples should be taken with the sampling frequency satisfying the Nyquist sampling theorem, say 10 times the frequency of the upper half power frequency. This can be used to define the way one should move down the frequency spectrum.

3. The previous lower half power point frequency should be made the new upper half power point frequency and sampling at a rate 10 times this frequency should be made. This will take care of the difficulty with observation time as the mean frequency of measurement becomes smaller and smaller.
4. Analysis of the  $N$  samples taken from each frequency interval can be performed and the mean square voltage,  $\overline{V^2}$ , calculated.

With a scheme of this nature since each band is joined to the next one at its half power point, the overall measuring spectrum will be flat. (See expected total response curve Fig.22). It can then be used to check the frequency dependence or otherwise of the noise. Other elementary percentage bandwidths in a similar way can be chosen and similar spectral curves drawn for the same total frequency interval.

An example of the scheme for 100 percentage bandwidth extending down to 1 Hz is presented in Table 2 and Fig.22.

With a 100% bandwidth or  $Q = 1$  since the time constant of the circuit will be  $Q/f$ , this will cater for the necessary increase of observation time as one goes down the frequency spectrum.

For such a scheme active filters should be used for realising the elemental responses. The scheme is like that used in the Muirhead-Pametrada Wave Analyser D-489-E.

Finally, if one has two active sources for fluctuation such

TABLE 2 : ILLUSTRATION OF SCHEME FOR MEASURING NOISE TO LOW FREQUENCIES. 100% BANDWIDTH OR  $Q = 1$ .

Frequency band Hz		Sampling Frequency taking 100 samples
Lower half power point	Upper half power point	
729	2187	21.87 kHz
243	729	7.29 kHz
81	243	2.43 kHz
27	81	810 Hz
9	27	270 Hz
3	9	90 Hz
1	3	30 Hz
0.33	1	10 Hz

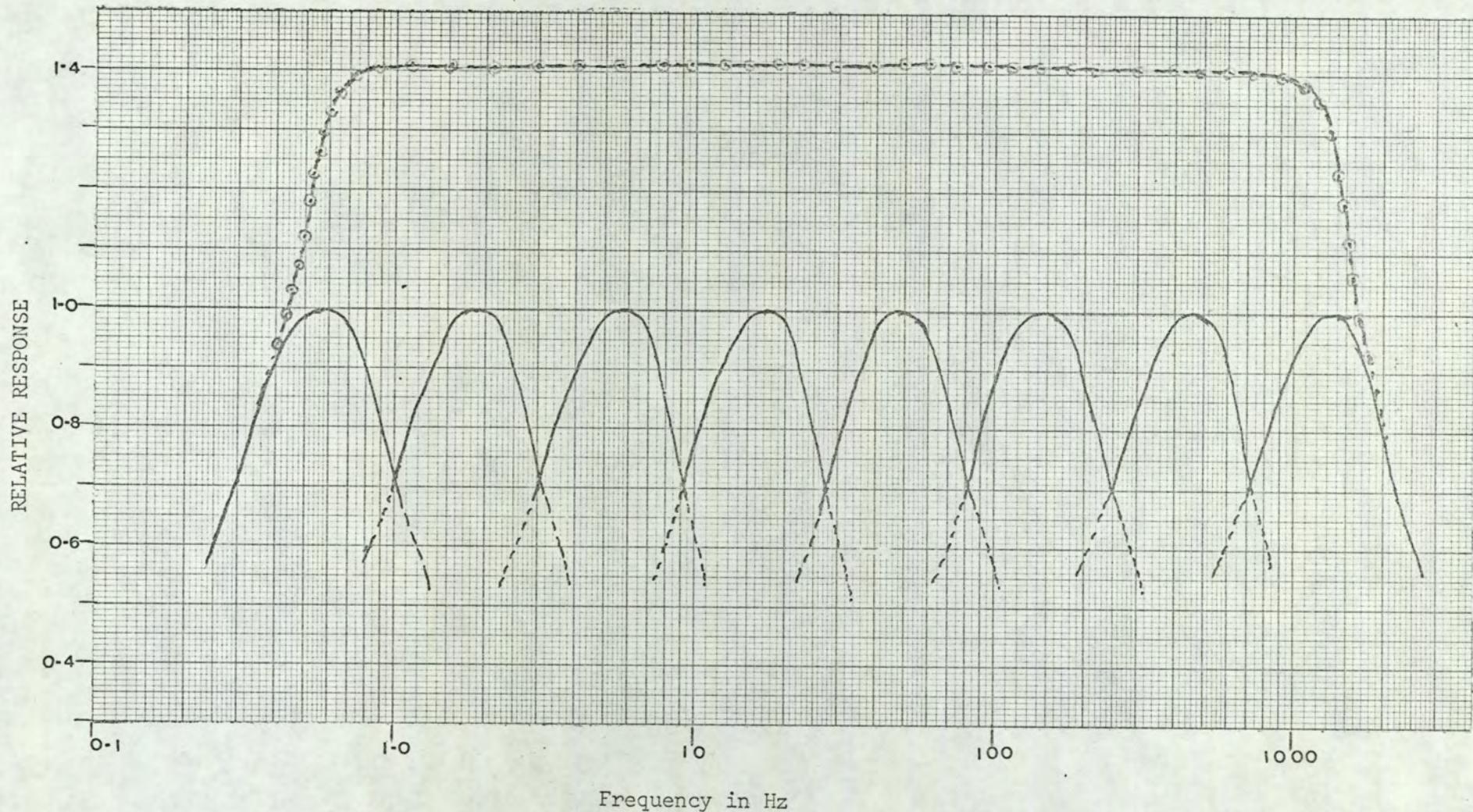


Fig 22. RESPONSE CURVES OF LOW FREQUENCY NOISE DETECTING SYSTEM (FOR SCHEME IN TABLE 2)

- Response Curves of Analysers
- Equivalent Total Response of a Detecting System comprising Analysers spaced logarithmically at eight frequency intervals

as 'shot noise' and 'thermal noise' and these span the whole frequency spectrum, it is possible that within any frequency band the voltages arising out of these sources of fluctuation will have frequencies,  $f_s$  and  $f_t$ , which are near each other. The sum of these voltages will therefore have peaks which will occur at their difference frequency,  $f_r - f_s$ . This will lead to a fluctuation occurring with a very low frequency. Could this be a possible source for "flicker noise"?

This can be checked by repeating measurements at low frequencies. Some such experiments might aid in the interpretation and analysis of noise into component, especially at low frequencies.

#### Noise due to signals or Excess noise:

There is a further source of noise attributed to the effect of signals. In other words increase in the inherent noise of a system when signal is applied. This is denoted as 'Excess noise'. Bull and Bozic<sup>(47)</sup> attribute this to changes in the characteristics of the device when signal is applied. In the present experiment this type of noise was not investigated as the differential signal of interest was in the microvolt region. It is possible, however, that in the presence of large common mode signals this type of noise might be manifested.

In the present system we are interested in recognising the foetal electro-cardiogram in the presence of noise and since the triggering mechanism used in analysers requires a fiducial point in the signal, the maximum peak of the intrinsic noise and not its mean square value was estimated.

The total inherent noise level was  $\approx 0.7\mu\text{V}$  peak to peak referred to the input in the frequency band from 1.2Hz to 130Hz. This noise level was found to be adequate as the estimated minimum foetal signal from abdominal recordings is  $\approx 5\mu\text{V}$  (R-wave).

### Other Sources of Noise:

Potentials from maternal abdominal muscles give rise to by far the greatest amount of noise other than that arising in the amplifying system. Since the heart itself is a muscle one would expect that the frequency spectra of both would be similar. This indicates that no filtering circuit can improve the signal to noise ratio appreciably. The only method seems to be to discriminate against unwanted myographic noise by having a high common mode rejection ratio. Thus myopotentials originating at points relatively distant from the detecting electrodes will have large in-phase components and hence their contribution will be reduced. The high common mode rejection ratio will also deal with interference arising out of external sources such as from the mains supply.

During initial tests since the main power of the electrocardiogram was thought to be centred around 20Hz, an active filter was constructed with a bandwidth of about 10Hz around 20Hz. This approach was found not to improve the signal to noise ratio. Not only did the signal "ring" but also with the low cut-off point at 15Hz the signal became unrecognisable. This phenomenon is discussed fully in the next chapter under "Presentation of Foetus".

In systems where the interest is the waveform and not the power of the signals, only the noise voltages which have frequencies near the frequency of the signal are those that mask the information. High frequency noise gives an electro-cardiogram the appearance shown in Fig. 23(a)

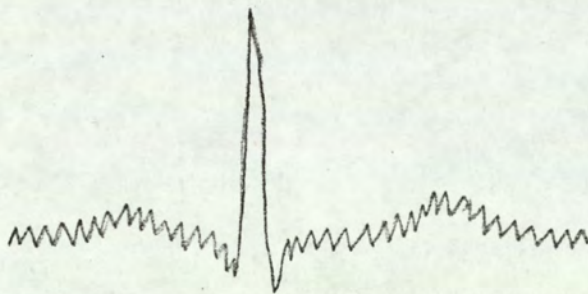


Fig.23 a.

The appearance of an electrocardiogram in the presence of noise at high frequency.

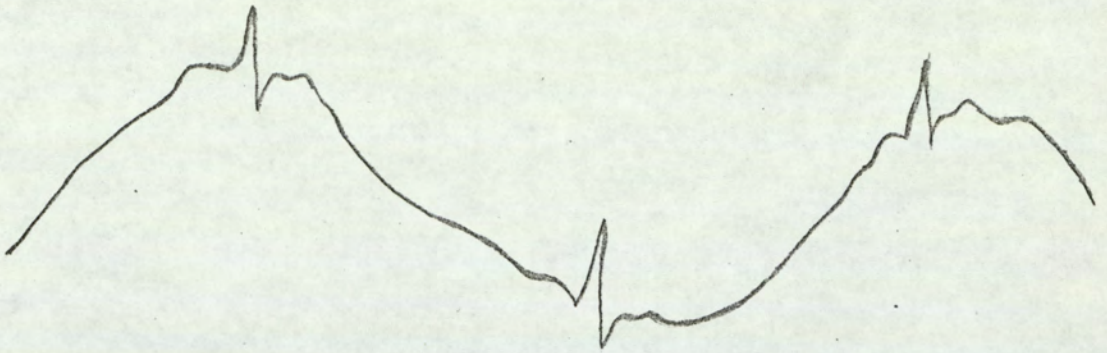


Fig.23b. Illustration of the effect of low frequency noise on the appearance of an electrocardiogram.

Noise frequencies lower than the signal frequencies alter only the base line and give the signal the appearance shown in Fig.23(b). Both of these can be dealt with using proper filtering or averaging techniques. One can conclude that it is the noise voltages which occur within the spectrum of the signal that mask it.

In concluding this section it can be said that the effect of inherent noise has been discussed because its level sets the limit to the electrophysiological potentials that can be detected after one has been able to remove the other source of noise. Interference from mains supply in the present system was not detectable as the records to be shown later indicate.

DETECTING ELECTRODES.

The choice of electrodes for detecting bio-potentials is very important. Its importance arises from the fact that the body is a volume conductor and the conducting material are the body electrolytes which constitute and bathe the tissues. The main electrolytes are sodium and potassium chlorides. Contact between a metallic electrode and the electrolytes leads to local dissociation which results in the formation of electrochemical cells, which have e.m.f.s and are also polarised.

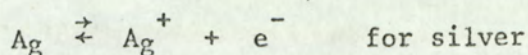
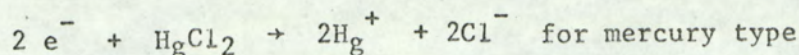
The extent of this polarisation can be inferred from the fact that Roy and Wehnert<sup>(48)</sup> have used the phenomenon to provide a battery to power an implantable cardiac pacemaker. They tried different anodic and cathodic materials and got the following results shown in Table 2.

Table 2 : GALVANIC CELL MEASUREMENTS (SALINE SOLUTION)

Cathode Material	Anode Material	Voltage (volts)	Anodic material loss (milligram/year)
Platinum Black	Zinc	0.9 → 1.0	550
"	Iron	0.5 → 0.6	468
"	Mild Steel	0.5 → 0.6	468
Silver	Zinc	0.8 → 0.9	550
Silver Chloride	Zinc	1.0 → 1.1	550

The usual method employed in electrophysiology (Roy and Wehnert) to avoid this contact potential, especially when recording down to d-c potential is, to use "non-polarisable electrodes". Usually such electrodes take the form of metallic mercury covered by a layer of calomel ( $H_2Cl_2$ ) or Silver Chloride ( $AgCl$ ). During measurement they are connected to the tissue by an agar bridge or an 'electrode paste' containing potassium or sodium chloride.

Used as a cathode the following reaction takes place:-



$\text{Hg}^{+}$  and  $\text{Ag}^{+}$  ions are exuded from the solution due to the low solubility of  $\text{HgCl}_2$  and high concentration of chloride ( $\text{Cl}^{-}$ ) ions. The reverse reaction takes place when used as an anode. The chloride ions in the  $\text{KCl}$  and  $\text{NaCl}$  swamp the fluctuation in chloride ( $\text{Cl}^{-}$ ) taking place.

The silver-silver chloride electrode is the easier to construct and therefore used more generally. Silver is electrochemically plated using 1.0 Normal hydrogen chloride ( $\text{HCl}$ ) as electrolyte. The electrode must be protected from light and friction. Therefore they must be kept in a solution of 0.9%  $\text{NaCl}$  preferably in the dark.

Polarisation depends on the ease with which an electrode material ionises in electrolyte solution. Carbon in the form of pure graphite, although a good conductor, does not ionise when in contact with a solution of even some of the strongest acids. It is low in the electrochemical series.

It was therefore thought that graphite could be a good non-polarisable detecting electrode material once it has been cleaned properly.

Graphite can now be produced in many forms, cloth, felt and blocks, and therefore can have very wide applications in electrophysiology.

In the present experiment graphite electrodes were constructed from solid graphite blocks (the type used as moderators in nuclear physics), and also from graphite cloth. Fig.24(a) and (b) show the

construction of the electrodes:-

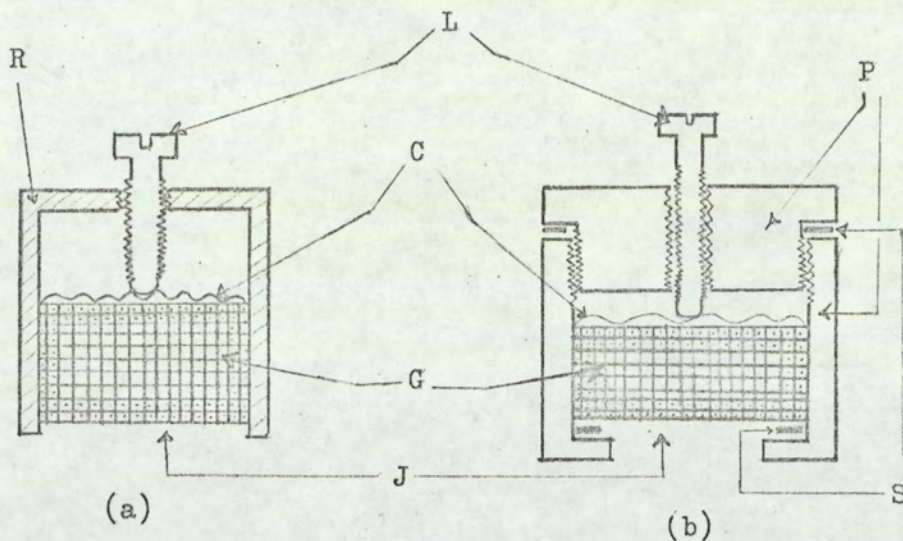


Fig.24.

CONSTRUCTION OF GRAPHITE BLOCK ELECTRODES.

R = Ebonite, L = metallic screw Lead, C = Corrugated metallic contact,  
G = Graphite cylinder ( cleaned ), J = recess for electrode Jelly,  
P = Perspex, S = rubber Spacer.

Both electrodes in Fig.24 are similar but the one in Fig.24(b) has the advantage that the graphite can be removed for cleaning if this became necessary.

Graphite is an abrasive material and it is known that during manufacture and machining it will retain films and particles of metal. The graphite electrode cylinders were therefore subjected to the following rather drastic treatment before they were used:-

1. Immersion in concentrated nitric acid overnight.
2. Boiling in distilled water.
3. Heating up in an oven.

After this treatment, it did not blacken the skin or other materials appreciably.

The best method for attaching such an electrode to the skin is by the use of a Beckman electrode polythene disc which is adhesive on both sides after filling the recess Fig.(24) with electrode jelly. 'Redox' electrode paste was found to be suitable. The electrode

system in this form can be used for recording electro-cardiograms from adults. With the provision of a groove for a rubber band (netting) to hold it down on the head it can be used for electro-<sup>c</sup>en<sup>^</sup>cephalography.

The graphite electrodes found to be best suited for foetal electro-cardiographic recordings from the maternal abdominal wall were, however, constructed from graphite cloth. (See Appendix II for a specimen).

Fig.25 shows the construction of the electrode from the cloth:-

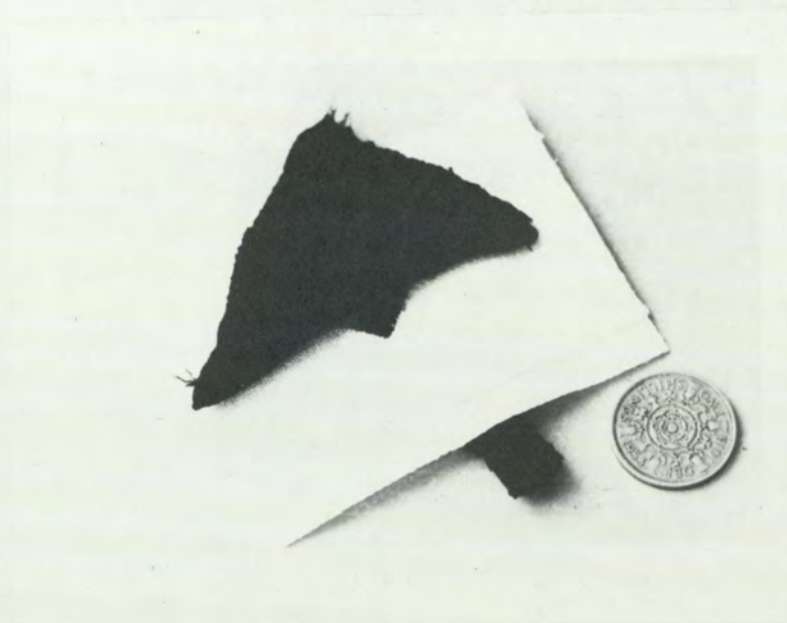


Fig.25. Shows the arrangement of the Graphite electrode and the 'Variband' support.

The graphite cloth is doubled up to make an isos<sup>e</sup>cles triangle and sewn with nylon thread (to withstand severe initial acid treatment). A doubled up tape is made and sewn on to the triangle making sure that the two graphite cloth surfaces (tape and triangle) are in good contact. After sewing the cloth electrode is dipped in concentrated nitric acid and rinsed in boiling distilled water.

It was found that washing in water with detergent or soap then made it so clean that it did not blacken the skin appreciably. It is then dried.

In this form the electrode was found to be very satisfactory.

The main advantage is that the material is soft and therefore follows the contours of the human skin, producing very good contact with the electrode jelly so that artifacts arising from stretching and bending on account of material movement were kept to a level smaller than with metallic electrodes.

In use a slit was made in a "variband" cloth through which the leading tape connecting the <sup>~</sup>triangular electrode was passed.

The maternal abdominal skin was washed with soap and water and Redox paste was rubbed into the area of interest. More paste was smeared on to the exposed side of the graphite triangle. It was finally secured on the abdomen with two tapes of plaster. Three such electrodes were needed. The protruding ends of the graphite tapes were connected by small crocodile clipped leads to the input of the detecting amplifier. Fig.26 shows a photograph of the electrodes in place as described:-

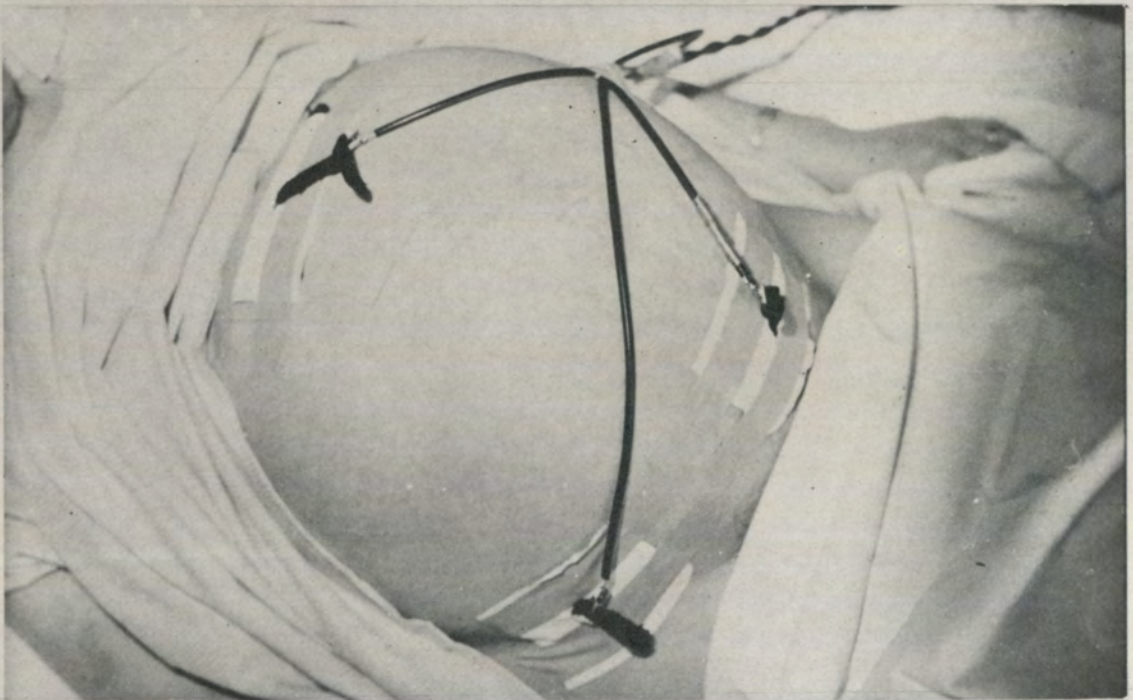


Fig.26. Connection of the cloth electrodes to the mother.

In an earlier work by Goddard et al<sup>(20)</sup> a scheme to reduce interference of the foetal signal by myopotentials from neighbouring

muscles was used. Eleven pairs of electrodes disposed as shown in

Fig.27 were attached to the maternal abdomen:-

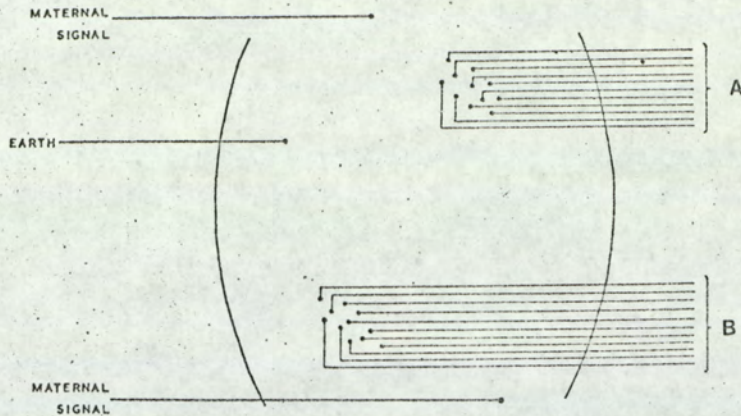


Fig.27. Arrangement of electrodes on abdomen in a scheme to improve the signal-to-noise ratio. (Goddard, et al.)<sup>20</sup>

A pair consisting of one lead from A and one from B was connected to one differential pre-amplifier (11 pre-amplifiers all together) and the outputs of the pre-amplifiers summed. Statistically, one would expect the disturbance to be reduced approximately by  $\sqrt{N}$ , N being the number of pairs of electrodes, in this case the expected improvement of signal to noise ratio was  $\sqrt{11}$ .

In the present system it was felt that the same effect would be obtained by doing the summing on the abdomen by having large electrodes (preferably having an area that of the total small ones) and an amplifier with high common mode rejection ratio.

It is here that advantage is gained in the use of the cloth electrode. The graphite cloth can be made any size and easily made to follow the body contours when in contact with the skin.

In the present experiment, therefore, three larger electrodes were used. One could envisage that in this case the improvement of

signal to noise ratio would be proportional to  $\sqrt{A}$ , A being the electrode area touching the abdomen.

A further matter of interest in the use of graphite electrode for detecting potentials arising out of organs in biological systems was provoked by the phenomenon of voltage fluctuations which take place at metal-electrolyte interfaces. Flasterstein<sup>(49)</sup> reviews previous work and describes this phenomenon as having polarisation effects and noise of electrochemical, electromechanical and thermal origins. He gives examples of these unpredictable voltages using a system of electrodes immersed in small glass containers of electrolytes. Their amplitudes range up to hundreds of microvolts and their frequencies overlap the physiological spectrum from d.c. upwards and are therefore difficult to filter out. The behaviour of open-circuited electrodes in solutions is affected by electrochemical corrosion.

Since carbon in the pure state would not suffer such electrochemical corrosion to any degree, it was felt that it will not produce such electrochemical artifacts. It must also be mentioned that since carbon is abrasive other metals with which it comes into contact during manufacture or its history can be occluded on it and initial drastic cleaning such as previously outlined is necessary.

In a trial with gold electrodes and fairly clean graphite electrodes it was found that when electrolyte, e.g. electrode jelly, was sandwiched between two such similar electrodes (gold-electrolyte-gold, graphite-electrolyte-graphite), shown in Fig.28, they both showed polarisation. On shorting terminals a and b (Fig.28) for some time and opening, it was found that the polarisation voltage on the gold system decreased to a small value and recovered to its original level, whilst that of the graphite system did not recover. It was

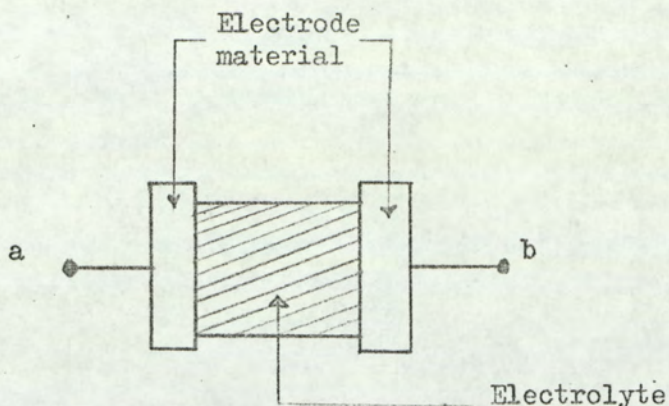


Fig.28.

Set-up for studying Polarisation effects  
at Electrode-Electrolyte interfaces.

also found that clapping one's hands produced far more effect on the gold system than on the graphite system. Secondly, the gold system seemed to be sensitive to mains hum pick-up. This behaviour has not been studied exhaustively and a more detailed study is called for. It can, however, be concluded that on account of its electrolytic inactivity, the contribution to the production of this type of artifact by the electrode material alone would be less for carbon (graphite) free from occluded metals.

In the measurements taken with the graphite electrodes described, very satisfactory results were obtained. It was found that gentle washing with soap and running tap water after a reading has been taken, was enough to clean the electrodes once the initial drastic cleaning had been carried out. A recording was made throughout labour using the abdominal graphite electrodes and with the mother's leg folded up. The only precaution was that the thigh should not touch the metallic crocodile clips used. These were covered with further strips of plaster. Apart from periods when the

mother was turned over, and periods when the Sister shouted "You are a good girl just give us another big push" with consequent increase in myopotentials, the foetal signal could be seen clearly.

#### INPUT IMPEDANCE OF DETECTING SYSTEM.

The source resistance of the foetal signal depends on the resistance of the tissues of both the foetus and mother intervening between the foetal heart and the electrodes, and to a greater extent on the condition of the maternal abdominal skin surface. The body being a volume conductor the resistance of the intervening tissues is small in comparison with the skin resistance. It is this surface resistance which is reduced by the use of the electrode jelly which permeates into the pores of the skin thus producing good contact with the internal tissues.

During breathing, however, it is expected that the intervening tissues will produce cyclical impedance changes correlated to the expansion and contraction. The detecting amplifier should have high input impedance so that these changes would not produce appreciable modulation of the amplitude of the detected signal.

Van Bommel<sup>(50)</sup> gives the abdominally recorded signal,  $a(t)$

as

$$a(t) = r(t) \left\{ m(t) + f(t) + n(t) \right\} \dots\dots\dots (72)$$

where  $m(t)$  is the component from the maternal heart

$f(t)$  is the contribution from the foetal E.C.G.

$n(t)$  is the additive noise components, mainly consisting of "muscle noise" electromyogram.

$r(t)$  is a multiplicative component especially due to movement e.g. respiration.

If  $r(t)$  is written as  $\{1 + g(t)\}$  where  $g(t)$  is the movement factor then it is felt that  $g(t)$  can be drastically reduced by using carbon cloth electrode which will keep the same contact area during movement of the

abdominal wall and produce less polarisation changes and by having high input impedance of the detecting amplifier.

In the present experiments, the differential input resistance was set at 20 megohm. For other applications which necessitate higher input impedance this could be increased to the input impedance of the field effect transistor used  $\sim 10^{10} \Omega$ .

To summarise on this chapter, a stable, high gain amplifier has been designed to have

- (a) High common mode rejection ratio.
- (b) Low noise.
- (c) High input impedance.
- (d) A suitable electrode system using graphite as electrode element has been tested and used successfully.

The importance of these topics in detecting foetal electrocardiograms in particular, and electro-physiological potentials in general, have also been discussed.

CHAPTER II

PROCESSING THE FOETAL ELECTROCARDIOGRAM

OBTAINED WITH ABDOMINAL ELECTRODES.

## CHAPTER II

PROCESSING THE FOETAL ELECTRO-CARDIOGRAM OBTAINED WITH ABDOMINAL ELECTRODES.

Fig.29 shows an oscillogram of a typical signal obtained at the output of the present detecting system.

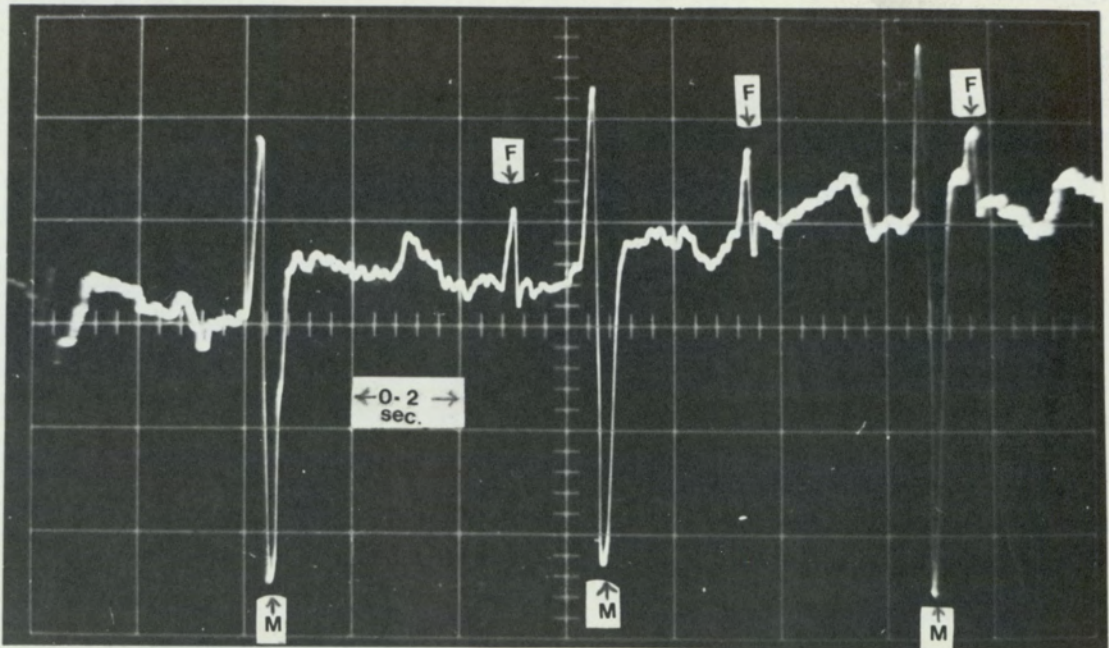


Fig.29. Oscillogram of Detected Signal. F=Foetal, M=Maternal.

The choice of a method for processing such a signal is dictated by the type of information one wants to extract from it for analysis.

Such information as far as the foetal part of the signal is concerned can be classified under two main headings:-

- A. The rate at which the foetal heart beats.
- B. The waveform of the foetal electro-cardiogram.

#### A : FOETAL HEART RATE

Sanctorius of Padua (1561 - 1636)<sup>(51)</sup> was the first to recognise the importance of the human pulse rate as a diagnostic tool. Before the invention of the stop watch Galileo (his classmate) and astronomers

like Kepler used the pulse beat as time reference. Galileo found that the period of oscillation of a pendulum depends on its length. Sanctorius used this idea to make the PULSILOGIUM:- He varied the length of a Galilean pendulum until the period of oscillation coincided with the beat of the heart and measured the length of the pendulum. Thus he correlated the different lengths with the state of his patients.

Since then the heart rate has been used as a diagnostic tool.

In the foetus the rate is about 140 beats per minute on the average. It has been found that during foetal stress the rate drops. The period after a contraction in labour when a drop occurs in the foetal heart rate is used for classifying the source of the distress.

It is therefore important that there should be continuous monitoring of the foetal heart rate.

Shelley<sup>(16)</sup> has outlined and discussed the various methods for foetal heart monitoring. These include the use of phonocardiograms and doppler tone detectors.

It can be seen from the signal picked up from the maternal abdomen (Fig.29) that one can take periodic records on an ordinary electro-cardiograph after amplification of the signal by the pre-amplifier and, knowing the chart speed, calculate the foetal heart rate. There are aids to calculation known as cursors to calculate the rate. One can also read the time interval between two complexes off an oscilloscope.

Suppose the oscilloscope time base is 0.2 sec/division and N is the number of divisions between two foetal signals

The period T is therefore 0.2 x N sec.

$$\begin{aligned} \therefore \text{The foetal rate } \frac{1}{T} &= \frac{60}{0.2 \times N} \\ &= \frac{300}{N} \text{ beats/min} \dots\dots\dots (73) \end{aligned}$$

In this example the heart rate is divided by the number of oscilloscope divisions between two complexes. A table was made for heart beats ranging from 50, ( $N = 6$ ), to 200, ( $N = 1.5$ ), beats per minute, so that the Sisters in the Maternity ward could read the rate (both foetal and maternal) off an oscilloscope.

These two methods would only give spot measures of the heart rate.

It can be seen from Fig.29 that the only way that continuous record of the foetal heart rate can be obtained from such a signal is first to remove the rather larger maternal complex and trigger a pulse interval counter with the resulting signal.

It is the technical difficulty of cancelling the maternal signal which has led some workers into the use of wire electrodes and other forms of direct electrodes, including trans-abdominal ones, to the foetal scalp or the presenting part. These methods have been reviewed in the introduction to this thesis.

I. A method of eliminating the maternal complex is to record a maternal complex free of foetal complex taken from another part of the body and subtract this from a signal like Fig.29 using analogue methods. Gureau and Trocellier<sup>S</sup>(17)(18) pioneered in this method.

Walden and Birnbaum<sup>(19)</sup> used suction electrodes in a scheme shown in Fig.30.

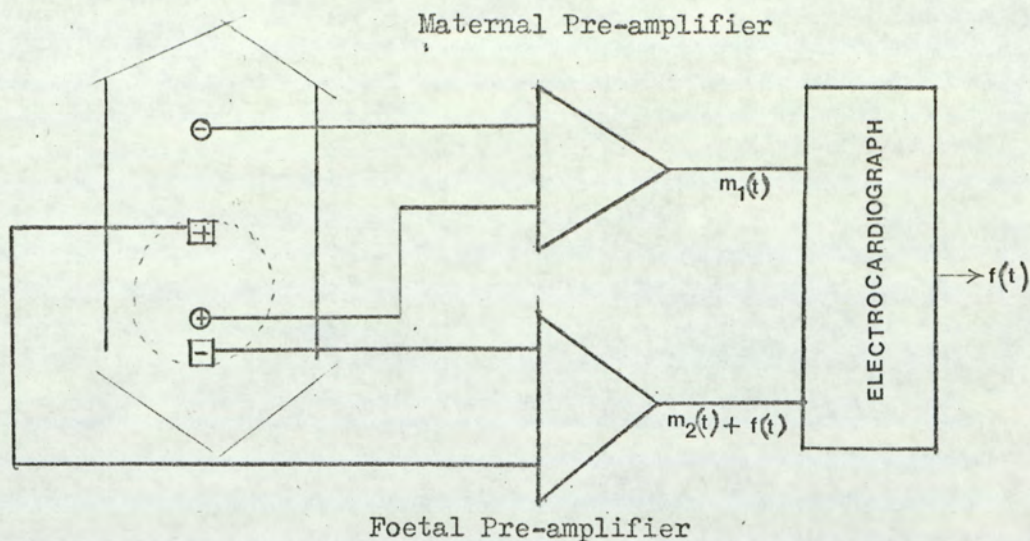


Fig.30. Method for Eliminating the Maternal Complex used by Walden and Birnbaum<sup>19</sup>.

This method depends on the maternal signal,  $m_1(t)$ , having the same form phase (or antiphase) and amplitude as the maternal complex in the total signal  $m_2(t) + f(t)$ .

Since the body is a volume conductor this means that the points which  $m_1(t)$  and  $m_2(t)$  are picked up must ideally lie on an equipotential. Secondly the maternal and foetal pre-amplifiers should have the same response characteristics. If these two conditions are not satisfied there will be a residual maternal complex whose amplitude should not be larger than the maximum foetal complex for triggering a ratemeter. Difficulties with the method are concerned with satisfying this condition by trial and error.

. In a system where two pre-amplifiers are not needed, Sureau and Trocellier<sup>(18)</sup> devised a method where the subtraction of the maternal complex is performed before amplification. Here the midline is chosen as being not far from an equipotential and by a potentiometric method voltages are chosen from fixed points straddling the midline for subtraction.

What could be a source of disadvantage is that once one moves away from the midline, one must search for a maternal complex for cancellation.

Fig.(31) is reproduced from Sureau's paper.

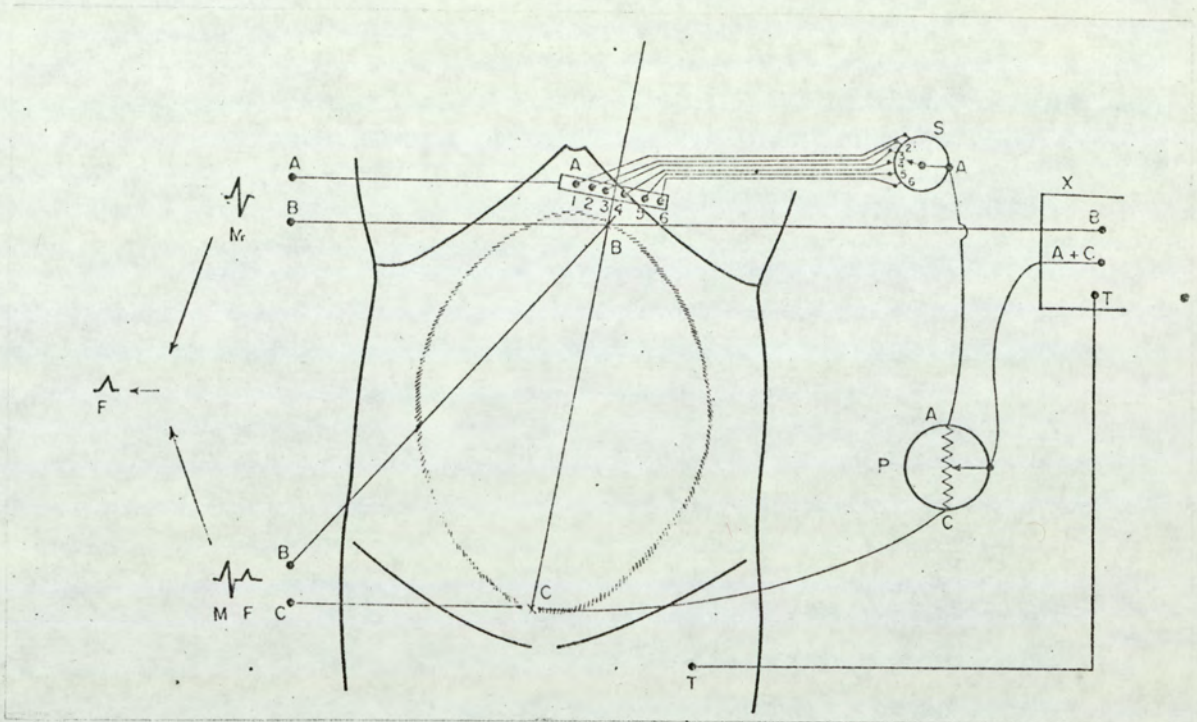


Fig. 31. Method used by Sureau et al. for eliminating the maternal Complex.

These methods have been used by many workers for measuring the foetal heart rate.

II. A second method for eliminating the maternal complex is to "blank it out". This is done by using a point in the maternal complex preferably the R-wave to trigger a gate through which a delayed version of the original signal passes. The method has been used by Kendall, Farell and Kane<sup>(52)</sup> and also by Goddard et al.<sup>(20)</sup>

Schematically the system is as illustrated in Fig.32

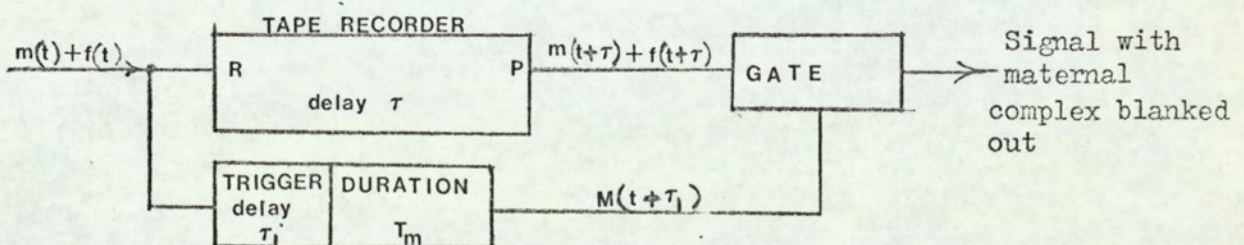


Fig. 32a. Schematic diagram of system for blanking out the maternal complex.

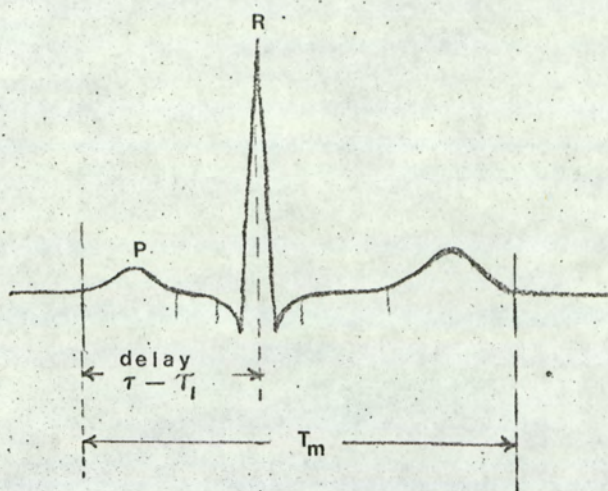


Fig. 32b. Timming for blanking out the maternal complex.

Since the time interval between successive R-waves in the electrocardiogram is not strictly constant, one cannot use a system where the triggering is done on a preceding R-wave. A typical complex to be blanked out is shown in Fig.32(b).

The gate is triggered with the peak of the R-wave as the fiducial point and the period during which the gate is closed should start at such a time that the beginning of the P-wave and the R-wave is equal to  $(\tau - \tau_1)$ .

The delay time is provided by the tape recorder. It is the time it takes a point on the tape to travel between the recording head and the playback head.  $\tau_1$  is a variable delay provided in the trigger circuit. This variable delay is needed because once the tape speed is chosen  $\tau$  is fixed.  $\tau_1$  is then varied to make  $(\tau - \tau_1)$  variable for different subjects.

This method was used in the present experiment and will be discussed in more detail later.

If one makes the duration of the blanking pulse short enough so that only the maternal QRS complex (the larger portions) are blanked out, the foetal signal could be used for triggering a rate meter. However, since the foetal and maternal heart-beats are not correlated, all foetal complexes which coincide with the maternal QRS will also be blanked out. A rate-meter will therefore not give a steady reading. If it is a pulse interval meter it will periodically indicate twice the expected pulse interval.

In the present system, however, the waveform and its properties were to be studied and not much time was spent over measurement of rate.

A scheme for a further method for eliminating the maternal complex using digital computer averaging will be put forward and discussed later in the thesis.

#### B : WAVEFORM OF THE FOETAL ELECTRO-CARDIOGRAM

The raw signal shown in Fig.29 has diagnostic value. It can be used to give information on:

- a) Foetal life.
- b) Presentation.
- c) Multiple pregnancies.

##### a) Testing for foetal life.

Foetal electro-cardiography has been used for confirming that the foetus is alive. However, if a record does not show any foetal complexes one does not conclude that there is no foetal life. It is possible that the electrode position is not suitable for picking up the signal. A positive signal, however, is a sure sign that the foetus is alive. An x-ray can show the presence of a foetus but until some pathological changes like the collapse of cranial structures are apparent, it cannot confirm foetal life *or death.*

b) Presentation of Foetus.

Foa<sup>(2)</sup>, as stated in the introduction, was the first to attach importance to the direction of the foetal R-wave in relation to maternal R-wave as a means of telling which way the foetus is orientated in the uterus. When the foetus is large, however, obstetricians use palpation or feeling the maternal abdomen to check for presentation.

It has been established by palpation, x-rays and simultaneous recording of the foetal electro-cardiogram with direct and abdominal electrodes<sup>(53)</sup> have shown that if a midline electrode system is employed and the foetal R-wave in a record such as shown in Fig.29 points away from the maternal R-wave, then the two bodies are orientated in opposite sense and the foetus is in the vertex or 'normal' presentation. The reverse holds for when the foetus is coming out leg first or is in Breech presentation. Workers, including Lark, Bernstein and Sureau, have however found some instances when this <sup>rule</sup> ~~rate~~ has not applied.

An investigation was therefore carried out in this experiment to find out more about the reasons for such exceptions.

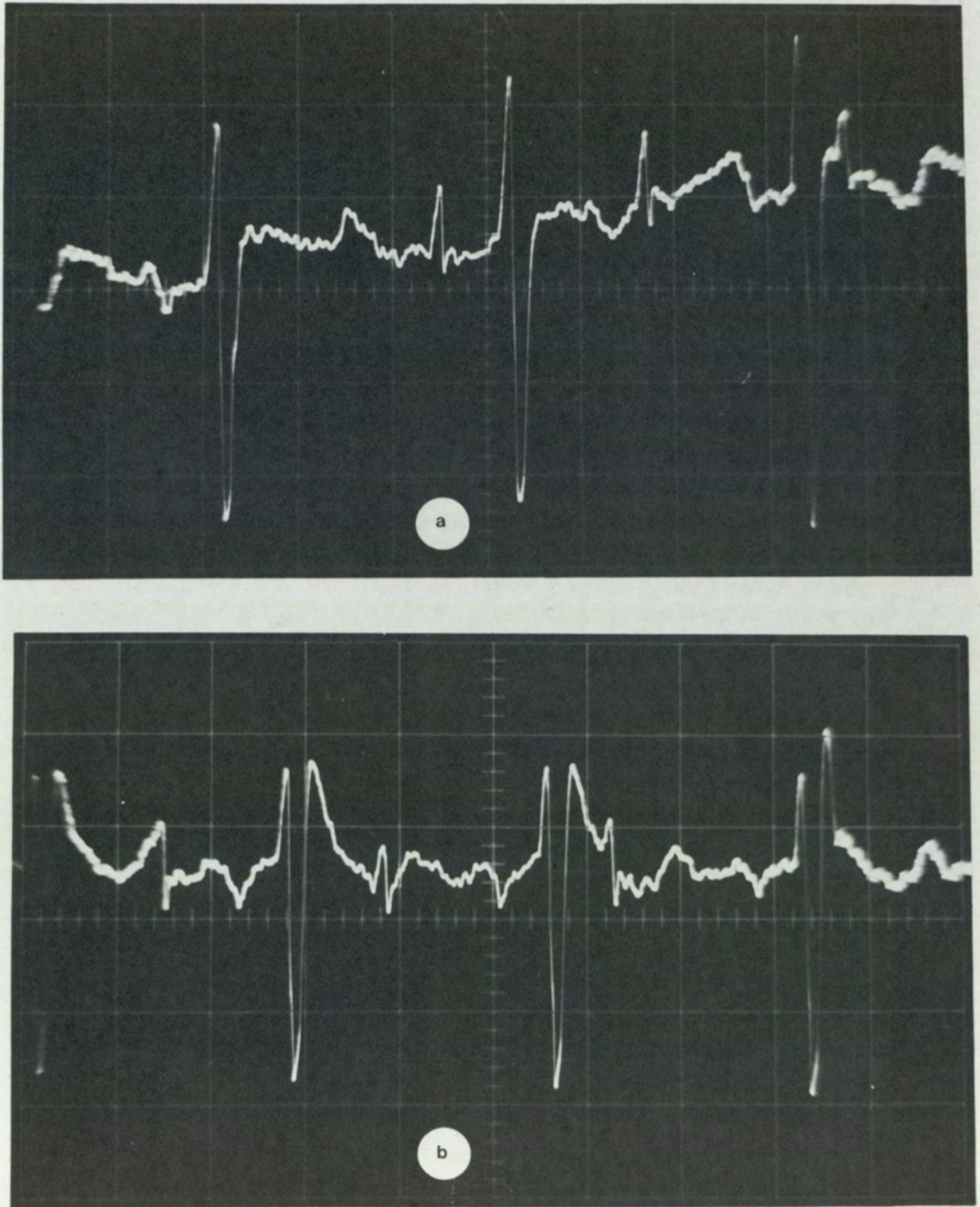
Effect of Low Frequency cut-off point on Waveform.

Fig. 33. Oscillograms to illustrate the effect of low-frequency cut-off point on the waveform of the detected signal.

Fig.33(a) and (b) are oscillograms obtained from the same electrocardiographic signals. The only difference between the traces in 33(a) and 33(b) is that in 33(b) the signal had been passed through a differentiating network of which the cut-off frequency was higher

than that used in 33(a). This record was taken with the detecting electrode in the midline position. The degree of differentiation can be inferred from the relationship of the inverted maternal Q and S waves. In 33(a) the S-wave is lower than the Q-wave. The rising base line from left to right shows that there is not much differentiation and the slow potentials originating as a result of maternal breathing are getting through. The foetal R-wave is clearly seen pointing (upwards) from the maternal wave (downwards). In Fig.33(b) the maternal S-wave is now level with the Q-wave as a result of the differentiation which has also flattened the base line. It can be seen now that the foetal signal is now bi-phasic and the foetal R-wave is almost as far up as the foetal Q-wave is down.

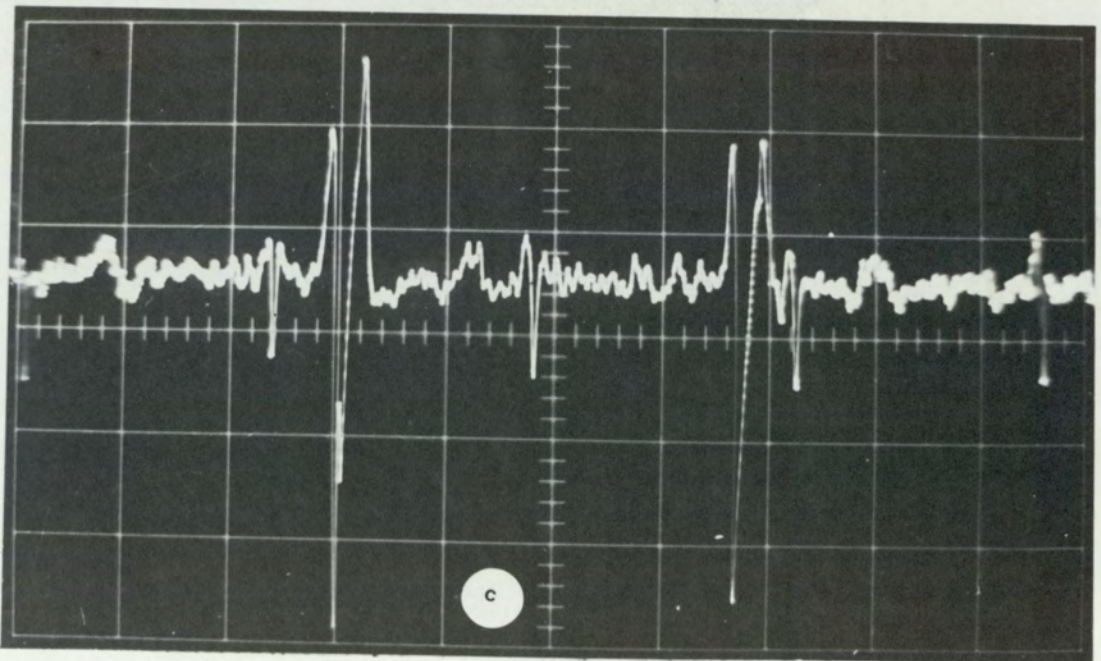


Fig.33c. Inversion of the foetal complex with further differentiation.

Fig.33(c) shows the effect of further differentiation. The maternal S-wave is now far above the maternal Q-wave and the foetal complex looks as if the R-wave is pointing downwards. Also it can be seen now that most of the slow waves in the signal have been removed. Using fig.33(a) one would say the presentation is Vertex or Normal. Using the same signal differentiated as in Fig.33(c)

one would say that the two "R-waves" (maternal and foetal) were pointing downwards, this suggesting breech presentation. Usually a flat baseline is regarded as being desirable, but it can be seen that in trying to obtain a flat baseline by cutting out the slow voltages in the signal, one can confuse or destroy completely information, such as that about presentation.

Fig.34(a), (b), (c) and (d) show a similar series obtained from an electro-cardiographic signal suggesting breech presentation in 34(a) and which, with successive differentiation, leads one to the mistaken diagnosis of normal or vertex presentation with Fig.34(c) and (d).

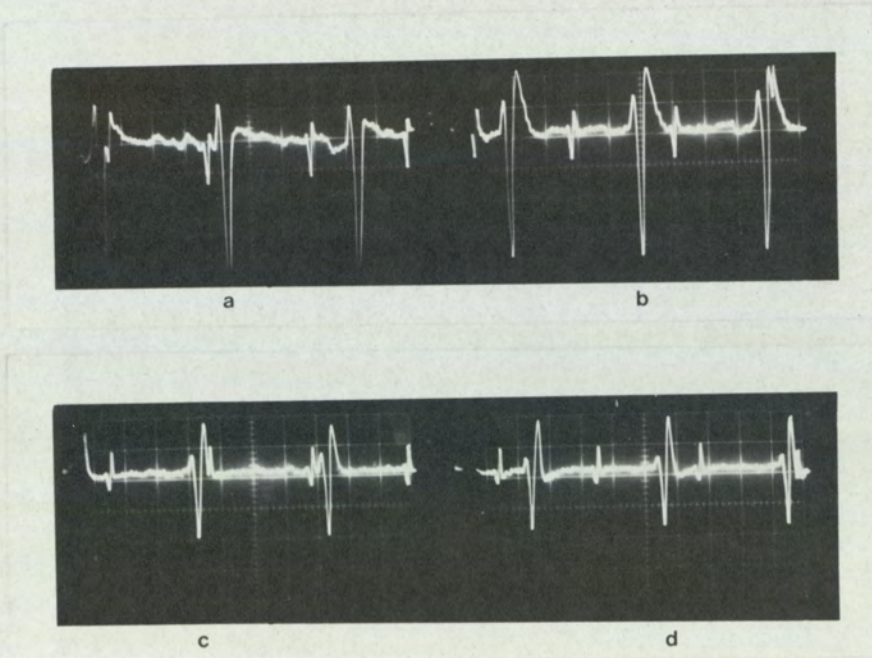


Fig.34. Inversion of the foetal signal (Breech presentation) as a result of differentiation of the signal.

The foregoing indicates that errors in the diagnosis of presentation using foetal electro-cardiography might have arisen from distortion of the signal produced by the detecting system. It was found that this inversion of the foetal waveform with severe differentiation of the signal occurred at different low cut-off frequencies for different electro-cardiograms. All, however, would have turned upside down by the time the cut-off point has been raised

to 15Hz.

It is thought that except in cases, if these exist, where the heart is actually placed upside down in the foetus, the rule that a foetal R-wave pointing away from a maternal R-wave (midline configuration) represents normal or vertex presentation therefore always holds.

In view of the above, it is thought that the rule concerning the orientation of the foetal waveform with respect to the maternal waveform could be extended to deal with cases in which readings taken with electrode configuration other than from the midline can be analysed.

Suppose we used a midline electrode configuration and labelled the electrode connected to the pubis RED and that connected to the top of the fundus BLACK and kept to this by making sure that the appropriate lead is correctly plugged into the detecting amplifier, then when the R-wave points upwards on our record we could conclude that this represents 'normal' presentation. We could translate this as pointing towards the BLACK lead (assuming the mother was standing upright).

If now we have a foetus in lateral position, although from a given record the foetal R-wave may point away from the maternal R-wave when we have used a configuration as shown in Fig.35, we cannot say that it represents a normal presentation. What we can say is that the foetal R-wave points towards the BLACK lead. With a small diagram on the record showing the electrode position (as is done in electro-encephalography) we could say which way the foetus is orientated.

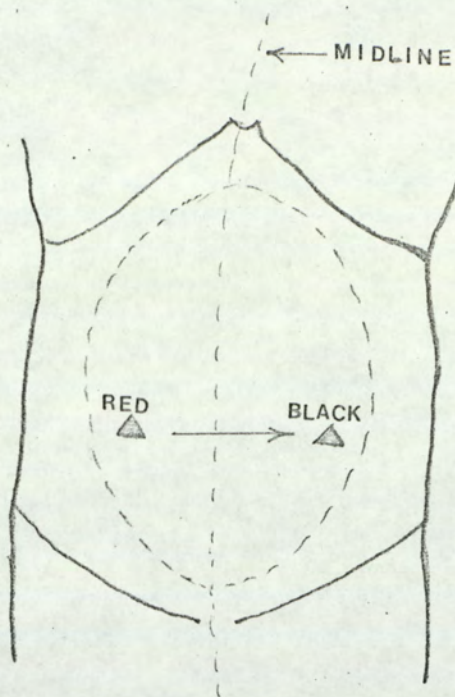


Fig.35. Standardisation for the diagnosis of foetal Presentation (see text).

In other words, we should relate the orientation of the foetus to our fixed electrodes and only use the direction of the maternal complex to check whether we have plugged the leads into the detector correctly.

A tentative explanation for the inversion of the waveform with differentiation is that the rise from Q to R is slower than from R to S in the electro-cardiogram and therefore the magnitude of the time derivative of the signal will be bigger for the R - S section than for the Q - R section.

The frequency at which the low frequency cut-off point is set in the detecting system becomes even more important when information concerning the waveform of the electro-cardiogram is sought, as one does not wish to confuse a differential S-wave with an upturned R-wave.

In this experiment, therefore, a compromise was made and the low frequency cut-off point was set at about 1.3Hz. At this setting one can still have some slow 'breathing' voltages and still maintain information about presentation.

It was found that passing the signal through an integrating network had the reverse effect in that it made the S-wave move towards

the base line and enhance the R-wave. It was also found that the nearer the foetus was to the surface of the maternal abdomen the more differentiated the foetal waveform appears. This might be due to a property of the tissues of the conducting medium between the foetal heart and the surface. This is discussed further after the section on computer averaging of the foetal complex.

It is concluded here that with proper labelling of electrode configurations and proper manipulation of the waveform with differentiating and integrating networks an error in the diagnosis of presentation of the foetus will only occur when the foetal heart itself is not properly sited in the foetus. This might even be useful diagnostically if the discrepancy is discovered early enough, but it appears to be a very remote possibility.

#### c) Diagnosis of Multiple Pregnancy

A knowledge of how many babies a pregnant mother is going to have is of importance not only to the parents to indicate domestic changes, but also to the obstetrician in managing the pregnancy. He might have to get others to help during delivery, especially if the Caesarian operation needs to be performed. In the case of multiple pregnancy the babies might have to be delivered within a specified maximum time of each other.

Current methods for diagnosing multiple pregnancies include palpation, or feeling with the obstetrician's hands, comparison of the size of the abdomen with the period of gestation, and confirmation by the use of X-rays. The use of X-rays has the disadvantage of unavoidable irradiation of the growing foetus and it is here that the superiority of the safer foetal electro-cardiograph becomes apparent.

In 1938, Bell took the first electro-cardiographic record of twins.

The criteria used in determining multiple pregnancy from an electro-cardiographic record are based on the fact that each of the

hearts beat independently of the others and therefore, in this connection, are like different oscillators having different frequencies and phases of oscillation. A record of the sum of voltages depicting the electrical activities of the different foetal hearts will show complexes which come together at some times and at others go apart. Within a short observation time the rates, although they are not strictly periodic, would not change appreciably. One can therefore look for periodicity to differentiate between several complexes, one for each heart.

By taking a record and using a cursor marked in beats/minute (for the known chart speed), one can search systematically for these separate rhythms or periods and diagnose the number of the constituent sources.

Fig.36a shows an oscillogram given by twins in 'breech' presentation.

In this case, apart from the foetal heart rates estimated at  $F_1 = \frac{450}{2.9} = 155$  beats/minute,  $F_2 = \frac{450}{3.4} = 132$  beats/minute, the amplitudes of the complexes marked  $F_2$  are larger than the amplitudes of the complexes marked  $F_1$ . The maternal complexes marked  $M$  are larger than both ( $F_1$  and  $F_2$ ).

It can be seen therefore that the amplitudes of the signals can be used to sort out the complexes.

Fig.36b shows an oscillograph of the same complexes a moment later when the foetal complexes occur almost simultaneously thus showing that the two hearts are beating at different rates.

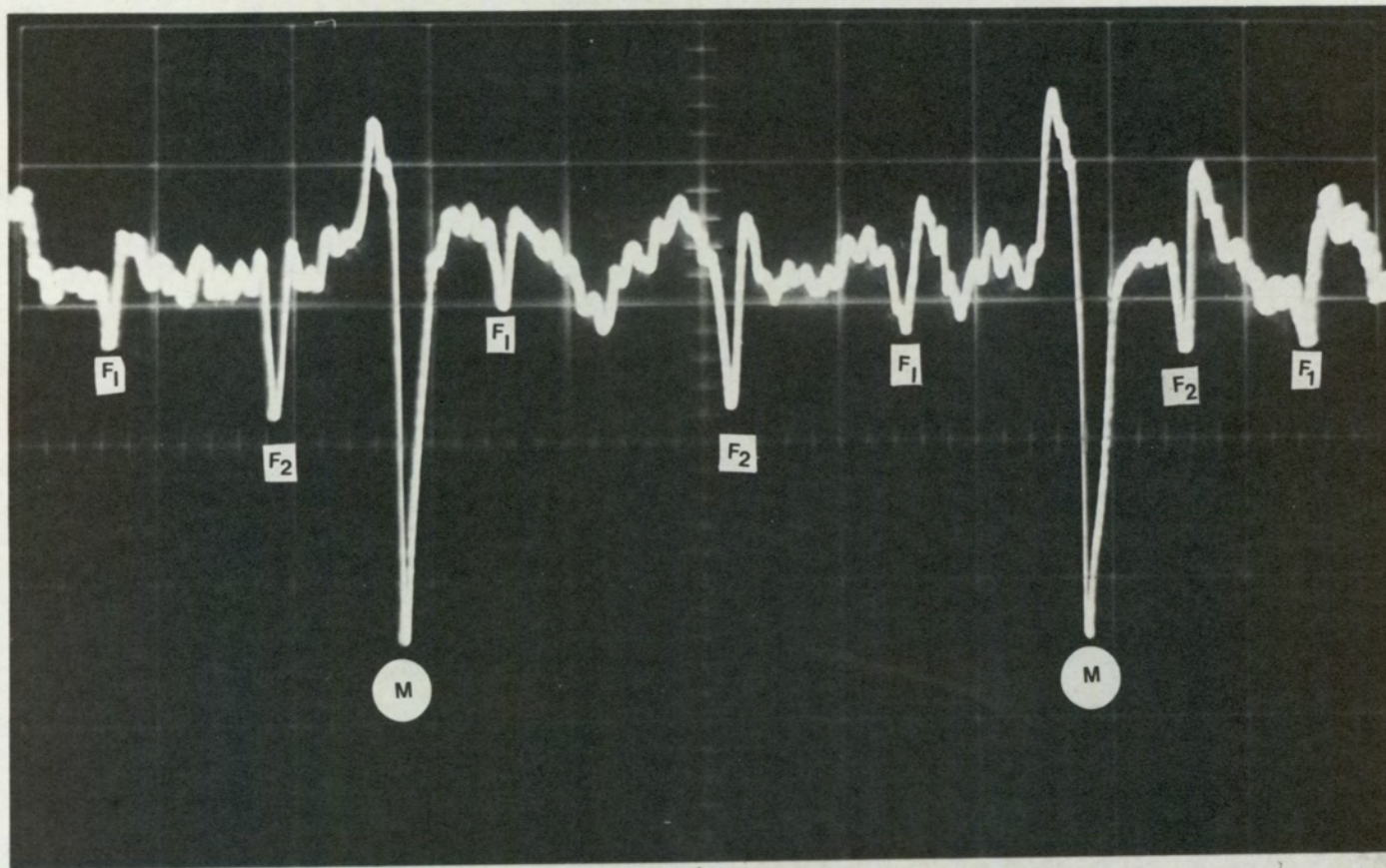


Fig. 36a.

Oscillogram showing the complexes of Twins in Breech Presentation (marked  $F_1$  and  $F_2$ ). M are maternal complexes.

Heart rate (beats/minute) =  $450$  / Large Division.

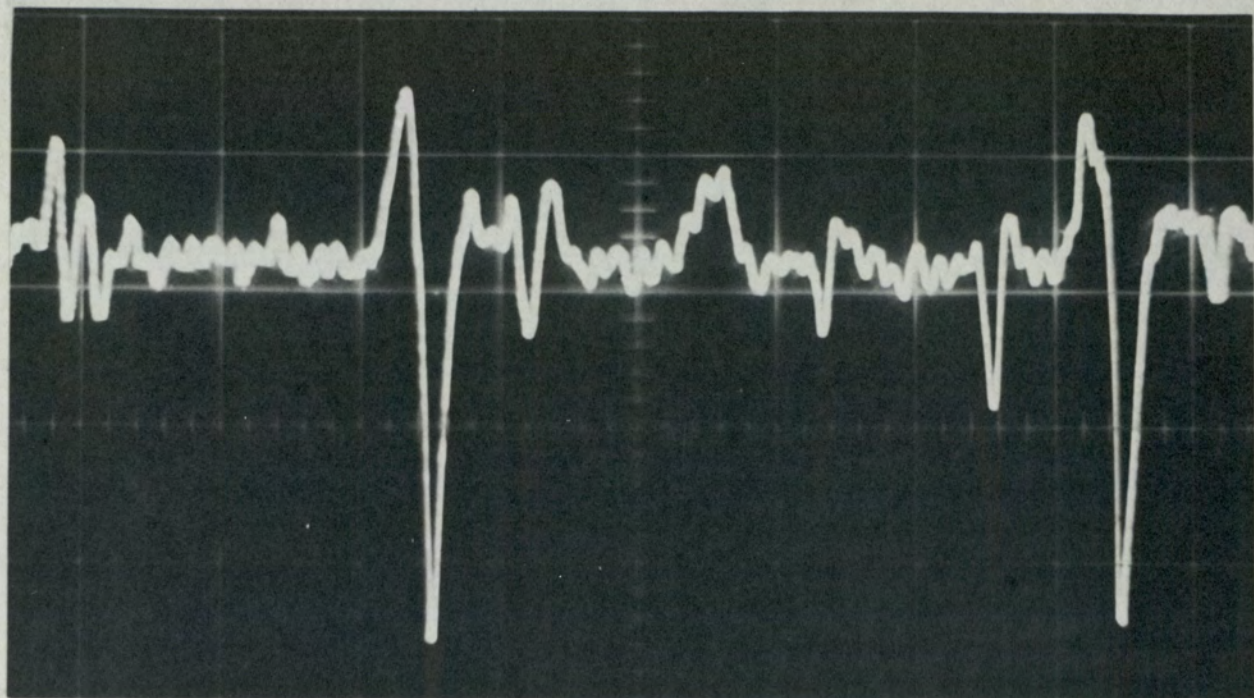
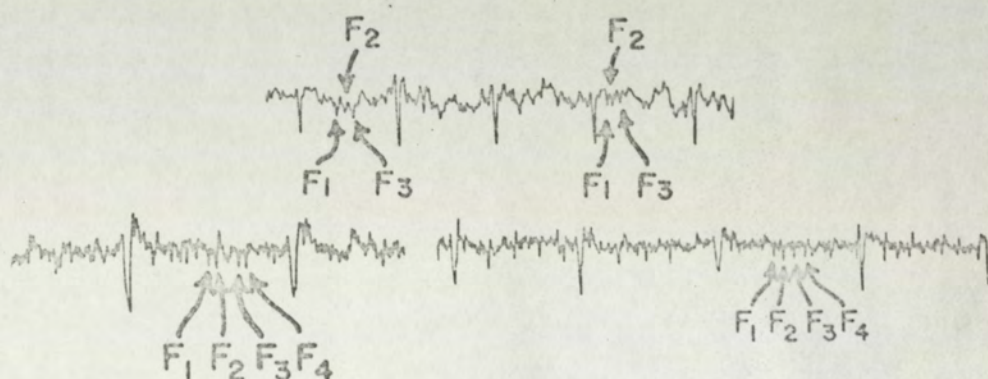


Fig. 36b

Recording Showing Foetal Complexes Coming together (extreme left).

The following recordings, taken from Larks' monogram, show the presence of triplets and quadruplets.



Recordings showing Multiple pregnancies, Upper-tracing, triplets; Lower tracing, quadruplets. ("From Larks, S.D., FETAL ELECTROCARDIOGRAPHY, 1961. Courtesy of Charles C. Thomas, Publisher, Springfield, Illinois and with the permission of Professor Larks").

In the course of the present investigations, the writer was asked to take foetal electro-cardiographic recordings on Mrs. Sheila Thornes at the Queen Elizabeth II Maternity Hospital, Birmingham. Sample sections of the record are shown in Fig.37(a) and 38.

It can be seen when compared with Figs. 36 and 37(b) that

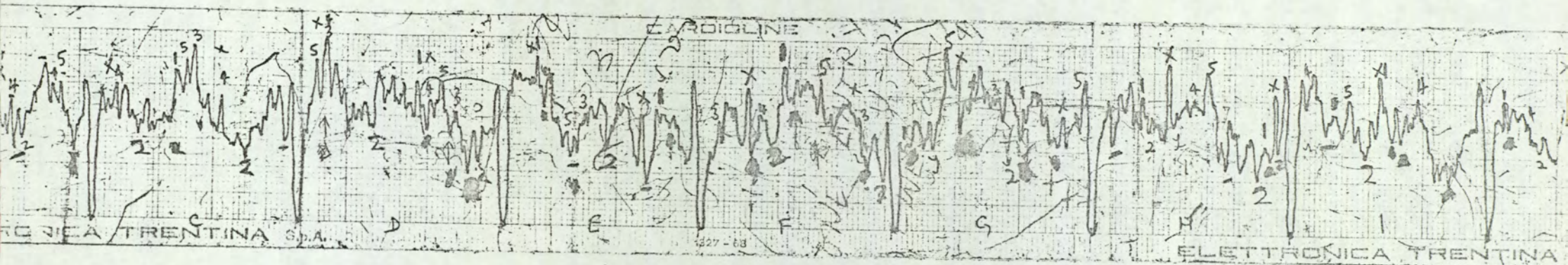
[ SEE NEXT PAGE FOR FIGURE 37 ]

there is a great deal and an unusual amount of activity between the maternal complexes.

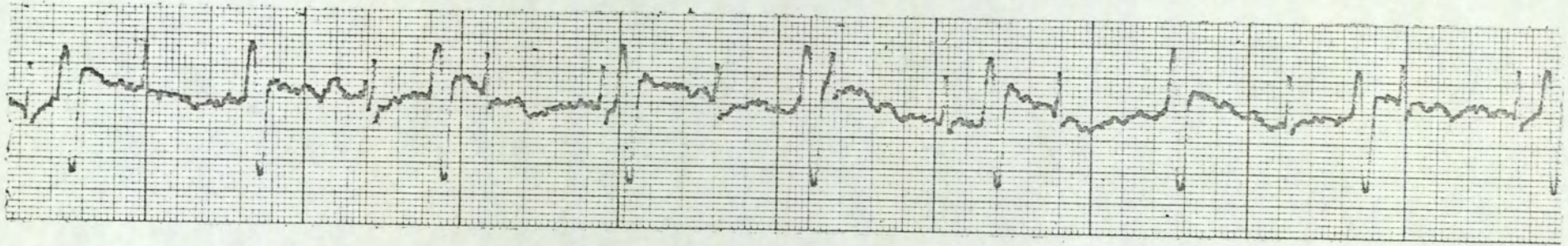
At first sight one might think that this activity originates from muscles other than the heart. Muscular noise signals, however, usually seem to be more regular and almost of constant amplitude. Secondly, the mother in question seemed extremely relaxed and if there had been only one foetus the record would have looked like the one shown in Fig.37(b). The maternal heart beat was about 79 beats/minute. The size of the abdomen also suggested there might be either a very large foetus or more than one.

C in

Trials were made starting at a point such as Fig.37(a), where most of the complexes had come together and try to find regular rhythms. If one could not obtain a regular pattern this particular attempt was



(a)



(b)

Fig. 37. Trace (a), Chart Record of Sextuplets ,compare with record of one foetus,trace (b).

abandoned and another made. The number of trials of this nature can be inferred from the state of Fig.37(a). Sometimes the pattern being followed would coincide with a maternal complex and if there is any indication that the shape of the maternal complex had changed where one expects the particular complex being followed, this point was marked and the search for periodicity continued. In Fig.38 the difference in size of the two maternal complexes suggests that such coincidence has taken place. One can guess that some of the upward pointing complexes have coincided and interfered with the first maternal complex to reduce its size. This procedure was then repeated for each of the complexes which one thought was foetal in origin. It was quite tedious. The pen writer on the ordinary electro-cardiograph could not follow the rapid changes in phase taking place due to the many complexes and so the graph Fig.37(a) had to be intensified by tracing over it with pencil. The last region on the extreme right marked X is an example of the undeeptened graph. Due to the high frequency response of the oscilloscope, the photographic record (Fig.38) from it is easier to use as the complexes stand out much more clearly.

The time base was 0.2 sec/large division.

Suppose one has been able to ascertain that the complexes seen were foetal in origin. Assuming also that the foetal complexes were occurring at the normal rate, 120 - 200 beats per minute, one could say that complexes marked a and b are too close to form one pattern. This is because the rate here is measured as rate/minute =  $\frac{300}{N}$ , (where N = number of large division) and the corresponding rate for N = 1 is 300 beats/minute. Similarly b and c could not be considered as forming a pattern. a and d however could form a pattern in the normal range of foetal heart rate. By marking off the interval a-d and trying it on a similarly spaced complex, this coincides with f. This interval represented by 2 divisions (N = 2) corresponds to a rate

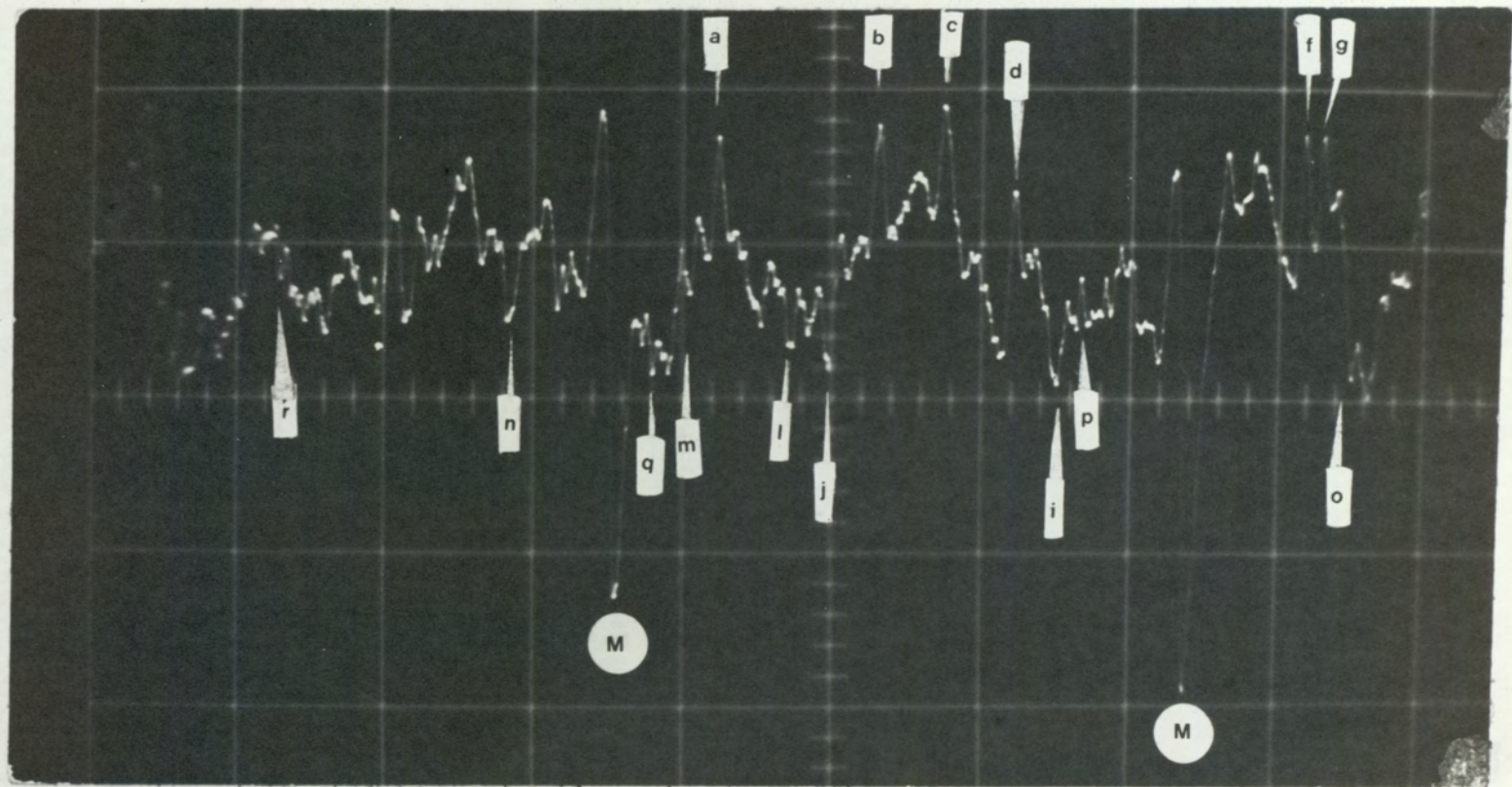


Fig .38 . Oscillogram of Sextuplets. The Foetal complexes have been marked with small letters; M represents the maternal complexes.  
Heart Rate ( beats/minute ) = 300/ Large Division.

of 150 beats/minute. A look at the disposition of foetal complexes with maternal complexes in the case where there was only one foetus (Fig.37(b)) shows that such a choice would be acceptable.

A choice between a and i (Fig.38) is ruled out because of the fact that these complexes seem to be in phase opposition (a representing normal presentation and i breech presentation).

By similar reasoning it can be seen that n, l, i, o seem to form another pattern with a rate of 158 beats/minute ( $N = 1.9$ ).

Considering the complexes occurring between the maternal (M) pulses.

1. Normal presentation (Pointing upwards)

a, d have been accounted for as forming one pattern

b, c are too close to be members of a pattern and one can conclude they represent two more foetuses.

At this stage one can conclude that there are at least three foetuses in Normal presentation.

2. Breech presentation

l, i form a pattern and l and j are too close to form a pattern. One can conclude that there are at least two foetuses in Breech presentation.

On this basis therefore, one could conclude that there are at least 5 foetuses, 3 in normal presentation and 2 in breech presentation.

If one considers further that m and p formed a pattern this will mean a rate of 110 beats/minute, projecting the corresponding interval to the left brings one to an indefinite "wobble" at r (not very much unlike p in appearance). If this is a true pattern then there would be six foetuses present:- four generally in normal presentation and two in breech presentation.

Usually there were at most two foetal complexes occurring in one maternal interval (See Fig.37b) except in cases as shown in

Fig.38a where a different foetus was under stress and the rate of 118 beats/minute was close to the maternal rate of 107 beats/minute. The foetal rate subsequently dropped to about 100 beats/minute and for some periods when they coincided one could not see the foetal signal, but it reappeared and went off again with a long beat period.

Using this ad hoc criterion of two complexes/maternal interval one can quickly count all complexes which might be foetal in origin and divide the count by two to guess at the number of foetuses present.

Applying this to Fig.38, in the interval between the maternal complexes one can count

$$a, b, c, d, p, i, j, l, m, q = 10$$

$$\therefore \text{No of foetuses} = 10/2 = 5$$

In Fig.38 it is easier to tell the presentation than in Fig.37(a). This might be due to the fact that the response of the pen writer used in Fig.37(a) was slower and could have affected the waveform. In Fig.37(a) whenever the complex marked X was seen the one marked 4 was not far away. Similarly, the complexes p,q,r in Fig.38 were not very definite so it was concluded ten days before the sextuplets were delivered that there were 5 foetuses with a possibility of a sixth one. Also that generally two were in breech presentation and three were in normal presentation.

The validity of this method of analysis rests completely on these assumptions:

- (i) The foetal heart rates were normal
- (ii) The heart rate does not change appreciably during the time of measurement.
- (iii) The waveform, (size and direction) can be used as discriminating criterion.

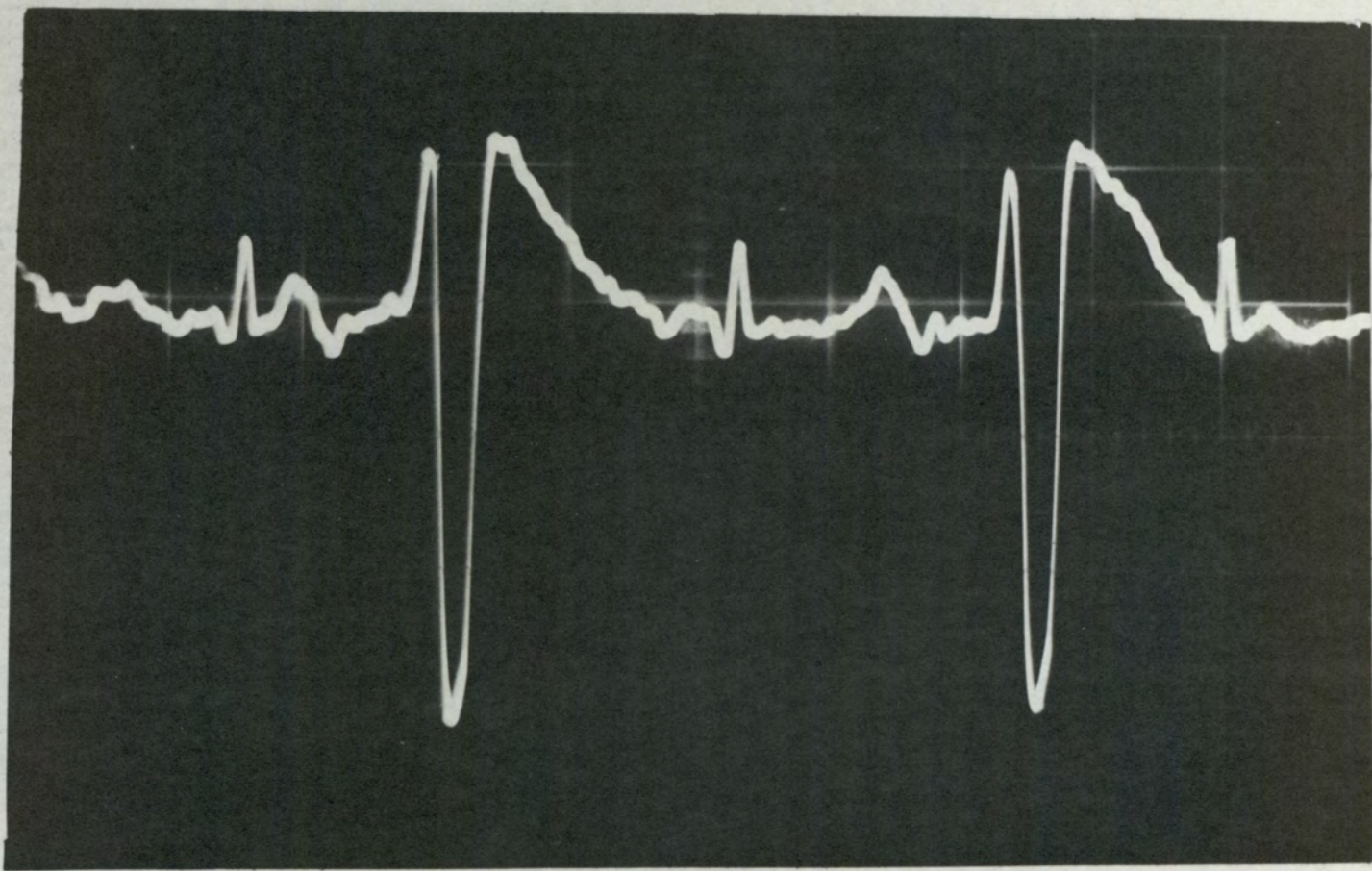


Fig.38a. A case where the foetus is under stress and the rate is comparable with the maternal rate

(Rate/minute = 450/Large Division)

when (i), (ii), (iii) are not satisfied there will be difficulty and errors in the diagnosis of multiple pregnancy using foetal electrocardiography.

In this section we have dealt with the type of information obtainable from the raw signal from the output of the detecting amplifier without further processing of the signal. It has dealt with normal signals in terms of rate. It can be said in addition that information concerning pathological cases such as tachycardias and bradycardias or arrhythmias can be obtained also by visual inspection.

THE USE OF COMPUTER TO OBTAIN THE WAVEFORM  
OF THE FOETAL ELECTROCARDIOGRAM

In order to get information from the detected signal concerning the waveform of the foetal electro-cardiogram, means must be found to remove all other confusing voltages masking important characteristics of the foetal electro-cardiogram. The first of these masking voltages to be removed are those constituting the rather larger maternal complex. When this is done computer averaging techniques can be used to improve the signal to noise ratio.

Digital methods should be used because if one has the low frequency cut-off set so that there are some "breathing" voltages periodically lifting the base line up and down then analogue computer summation will not be able to cope with the fact that the signal is in effect occurring at varying d.c voltage levels. The result of superimposing several foetal complexes will be a blurred average as would happen when one uses an oscilloscope with long fluorescent decay time directly.

Among the digital computer auxiliary apparatus or peripherals should be an analogue-to-digital convertor. There should also be a system to initiate digitilisation and storage.

The natural point in the electro-cardiogram for triggering the computer is the R-wave or a correlated function derived from it. In Fig.39 the usual definitions of the various portions of the electro-cardiogram are indicated by the lettering.

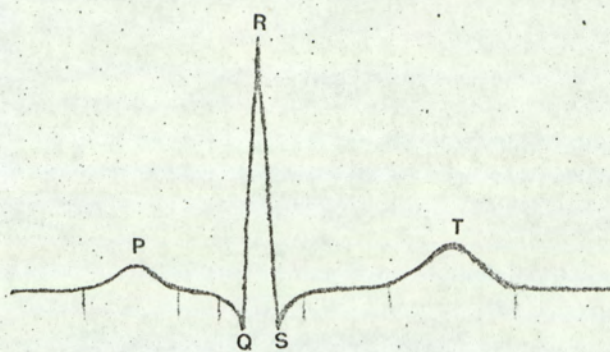


Fig.39. Nomenclature for the Main Waves of an Electrocardiogram.

A system for the elimination of the maternal complex based on the method used by Goddard, Newell et al<sup>(20)</sup> was designed and used in this experiment. The signal is first delayed using a tape recorder employing frequency modulations (F.M) and so having a response extending to d.c. The delay time,  $\tau$ , is the time it takes for the tape to travel from record head to playback head. The maternal R-wave in the undelayed signal is used to produce a pulse of known duration,  $T_m$ , shown in Fig.40.

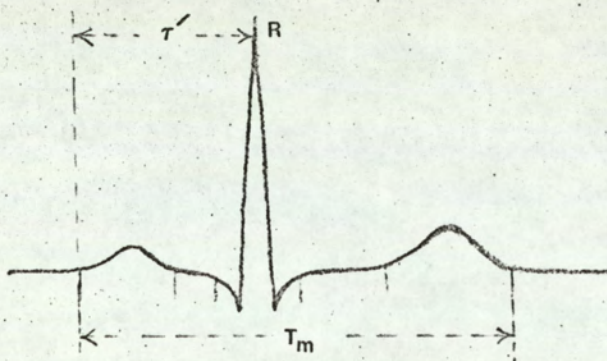


Fig.40. Timing for Maternal Blanking. (see text ).

This pulse is used to operate on a gating device at the output of the tape recorder so that during the period,  $T_m$ , no signal is obtained from the gating device. Thus only foetal signals which occur outside the periods such as  $T_m$  can subsequently be used for triggering the computer.

A delayed maternal complex triggered with its undelayed R-wave counterpart will only be blanked out if the timing is such that (see Fig.40)

$$\tau' = \tau - \tau_d \dots\dots\dots (74)$$

where  $\tau'$  is the period shown in Fig.40.

$\tau$  is the time delay produced in the tape recorder.

$\tau_d$  is the time delay in the triggering circuit before the gating voltage is produced.

Fig.41 is a block diagram of the system constructed to realise this situation. The detecting system and information that can be obtained without the use of computers have been described in the previous sections. The following is a general description of the remaining blocks in Fig.41.

Path b.

The signal along this path is first passed through an R-C (resistance-capacitance) differentiating network to remove low frequency base line drift and thus ensure constant triggering level. The negative going pulse, maternal R-wave, triggers the Schmit circuit to produce a waveform having a shape shown at its output. There is a variable time delay,  $\tau_d$ , between the arrival of the trigger point on the maternal R-wave and the negative going point of the output waveform. This derived negative going pulse triggers the Master Flip-flop circuit and at the same time opens the F.E.T. 2 gate for signal from the variable free-running oscillator to reach the "Divide by 400" circuit.



After counting 400 oscillator pulses the "divide by 400" circuit produces a pulse which resets the master flip-flop, thus producing the square wave shown. The duration of this square wave,  $T_m$ , is the time it takes to count 400 oscillator pulses..

$$\therefore T_m = \frac{400}{f} \dots\dots\dots (75)$$

where  $f$  is the oscillator frequency.

By varying  $f$ , therefore, the time  $T_m$  can be changed smoothly over a wide range.

The pulse of duration  $T_m$  is then used to close F.E.T. Gate I so that during this period ( $T_m$ ) no signal gets to the amplifier marked AT.

#### Path a.

The signal along path a is recorded and played back by the F.M. tape recorder. The fixed delay time,  $\tau$ , between record and playback being the transit time of the magnetic tape between the record head ( $R_e$ ) and playback head ( $P_e$ ).

Suppose the distance along the tape is 1 inch and the tape speed is  $3\frac{1}{4}$  inches per second then

$$\tau = 267 \text{ m sec.}$$

The delayed signal is unaffected except for addition of noise from the tape recorder system, mainly at twice the demodulating frequency.

#### Path d.

The signal along path d goes through an analogue amplifier, AA, which is used to cut-off most of the ripple voltage from the F.M. demodulator and set the amplitude of the signal at the correct level for the computer input. This <sup>m</sup> amplifier can have filters for studying the effect of filtering on the computer averaged waveform.

Path c.

The delayed signal is first passed through a high pass filter to remove base line drift, and presented to F.E.T. Gate I which is closed when a maternal complex occurs.

The filtering should be done before gating or "Blanking" for the following reason:

Suppose the waveform of the input to the F.E.T. Gate I were as shown in Fig.42. The gate output would be represented by the solid line, the dotted line representing the position of the blanked out maternal complex.

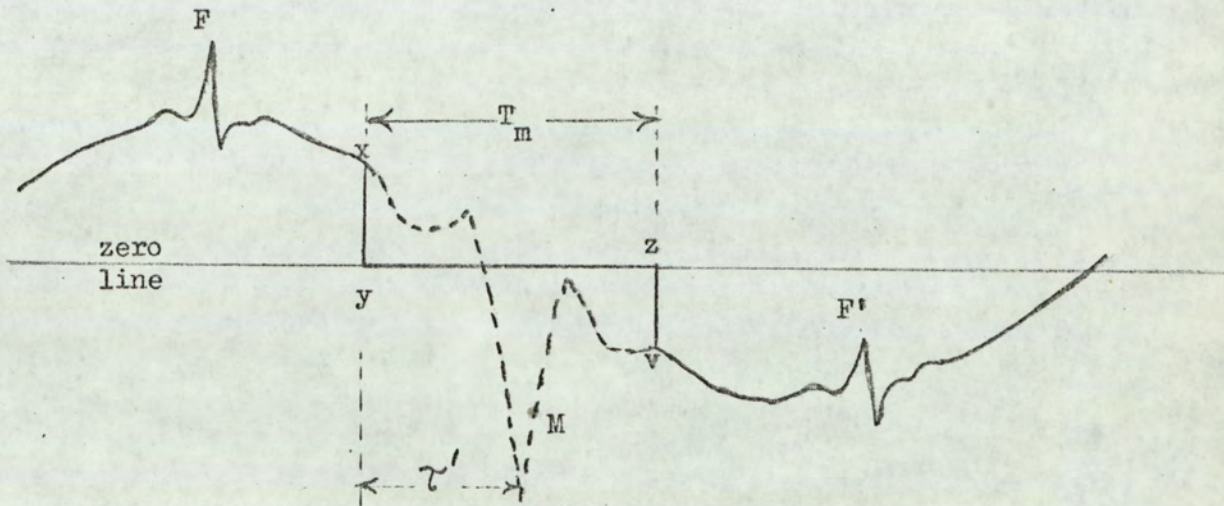


Fig. 42'

Illustration of the Necessity to differentiate the waveform to be used for triggering the foetal complex before blanking.

It can be seen that the foetal complexes F and F' cannot both be used for triggering the computer since its threshold will have fixed polarity. In the PDP8/I the trigger pulse should be negative going and must have amplitude between -0.5v and -3v.

One would therefore differentiate the signal to remove the interfering low frequency voltages. When this is done the discontinuities at y and z will give rise to spikes which can also trigger the computer to initiate the averaging process. It is to avoid such a

situation that the filtering must be done before the maternal blanking.

One can have the foetal complex pointing upwards (normal presentation) or downwards (breech presentation) and since one polarity is needed for triggering the computer, a reversing switch is needed. This is provided in amplifier  $A_T$  which also controls the amplitude of the trigger pulse.

It can be seen that there is no time delay between analogue signal at  $e$  and its counterpart used for triggering at  $f$ . The time delay needed to start averaging from the beginning of the foetal P-wave when triggering is done with the R-wave is provided internally by the computer.

It can be seen that with a system as outlined in Fig.41 the signal to be averaged is not distorted by the differentiation used in the production of the trigger pulse, apart from any intended modification of the waveform in amplifier  $A_A$  for studying the waveform.

The following is a description of the system blocks, Fig.43 shows the actual circuits constituting the maternal blanking system.

#### Maternal Triggering Pulse Circuit.

After passing through the differentiating network provided by  $C_1$  and  $R_1$  the threshold for ensuring proper triggering is set by the potentiometer  $R_1$ . The output of the trigger circuit is a square wave whose duration,  $\tau_i$ , can be varied with  $R_2$ . The combination of  $R_2, C_2, C_3$  provides a wide range for  $\tau_d$  (see equation 74) in the manner suggested by Green.<sup>(54)</sup>

#### Master Flip-flop.

The maternal flip-flop circuit is a conventional one with  $D_2$  and  $D_3$  added to ensure reliable switching. It is triggered by the negative going portion of the output of the maternal trigger circuit.

With the arrival of the maternal trigger pulse transistor  $T_3$



is turned off and the point F moves to zero potential.  $T_4$  is turned on and the point G becomes negative with respect to earth potential. This point, G, is connected to the gate terminal of the P-channel m.o.s. f.e.t. constituting F.E.T. Gate 2. With the negative voltage ( $\approx -6v$ ) on its gate terminal it starts conducting and allows pulses from the variable frequency oscillator to reach the input of the "divide by 400" circuit. After 400 oscillator pulses have been counted, a negative going pulse from the output of the "divide by 400" circuit switches off  $T_4$  and the point G returns to zero potential turning F.E.T. Gate 2 off.

Point F is connected to the N-channel m.o.s. f.e.t.  $S_2$ , in F.E.T. Gate 1 and point G to the gate terminal of  $S_1$  another N-channel m.o.s. f.e.t. with the arrival of a maternal pulse  $S_2$  is turned on and  $S_1$  is turned off. This state persists until the "divide by 400" circuit has counted 400 oscillator pulses. After this, with G going to ground potential and F going to negative potential,  $S_1$  is turned on and  $S_2$  off. Thus only foetal signals occurring in the absence of maternal pulses can get to the foetal trigger amplifier  $A_T$ . The drain to source resistance of the f.e.t.'s when they are on is about  $200\Omega$  and  $10^6\Omega$  when they are off. They therefore constitute good and reliable switches. Resistances have been put at their gate terminals to protect them from transients. It is for the same reason also, that the  $100k\Omega$  resistor has been connected across m.o.s. f.e.t.  $S_2$ .

When F.E.T. Gate 1 is conducting  $C_4$  and  $R_4$  provide the high pass filter which is needed to avoid the effect described in Fig.42.

#### Variable frequency oscillator.

Fig.44 shows the circuit of the variable frequency oscillator.  $R_7$  and  $R_6$  provide the coarse and fine frequency adjustments respectively.  $R_5$  and  $C_5$  determine the duration of the oscillator pulse. The present setting of  $R_7$  is such that when  $R_6$  is varied the oscillator frequency varies from 670Hz to 4000Hz. After division by 400 this gives a

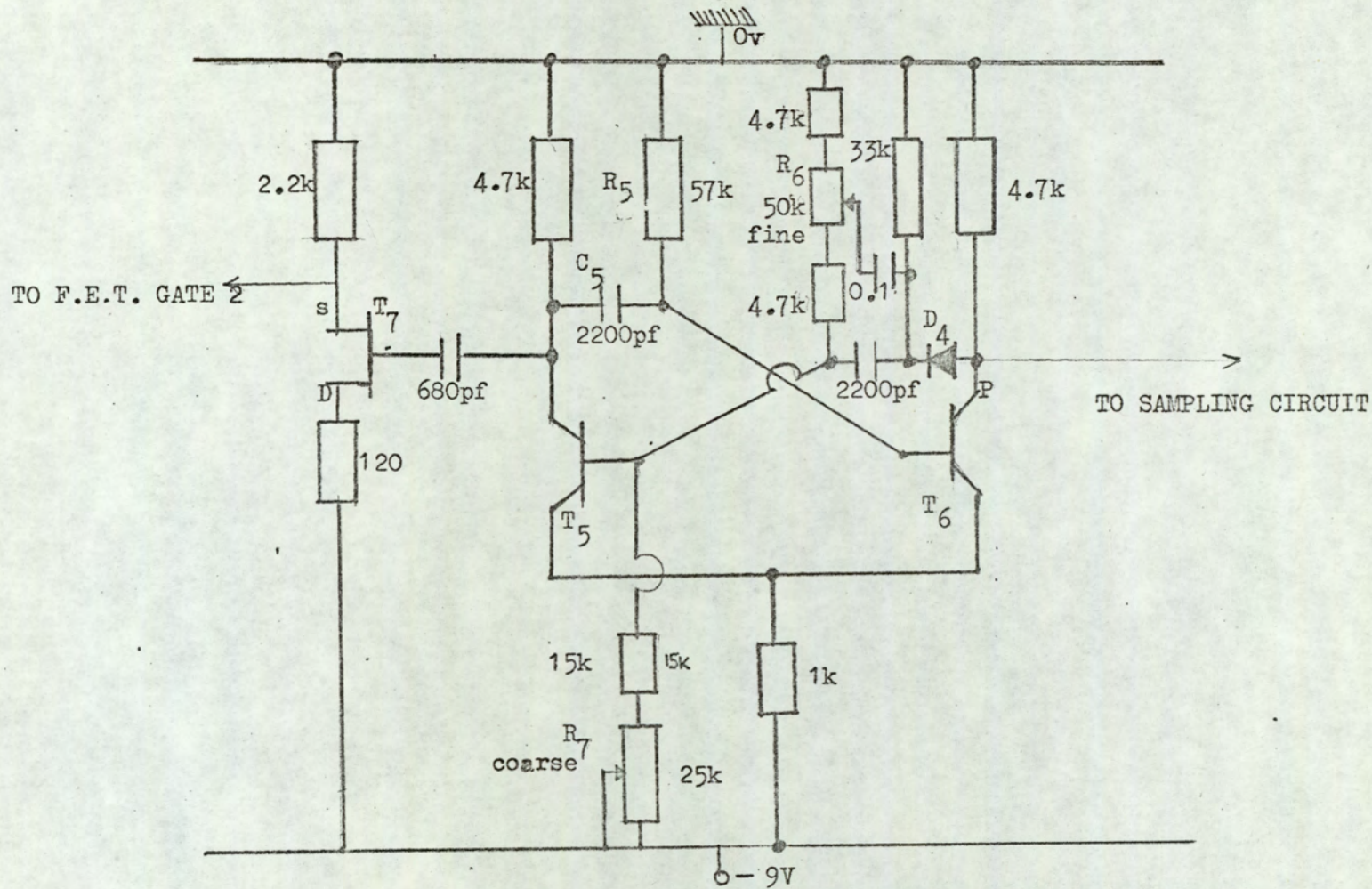


Fig.44. FREE RUNNING VARIABLE FREQUENCY OSCILLATOR CIRCUIT.

smoothly variable duration of the maternal gating pulse,  $T_m$ , from 100 millisecond to 600 milliseconds. This covered the range of the  $T_m$  met with in the present work. There is facility for changing the value by varying the setting of  $R_7$ .

"Divide by 400" Circuit.

The "divide by 400" circuit was constructed from two commercially available decade counters and one dual master-slave flip-flop, Texas SN7490N and SN7473N, respectively. They were connected as shown in Fig.45.

Originally the circuit was intended also to be used for taking 400 samples during the gated period. With the oscillator set at any frequency one could obtain 400 samples irrespective of what the actual frequency is. In other words, one could take 400 samples, irrespective of the length of the complex, for normalising the length of complexes in case different foetal complexes were to have been summed to produce a standard average foetal complex. This can be done by putting another gate circuit in the path of the signal to be sampled and sample with the oscillator pulses which passed through F.E.T. Gate 2.

When the PDP8/I computer was installed it was found that there was facility for taking such samples, and so the circuit was used only to provide  $T_m$  for maternal blanking.

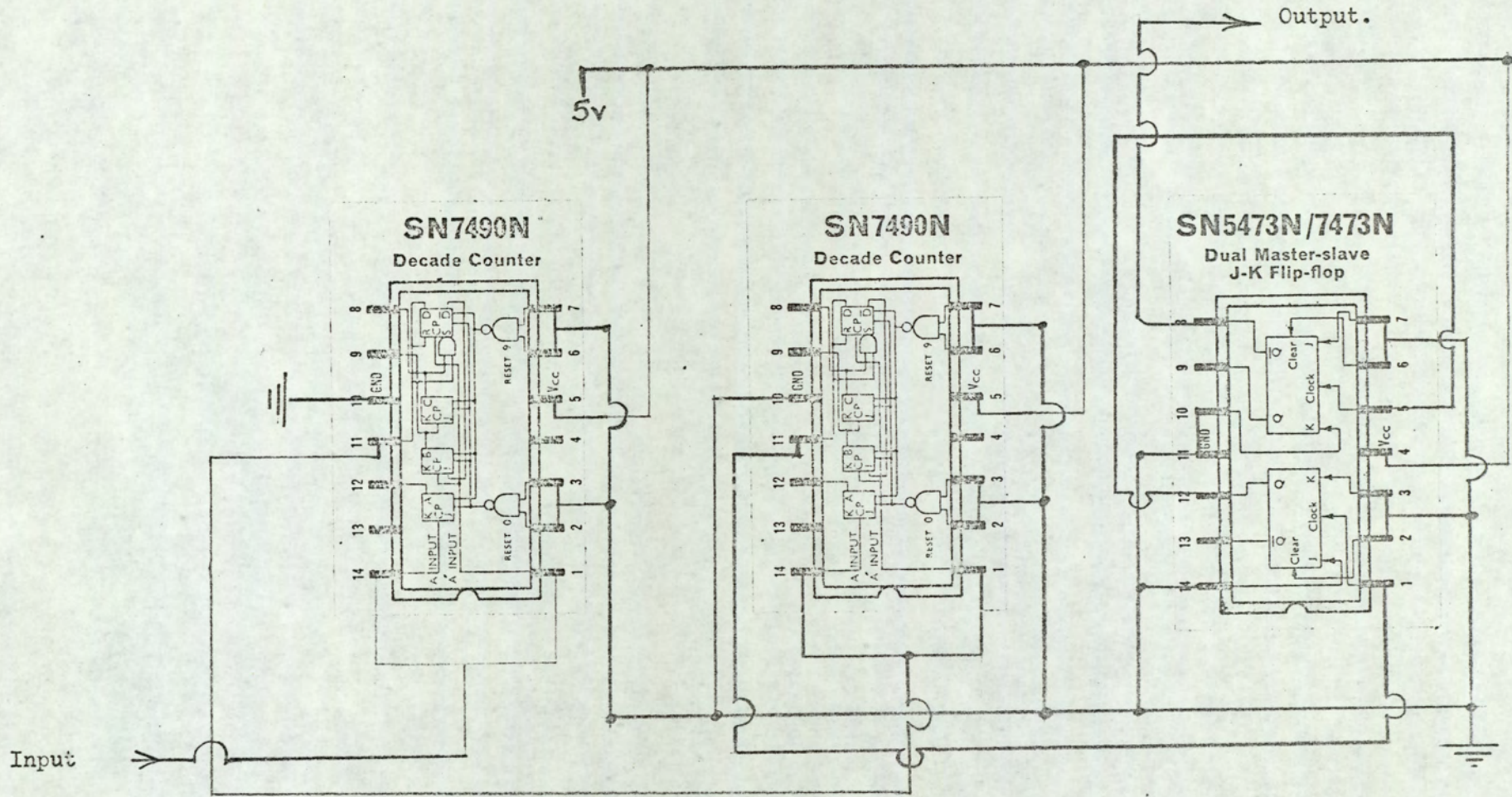


Fig.45 DIVIDE BY 400 CIRCUIT.

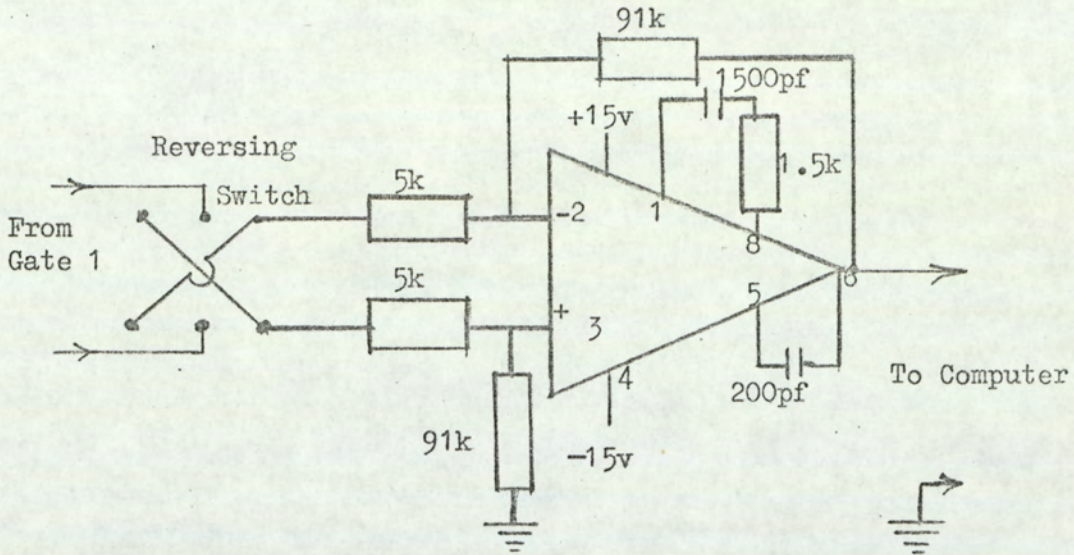
Foetal Trigger Amplifier, AT.

Fig. 46. Circuit Diagram for Foetal Trigger Amplifier,  $A_T$ .

Fig.46 shows the diagram of the foetal trigger amplifier,  $A_T$ .

The amplifier has a reversing switch at its input. This is used to obtain a negative going trigger voltage of about  $-2.5v$  irrespective of the presentation of the foetus. The amplifier is built around a commercially available operational amplifier. The stage gain is about 20. The amplification of the main detecting amplifier is  $10^4$  so that if the amplitude of the foetal signal is say  $15\mu V$  at the detecting electrode, the triggering foetal R-wave will have an amplitude of  $20 \times 10^4 \times 15 \times 10^{-6} = 3v$ . Fine adjustment was provided by the amplifier gain control in the tape recorder. There is also a variable amplitude control at synchronising input of the PDP8/I computer.

The networks on pins 1 and 8, pins 6 and 5 were used to provide frequency compensation.

### Analogue Amplifier, A<sub>A</sub>.

The analogue amplifier, A<sub>A</sub> in the block diagram is actually the input differential amplifier of the dual beam oscilloscope, Tektronix 583 . It has variable low and high frequency passbands. It was also used to control the amplitude of the foetal signal to be averaged as the amplitude of the input signal to the computer should be in the range  $\pm 1$  volt. The variable passbands facilitated the study on the effect of high and low frequency cuts on the averaged foetal signal.

### Tape Recorder.

The tape recorder used employs frequency modulation to extend the frequency response down to d.c. This is done by adding F.M. modulator and demodulator units to a Tandberg Tape recorder deck, the apparatus being sold as the Elliot-Tandberg F.M. Tape Recorder. The characteristics of the Tape Recorder are shown in appendix 3.

Due to modulation and demodulation noise, mainly at the ripple frequency of demodulation, is added to the signal. The noise level is quoted at 50 mV peak-peak after a stage gain of 2. This is equivalent to 2.5 $\mu$ V peak to peak referred to the detecting amplifier input and is higher than the intrinsic noise of the detecting amplifier. It is, however, low enough to contribute little to the averaged signal after about 100 foetal complexes have been averaged. A better tape recorder would, however, be needed if smaller foetal signals than those studied in this work were to be examined.

In the block diagram, Fig.41, waveforms obtained at various stages in the processing of the signal for computer averaging have been included. The waveforms with durations  $t_d$  and  $T_m$  are correlated with the maternal pulses. The foetal waveform to be averaged and the trigger pulse derived from it are shown as e and f respectively. A typical averaged foetal complex is shown as on the oscilloscope of the PDP8/I computer. This is discussed later.

Fig.47a is a more detailed form of the waveform at the input of the computer. Here the signal to be averaged is shown on the lower trace. In this particular case the signal is differentiated.

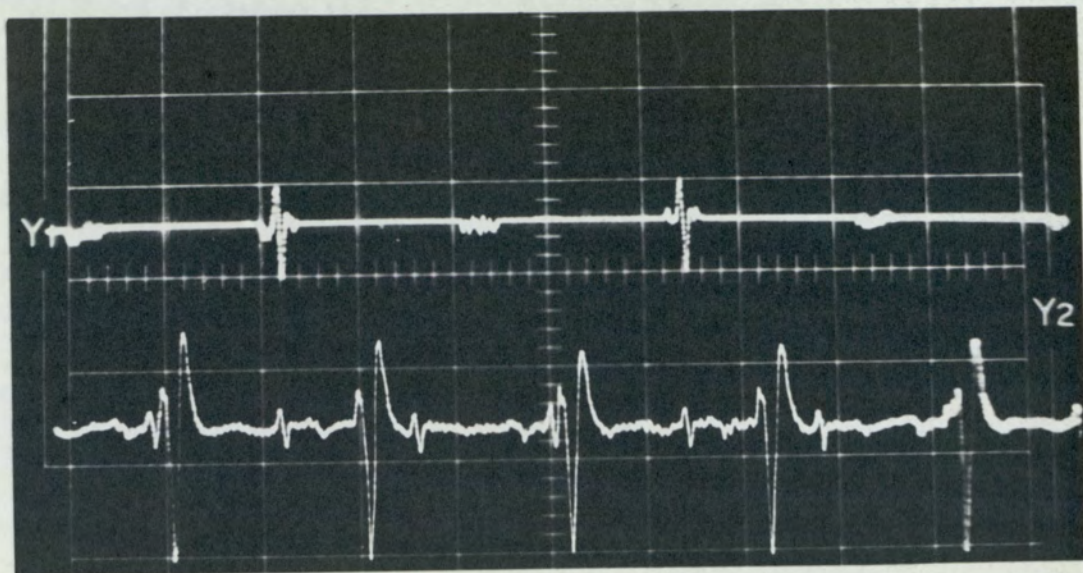


Fig.47a. Lower Trace, Signal to be Averaged.  
Upper Trace, Derived Trigger Pulse for computer to initiate the averaging process.

Normally it is as shown in Fig.47b. It will, however, suffice for explaining the action of the system.

The signal with the maternal complexes blanked out is shown on the upper trace. The blank spaces represent the positions at which the maternal complexes occurred. It can be seen that all foetal complexes occurring close to the maternal complexes are also blanked out and only those occurring away from the large maternal complexes, i.e. in the refractory period of maternal cardiac cycle, are used for triggering the computer to initiate the averaging process. By adjustment of  $\tau_d$  and  $T_m$  one can choose foetal signals occurring anywhere in the interval between maternal complexes for averaging. This makes it possible to reduce the influence of the maternal complexes on the averaged foetal electro-cardiogram. The maternal heart cycle is going on all the time and so, theoretically, one cannot choose any portion of the signal where its influence is absent. The maternal complexes

occur without correlation with the foetal signal and by removing the larger portions of the maternal complex and summing a number of foetal complexes the effect of the remaining maternal heart complexes should be reduced.

Fig.47b showing the undifferentiated form of the signal shown in Fig.47a, illustrates the fact that when the maternal heart

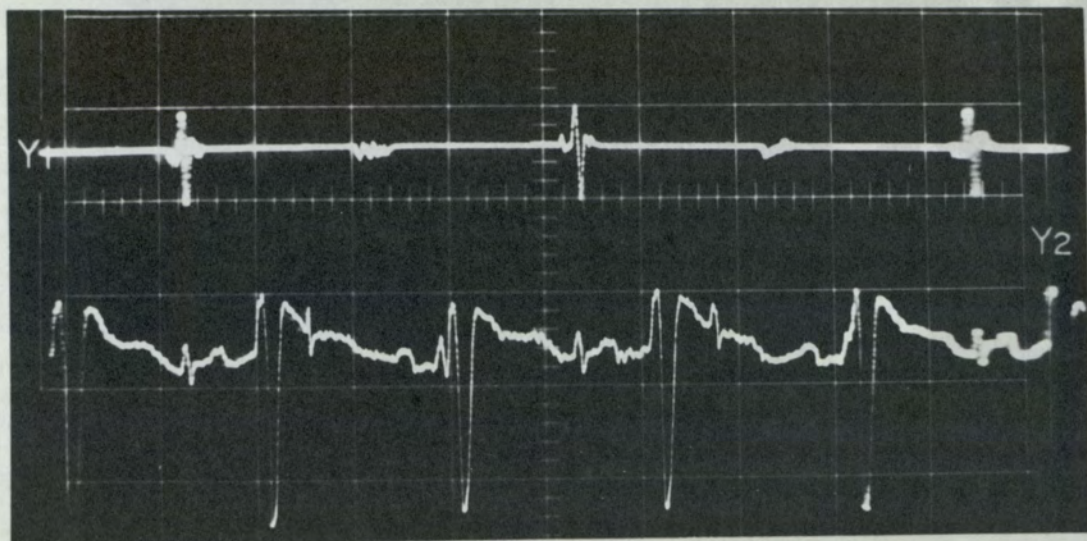


Fig.47b. Lower Trace shows the Undifferentiated form of the signal in Fig.47a illustrating the influence of the maternal complex (see text).

rate is fast, the refractory period in the heart cycle becomes short and the foetal waveform always sits on top of the slow parts of the maternal complex even when most of the maternal complexes (QRS) have been blanked out.

As a result of differentiation as shown in Fig.47a the amplitudes of the low frequency portions of the maternal complex are reduced and a wider interval of choice of foetal complexes can be achieved by decreasing  $T_m$ .

Since the foetal signal has a constant probability of occurring in any part of the interval, a wider interval of choice makes the averaged complex less dependent on the maternal complex. By restricting this interval to avoid large sections of maternal complexes one makes the choice of foetal signal less random. In other words, the foetal signal

chosen for averaging tends to occur at about the same period after a maternal R-wave.

Differentiating the signal has been shown earlier not only to lead to deformation of the waveform but also to remove the low frequency portions of the foetal signals as well. This difficulty is a limitation in this system of removing the maternal complex by blanking it out.

However, in normal circumstances where the maternal rate is not high the refractory interval is long enough for the system to be used. Fig.47c is such a normal case. Even without differentiation the maternal refractory period is long enough to produce good averaging.

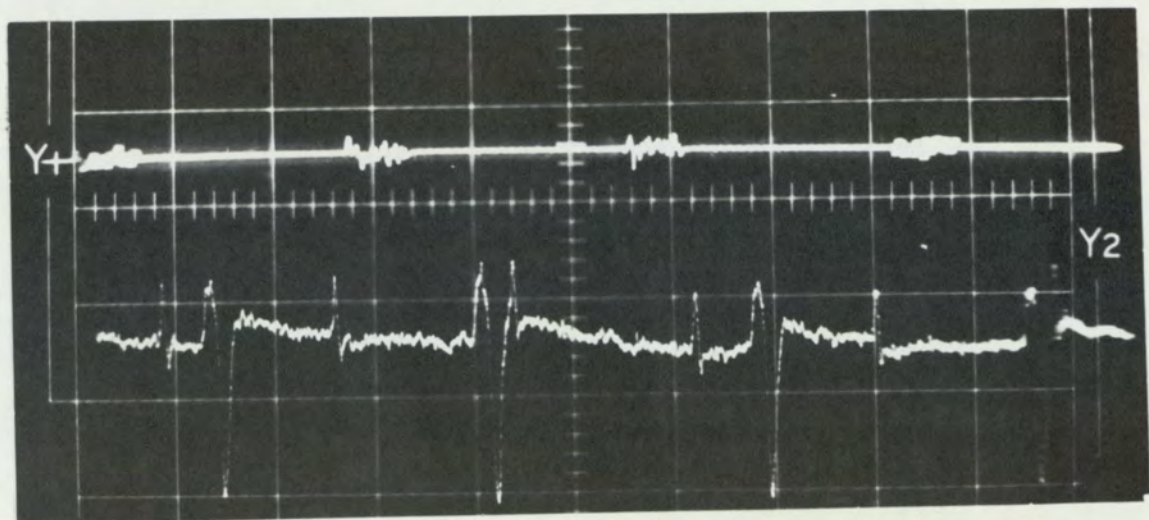


Fig. 47c. The averaging process in the case when the maternal heart rate is normal (see text below).

It is shown with the same timing adjustments ( $\tau_d$  and  $T_m$ ) as was used for Fig.47(a) and (b). It can be seen that both values of  $\tau_d$  and  $T_m$  can be reduced to enable more foetal complexes to be averaged in a given time.

With the values of  $\tau_d$  and  $T_m$  used in Fig.47c no foetal complex could have been chosen for averaging in the interval of time represented by the photograph. This means that the total averaging time (for say 100 complexes) is longer when the duration of the blanking pulse,  $T_m$ , is long.

After discussing the results of computer averaging using this system of maternal blanking, a scheme for computer averaging which can avoid this difficulty, especially when fast maternal heart beats are encountered, will be outlined, even though this has not been tested experimentally on account of lack of available time.

AVERAGING OF SIGNALS IMMERSSED IN NOISE TO ENHANCE  
SIGNAL TO NOISE RATIO.

In the previous section the method for processing the signal and correlated trigger voltage for presentation to the computer was outlined. The following will deal with the averaging process itself.

General Techniques.

A frequently used technique (Katzman)<sup>(55)</sup> for computing an average response, or 'averaging' a signal immersed in uncorrelated interference is first to produce a signal which is time-locked with the signal of interest such that after a pre-selected time of this signal occurring, a summing device stores correlates of the signal for a pre-selected time, notably the duration of the signal of interest.

This process is repeated say N times.

If the noise results from an additive, statistically independent random process, the signal-to-noise ratio of the sum of N signals is given by:-

$$\frac{\sigma_s^1}{\sigma_n^1} = \frac{N^2 \sigma_s^2}{N \sigma_n^2} = \sqrt{N} \frac{\sigma_s}{\sigma_n} \dots\dots\dots (76)$$

where  $\sigma_s$  is the r.m.s. value of the signal.

- $\sigma_n$  " " " " " " noise.
- $\sigma_s^1$  " " " " " " signal after averaging.
- $\sigma_n^1$  " " " " " " noise " "

There is therefore an improvement of signal-to-noise ratio by a factor of  $\sqrt{N}$ .

Cox<sup>(56)</sup> discusses the limitations in the use of this technique especially as to the validity of the assumption utilised that the noise is uncorrelated with the signal.

In electrophysiology the technique has been used to compute or obtain average of evoked responses, such as the effect of a stimulus

on the electrical patterns occurring in the brain.

The most important part of the technique is the production of the fiducial, or starting, signal which also initiates the averaging process.

In foetal electro-cardiography the natural fiducial point is the R-wave. Normally the highest point in the electro-cardiogram. Since it occurs in the middle of the waveform of interest it is important, as stated earlier, by the use of the tape recorder, to produce a delay  $\tau^1$  (see equation 75) in the signal to be averaged and the particular R-wave which initiates averaging.

In averaging biological signals, such as evoked responses from the brain, where one does not expect the base line to drift up and down, analogue systems can be used in obtaining the average. In such cases the storage device could be a photographic plate on to which the exposures are triggered with the fiducial stimulus. It can be appreciated that any such system will give a blurred image when used to operate on signals with changing base lines such as is the case in foetal electro-cardiograms recorded with maternal abdominal electrodes. This blurring is avoided if the signal is first converted from the analogue to digital form before sequential summation of the elemental samples.

An analogue-to-digital converter (ADC) is therefore required as part of the peripheral instruments for computation of the average.

The first step in the analogue-to-digital transformation is a sampling process, in which values of the analogue signals are chosen and stored at discrete points in time. This is followed by a quantisation process in which amplitude values are assigned to each sample.

In the present experiments the PDP8/I computer was used in averaging the foetal electro-cardiogram. It has facility for analogue to digital conversion. This computer uses PAL III language and included in its software is a program for averaging. On command by a negative going pulse of amplitude between -0.5v to -3 volts, it will sample and display an analogue signal of amplitude  $\pm 1$  volt.

Instructions as to the sampling time, delay time, number of samples to be taken during the sampling time can all be typed into spaces available in the program to suit the signal being averaged. The program demands these instructions at appropriate stages for the insertion of such information by the aid of a tele-typewriter.

Fig.48 shows a sweep summary typed out by and displayed on the oscilloscope of the computer after the operator has given correct instructions to the computer for averaging.

```

      SWEEP SUMMARY
      BEGINS-AT RATE-ENDS
      -30.00M 375 U 44.62M
      -97.12M 1.125M 126.7M

      AVERAGES
      CHAN RATE TYPE SORT
      1 L 1 0
      1 H 1 0

      SYNC ON CHANNEL: S1
      64 SWEEPS AT 300.0MS
      (VBP,0,230 -6277)
      !
      [
      TIMING...R
      TRIGGER...
      !
      [<
  
```

Fig. 48. Example of Computer Sweep Summary for averaging.

In this run the computer was to provide 200 data points in the assigned sampling period. There is a built-in delay time of either sign. That is if the sampling is to commence at a point of the waveform occurring before the trigger signal (say the R-wave), then one needs a negative time delay. The system is equivalent to using the tape recorder to delay by  $\tau_d$  as used in the maternal blanking system.

In Fig.48 the -30.00M means that the delay is -30 milliseconds "before" the trigger signal and 44.62M means 44.62 milliseconds after the arrival of the trigger signal. The sampling period is therefore  $(30 + 44.62 = )$  74.62 milliseconds and within this period 200 samples should be taken. The computer therefore points out the time it spends

on each data point 375U (U = microseconds) in the middle.

Similarly, the next line shows that 200 samples are taken between -97.12 milliseconds and +126.7 milliseconds, using the R-wave as the starting point, at 1.125 milliseconds per data point. The total sampling time is  $(97.12 + 126.7 = )$  223.82 milliseconds.

In this program the computer is being instructed to produce two types of averages from the same electro-cardiogram. One represents a duration which would cover the 'whole' electro-cardiogram or what one thinks subjectively will be sufficient to include the PQRS intervals of the foetal electro-cardiogram. The other is the average for a portion of the electro-cardiogram QRS. If the same number of data points is called for then the rate of sampling in the latter case must be higher than in the former. In the computer language the former is obtained at 'low', L resolution and the latter at 'high', H, resolution.

The section on AVERAGES in Fig.48 describes how the averages are obtained. The channel, CHAN, describes the source from which the signal is being chosen for averaging. In this case it is the signal on input I of the computer. RATE : means that the average displayed at the top Fig.49 is obtained by ~~Low~~ low, L, resolution sampling and the average displayed below it is obtained by high, H, resolution sampling.

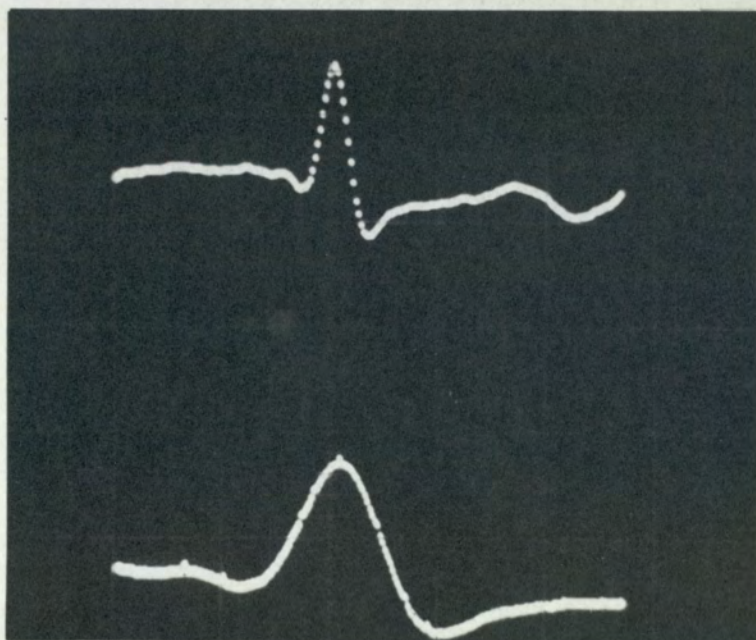


Fig.49

Illustration of the result of High and Low Resolution sampling. The lower average represents the middle portion of the average in the top trace.

The next line on Fig.48 means that the fiducial or synchronising signal (in this case the derived R-wave) is applied to input  $S_1$  on the computer. The next line says that 64 such foetal complexes are averaged.

Because the computer is performing other functions such as storing and locating sampled data it computes the minimum interval of time within which it can accept successive complexes for sampling. In this case this minimum time might be 300 milliseconds. It then requests the operator to type in any time more than 300 milliseconds and uses the extra time to modulate the brilliance of the display oscilloscope during averaging. In this case by typing in 330 milliseconds, it illuminates the scope for 30 milliseconds.

Having computed these characteristics of the sweep, the computer calls for calibration of the TIMING mechanism to cater for this particular average. This timing calibration is made against an internal standard clock. The calibration involves rotating knobs on the computer to align displayed (X) crosses. Once this is done the statement TRIGGER is put up. This means that a sample of the synchronising pulses to be used to trigger the computer must be put on input  $S_1$  and the trigger threshold adjusted until reliable triggering is obtained. If the level is set too low, noise voltages can initiate sampling, if it is too high the amplitude of the foetal R-wave will be too small to initiate sampling. When good reliable triggering is obtained the computer types  $\llcorner$  to indicate that it is ready to do the averaging.

In the averaging process itself, the quantised values of the analogue signal are assigned special locations in the computer. Suppose these locations were  $q_1, q_2, q_3 \dots q_r \dots q_n$ , then the first sample of each of the complexes is added to  $q_1$ , the second to  $q_2$  and so on. After a number,  $N$ , of complexes have been sampled the display of the contents of these locations will represent the averaged waveform.

The computer can be programmed to make statistical computations

such standard deviations and trends on the contents of these locations and display confidence levels.

Figs. 50(a) and (b) show displays of 95% confidence levels meaning that 95% of the complexes chosen for averaging had the range of waveforms shown. The average is the one displayed in the middle.

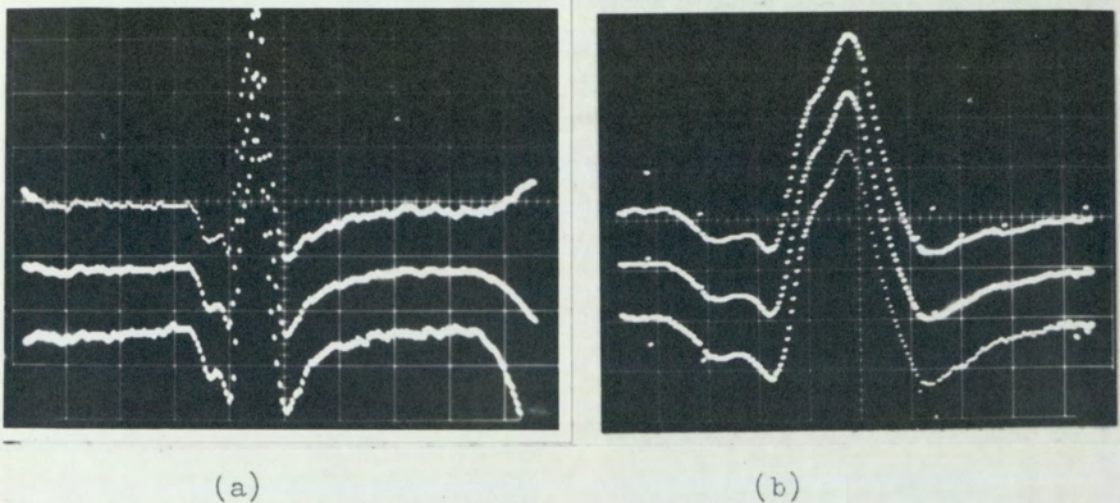


Fig .50.  
Computer display of 95% Confidence Levels.  
(b) represents the expansion of the middle portion of (a).

The computer can also print out the values of the mean and standard deviation for each of the  $q$  locations used to obtain the average.

Thus once a good signal is detected and a good trigger pulse is derived from it, one can use a computer to obtain averages of the foetal electro-cardiogram.

The above is a description applicable only to the PDP8/I. In any actual situation one will have to make use of the computer available. Each computer has its own particular set of facilities. One general feature exists, namely that most errors in averaging arise from failure to trigger accurately.

THE AVERAGED FOETAL COMPLEX

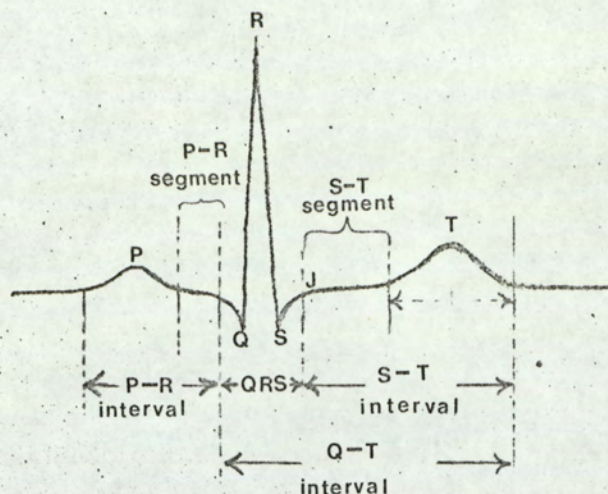


Fig.51. The Main Components of an Electrocardiogram.

Fig.51 shows the normal components one is looking for in an averaged foetal electro-cardiogram using the techniques developed here. It represents a normal electro-cardiogram of an adult and the standard nomenclature used in electro-cardiography (Burch and Windsor)<sup>58</sup>. The nomenclature, P.Q.R.S.T., has been used since the time of Einthoven.

It is not necessary that one gets every one of these portions in an electro-cardiogram when one applies two electrodes to the human being. The diagram contains the important waves which characterise the expected electrical activity of the normal heart.

In general the three limb leads placed as shown in Fig.52 are used in the diagnosis of the state of the heart.

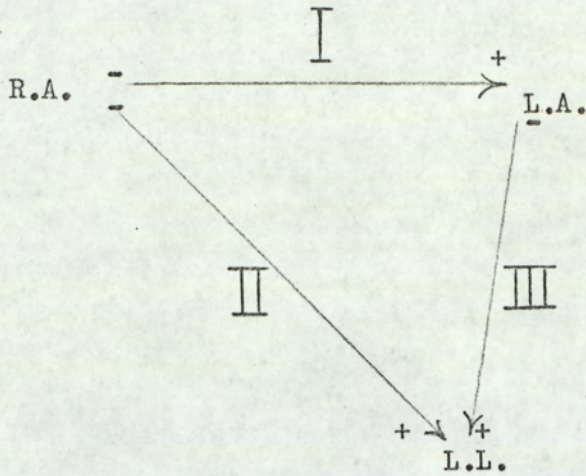


Fig.52. The Main LIMB LEADS used in Electrocardiography.

R.A.= Right Arm Lead ,L.A.= Left Arm Lead, L.L.=Left Leg Lead.

The right leg is usually used as a common terminal.

Fig.53 is a diagram of the conducting system of the heart.

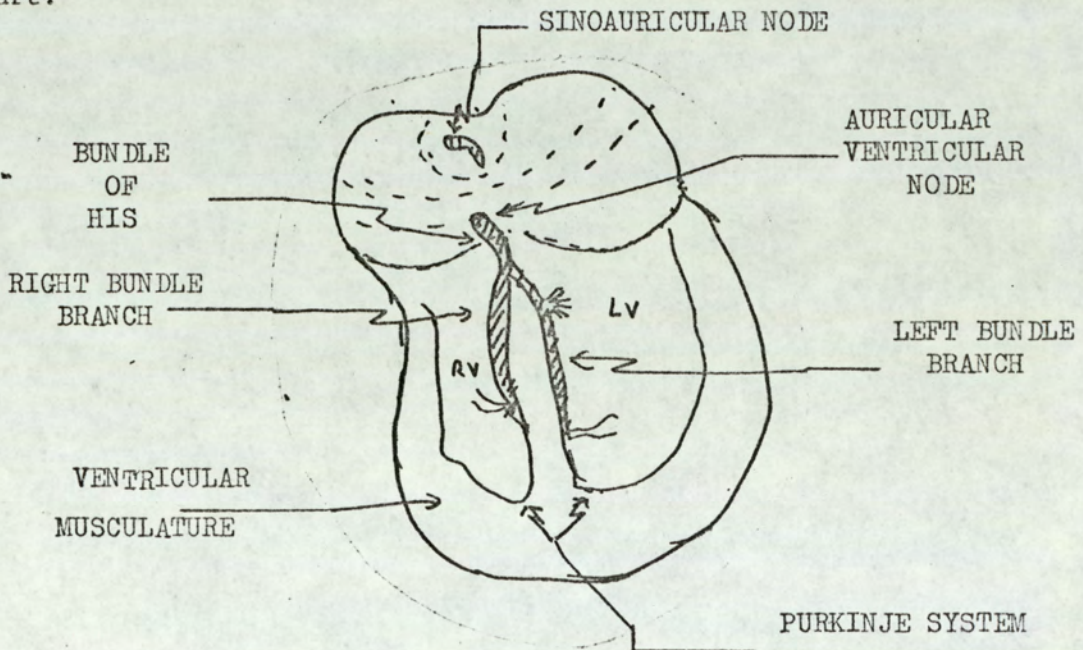


Fig.53. Diagram showing the CONDUCTING SYSTEM of the heart.

Briefly, a signal from the heart's pacemaker in the sinoauricular region sends an electrical wave which, having reached the bundle of

His, in the auricular ventricular node stimulates and sends a wave of depolarisation into the muscles of the ventricles causing them to contract and pump blood round the body. Electrodes placed, as shown in Fig.52, on the body which is a volume conductor can detect the electrical changes taking place during this heart action.

The P-wave (Fig.51) is therefore representative of the pacemaker action. The pacemaker can be regarded as a relaxation oscillator which is sustained by bio-chemical action in that muscle.

The QRS portion represents the mechanical pumping action of the ventricles.

The T-wave represents the repolarisation of the muscles in readiness for a signal from the pacemaker to initiate the next heart beat.

The P-R interval represents the transmission time for the depolarisation wave to travel from the sinoauricular region to the auriculoventricular region.

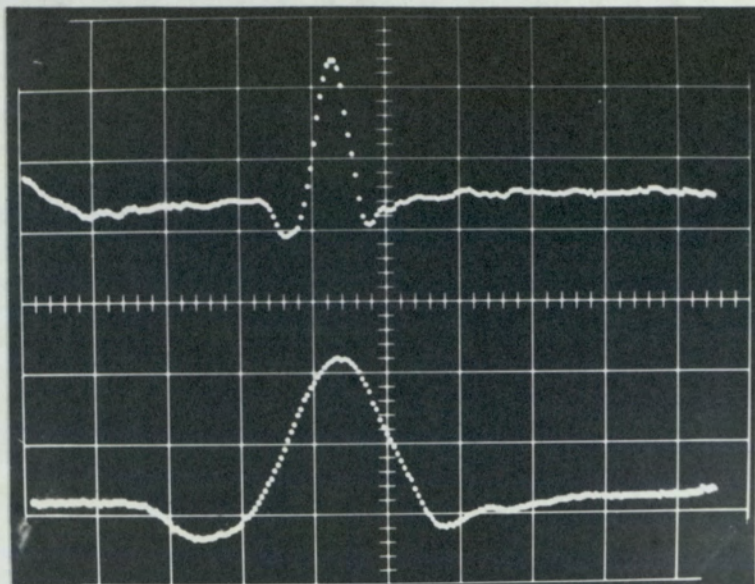
The S-T interval represents the time it takes the electrolytes in the cells of the muscles to return to equilibrium.

It can be seen that a study of the electrical correlate of the heart action can give information which can be used in the diagnosis of disorders in the heart. These disorders are characterised by blocks and shunts in the conducting paths which can lead to slowing down, complete cut-off or speeding up of heart action. Other forms of disorder are due to erratic behaviour of the pacemaker (oscillator) system. The effects of all these departures from normal behaviour have been studied and catalogued under the general title of ELECTROCARDIOLOGY.

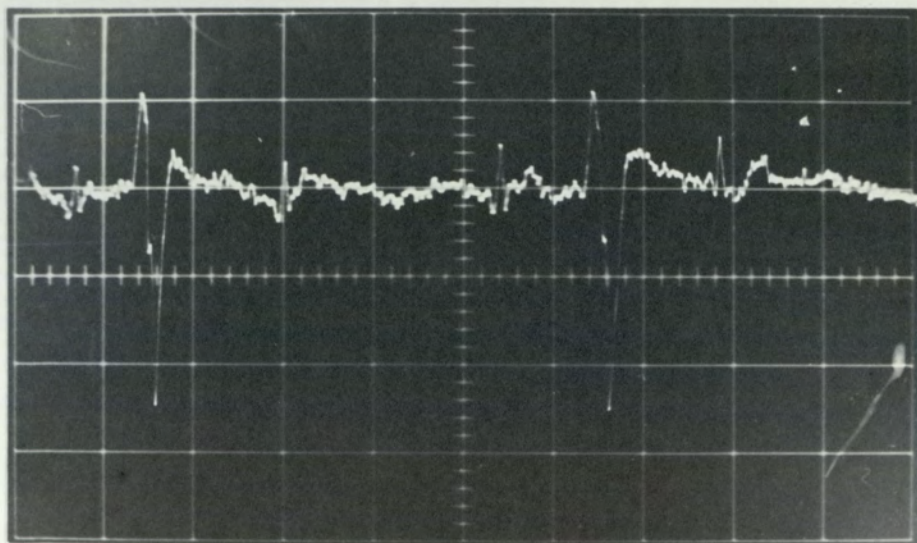
It is in the effort to extend this knowledge to the foetus to help in its management during pregnancy and perhaps after it has been born that it is important to get as much information as possible from a recording made by placing electrodes on the maternal abdomen.

Results of Averaging using the System.

Fig.54(a) represents the result of averaging foetal complexes from a detected signal shown in Fig.54(b) using the present system. The QRS complex can be seen clearly.



(a)



(b)

Fig.54.

(a), Computer Averages of the foetal complexes in (b). The lower trace in (a) is the expansion of the middle portion of the upper trace.

Fig.55 is also an average obtained with the system from an electro-cardiogram of a seven month baby (Lead II see fig.52).

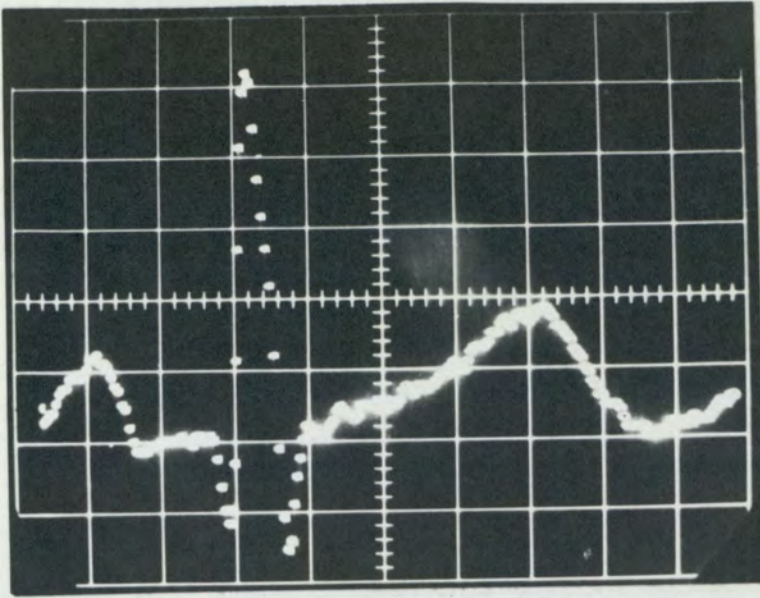


Fig. 55. The average of an electrocardiogram obtained from a seven months old baby, using Lead II

Comparing the top trace of Fig.54(a) with the trace in Fig.55, it can be seen that the P and T waves which are quite clearly shown in Fig.55 are not apparent from the trace in Fig.54(a). Kahn and Koller (59) predict that theoretically there should be an attenuation of the slow waves in the foetal electro-cardiogram due to the filtering effect of the tissues between the foetus and the detecting electrodes.

It is felt that even when this filtering is taken into account there should be some residual slow waves which can at least indicate the beginning of these waves (P & T) to help in calculating the P-R and S-T intervals. With the present system these small voltages are obscured by the effect of the maternal complexes which is nowhere zero. The foetal complexes chosen for averaging are limited to those which occur within a particular region of between the larger portions of the maternal complex. This means that the two complexes (maternal and foetus) cannot be regarded as occurring with no correlation with each other. Even greater correlation will occur when the maternal heart rate is high and the maternal complexes are close together thus limiting the

area of choice.

A look at Fig.50(a) which shows displays of the 95% confidence level reveals that the tail end of the averaged complex is not reliable. This means that the foetal complexes were chosen too near the subsequent maternal complexes. By increasing the delay  $\tau'$  in the maternal blanking system one finds that the region of unreliability is transferred to the leading part of the averaged electro-cardiogram meaning that foetal complexes are being chosen too near the preceding maternal complex.

An improvement of the system to avoid this situation is put forward after discussing results obtained with the system as it is now.

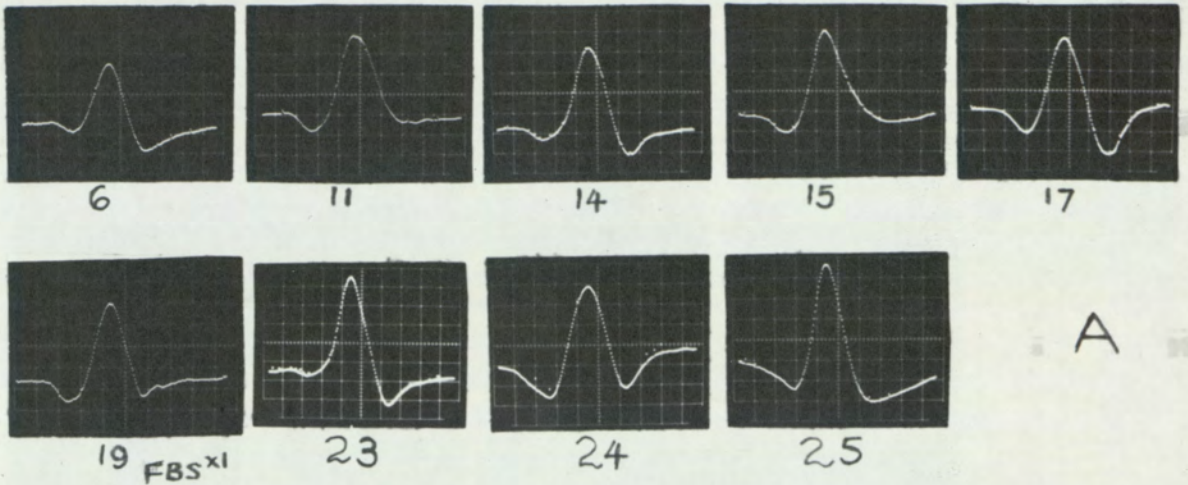
It can be seen, however, that in the neighbourhood of the R-wave (the trigger point), the level of confidence is quite high. This is exemplified by the similarity of the waveforms depicting the QRS portions in Fig.50(b).

It is concluded that the present method of maternal blanking is at least adequate for the study of the QRS complex of the foetal electro-cardiogram or the action of the foetal ventricles.

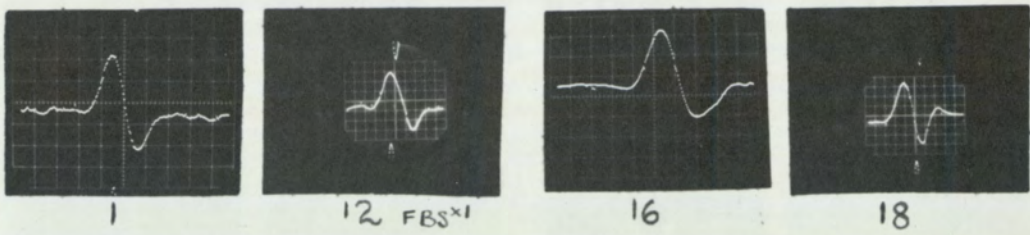
Fig.56 shows examples of the different types of averages of the foetal QRS complexes encountered in the present work. They have been grouped under categories A, A<sup>1</sup>, B, C and D as a result of visual inspection of the waveforms.

Starting with those in category A, it can be seen that all the waveforms show a smooth rise and fall with respect to time. The main difference in the shapes of the complexes in this group is that in the complexes numbered 11, 15, 19 and 24, the troughs of the Q waves are smaller in amplitude than the S waves. In those numbered 6, 14, 17, 23 and 25 the S waves are larger in amplitude than for the Q waves.

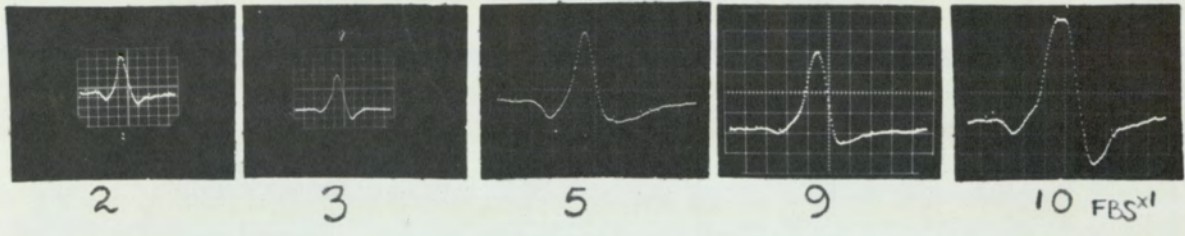
Those in category A<sup>1</sup> also show a smooth rise and fall of the complexes with respect to time. In general, however, the S waves are predominantly larger in amplitude than the Q-waves and the ratio of S wave to the total RS amplitude is much bigger. The waveforms can be described



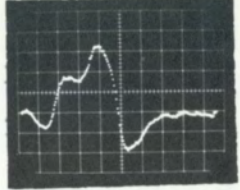
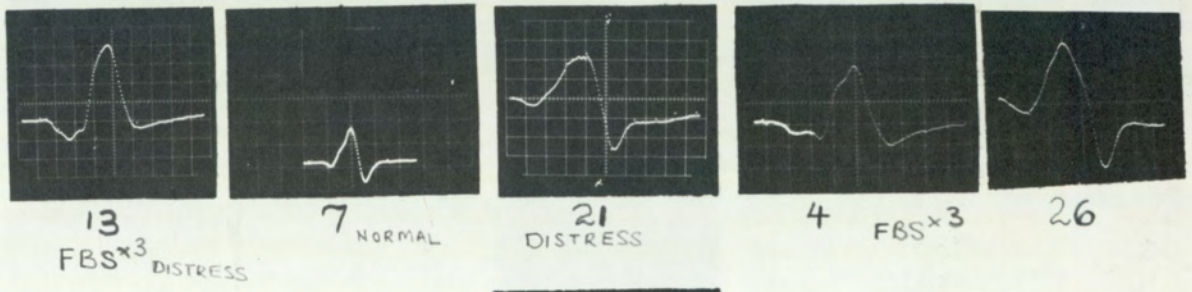
A



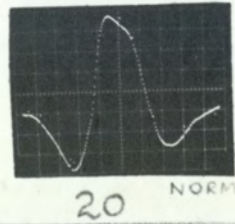
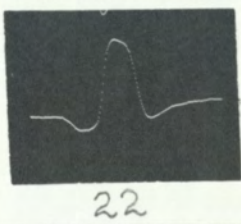
A'



B



C



D

Fig.56

SAMPLES OF AVERAGED FOETAL QRS COMPLEXES.

as 'equally' biphasic.

In those under category B, however, there is a clear initial "slowing down" of the waveform followed by a smooth waveform except for a slight subsequent slowing down at the top of the R-wave of the complex marked 10. The differences in the magnitudes of Q and S-waves are not very great.

In category C the slowing down takes place later than for those in category B but it occurs before the peak of the R-wave. The complexes marked 4 and 26 come from the same foetus but the readings were taken at 24 weeks and 40 weeks of gestation. They have been arranged in increasing order of changes in the rate of rise from the baseline of the QR segment. The complex marked 8 shows the worst amount of slowing down. In this group, also, there is some difference in the relation of the amplitudes of the Q and S waves.

The remaining two complexes classified as category D, show the slowing down after the peak of the R-wave. Also, in both, the Q wave is of greater amplitude than the S wave.

There is a slight slowing down after the peak of the R-wave in the case of the complex marked 26 in category C.

Since sampling at constant rate had been employed in the analogue-to-digital conversion process, the 'slowing down' can be inferred from the closeness of the data points in the regions discussed and used for grouping the complexes.

In all cases the duration of the complexes shown was 74.62 milliseconds (Refer to the computer Summary Fig. ) and with the horizontal scale measurements could be made of the intervals of the portions of the waveforms constituting the QRS of the foetal complexes.

The mechanism or route by which the foetal electro-cardiographic signals reach the maternal abdominal wall is not properly known.

It has been suggested<sup>(59)</sup> that since an insulating vernix caseosa whose conductivity has been estimated as  $1.2 \times 10^{-8}$  (ohm cm<sup>-1</sup>)

by Wimmer<sup>(60)</sup> and  $1.4 \times 10^{-8}$  (ohm cm)<sup>-1</sup> by Bolte<sup>(61)</sup> forms round the foetus the signal can only reach the surface via the umbilical cord-placenta pathway. The other route being the mucous lined passages of the foetus (i.e. naso-pharynx and oropharynx).

"The growing foetus attached by its umbilical cord to the placenta is bathed by the amniotic fluid which is contained within the 'bag of membranes' consisting of amnion and chorion -----Amniotic fluid is fairly freely exchanged with the maternal fluids, it is mainly an excretory product of the amniotic epithelium but it also contains urea and bile salts derived from the foetus. The foetus swallows amniotic fluid and absorbs water and solid constituents in its intestines; the water absorbed is excreted by the foetal kidneys into the amniotic cavity and is again swallowed by the foetus which in this way regulates the volume of the amniotic fluid ----- The function of the amniotic fluid is to provide space for foetal growth and movements and to distribute the pressure due to uterine contractions evenly over the foetus." With this quotation from<sup>(62)</sup> it can be inferred that the amniotic fluid which also fills the foetal lungs is reasonably conducting and could be the return path by which the signal could reach the maternal abdominal surface. If this view is correct then the foetal signal detected from the maternal abdominal surface could represent the electrical activity from a fixed bipolar reference point and with more knowledge empirical formulations can be made to aid in the interpretation of the foetal electro-cardiogram.

From a study of 95 cases by Roche and Hon<sup>(63)</sup> in which one electrode was fixed on the symphysis pubis and the other used to explore the maternal abdomen, both front and back, the following conclusions can be made:-

- (a) In 95% of the cases maximum foetal electro-cardiographic signal amplitudes were found in an area adjacent and above the maternal umbilicus and bounded by the anterior auxiliary lines.

- (b) In 10% of the cases the amplitude remained essentially constant as the electrode was moved across the abdomen and round the back.
- (c) No clear relationship was observed between the area of maximum amplitude of the foetal electro-cardiogram and the position of the placenta. The placenta was located on the anterior wall of the uterus, in the midline, or slightly to the right or left of it in 50% of the cases. On the posterior wall, in the midline or slightly to the left or right in 27% of the cases and in the lateral wall in 3 of the cases.
- (d) The mean amplitudes were 27.4  $\mu$ V, 28.7  $\mu$ V and 27.7  $\mu$ V (SD  $\approx$  75%) for anteriorly located placentas, posteriorly located placentas and laterally located placentas respectively.
- (e) In most patients there was little or no difference in the configuration of the foetal electro-cardiogram record from different positions on the maternal abdominal wall and back. In 7 patients some differences were observed.
- (f) In 71 of the cases in vertex presentation the waveform pointed upwards. In 20 cases the waveform was bi-phasic. In 16 out of 20 of these the main deflection was upwards and in 4 downwards. In 3 of these the signal varied so that it was mainly upwards in certain areas.

They remarked that the umbilical cord-placenta pathway may be an important pathway in the transmission of the foetal electro-cardiogram. They also suggested that the frequent changes in foetal position in utero might help to explain why the amplitude varies during pregnancy.

Remarks (a), (b), (c), (d) and (e) suggest that the resistance of the maternal tissues and the placenta is not high and that once the signal reaches these tissues it can be picked up equally well from any point nearby.

Roche and Hon<sup>(63)</sup> discussed only one route for the signal. With

the other possible route through the amniotic fluid it can be surmised that there will be changes when the orifices were pointing posteriorly or anteriorly with respect to the detecting electrodes, say the fixed one on the symphysis pubis which might be nearer the "bag of membranes".

One could surmise that, if one uses the very simplified travelling dipole model, then the nearer the foetus is to the surface, the more biphasic the signal would seem to be. This was actually seen in the case of the waveform marked 16 in Fig.56. The foetus was so near the surface that the heart beats could be seen. Fig.57 shows a longer recording of this signal from which this average was obtained.

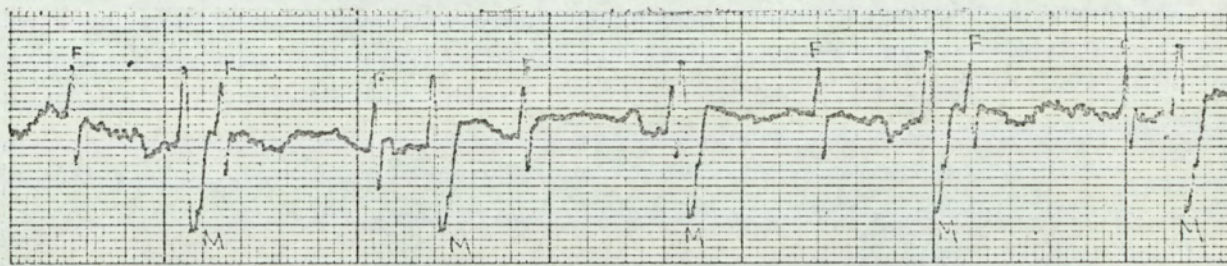


Fig. 57. A chart recording of the signal from which the average numbered 16 (Fig.56) was obtained.

Another indication that the orientation of the foetus could account for the signal being either predominantly mono-phasic or diphasic is exemplified by the complexes marked 4 and 26<sup>in Fig 56</sup>. These were obtained from the same foetus at 24 weeks of gestation when it was in breech presentation and at 40 weeks of gestation when it had turned round to vertex or normal presentation respectively. If the electrical axis of the foetal heart had not changed in the period from 24 weeks to 40 weeks then the orientation could account for the changes in waveform.

Larks<sup>(64)</sup> had concluded that the electro-cardiogram detected from the midline resembles that of the lead II (Fig.52) of the adult

and using the empirical Einthoven triangle<sup>(65)</sup> used it to calculate the electrical axis of the foetus and compare it with that of the neonate. There was some agreement. This also adds some credibility to the supposition that the electrocardiogram comes from a fixed area in the foetus.

However, Wimmer<sup>(60)</sup> and Bolte<sup>(61)</sup> measured only the d-c conductance of the vernix caseosa. It might be that this thin film might have a large capacitance, the impedance of which might be sufficiently small to pass a-c signals. If the capacitance is shunted immediately outside the protective covering by a low tissue resistance it might account for another mode of transmission in which the slow waves of the complex are filtered out i.e. the observation that the P and T waves are smaller in amplitude when the signal is taken from the maternal abdominal wall.

Studies of the conducting properties of the vernix caseosa both with a-c and d-c, the conductivity of the amniotic fluid and uterine tissues coupled with correlation of electro-cardiogram and foetus position are required to throw more light on the interpretation of the different forms taken by the averaged electro-cardiograms obtained in these experiments and shown in Fig.56.

In calculating the electrical axis of the heart or the resultant direction of depolarisation in the heart, Larks<sup>(64)</sup> uses only the ratios of the amplitudes of the Q, R & S waves. It is necessary, however, to stress that there should be an agreed standardisation of detecting systems as far as the low frequency cut-off point is concerned as there can be artificial variations in these ratios as a result of differentiation. The amplitude of the S wave increased in all cases when the low frequency cut-off point was raised. This is exemplified by Fig.58(a),(b),(c),(d) and (e).

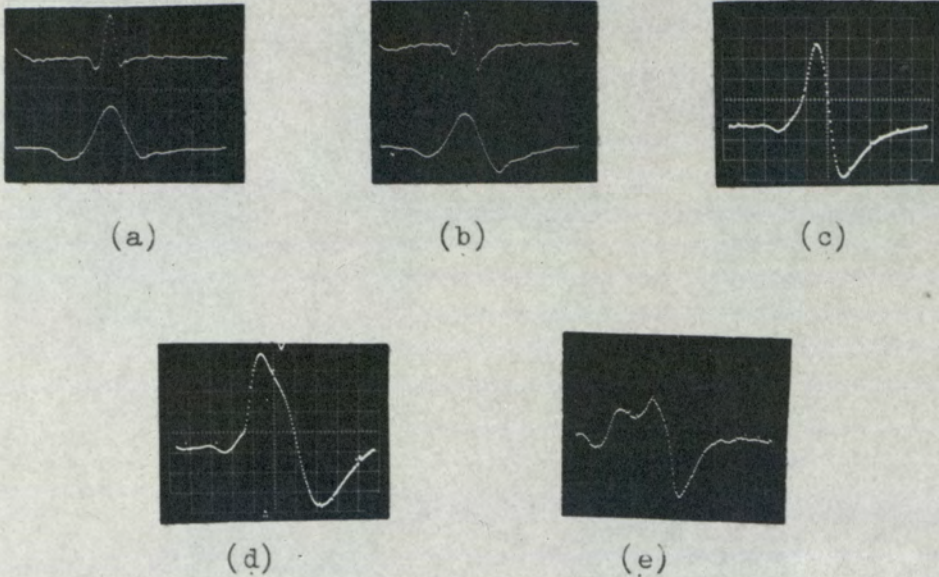


Fig.58. Samples showing the effect of differentiation on the averaged foetal complex (see text ).

Fig.58(a) and (b) are the averages of the same electro-cardiogram numbered 19 in Fig.56. The top traces are the total electro-cardiogram (total time 224 m.sec), and the lower traces the QRS complexes only (duration 74.62 milliseconds). Fig.58(b), however, is the differentiated form of Fig.58(a). It can be seen that this differentiation has increased the amplitude of the  $\mathfrak{S}$  wave. In like manner the complexes in Figs.58(c), (d) and (e) are the differentiated forms of the complexes numbered 9, 20 and 8 in Fig.56. It can also be seen that not only are the  $\mathfrak{S}$  waves of (d) and (e) (compare to 20, 8 artificially increased in amplitude but the 'slow' portions or "kinks" have been displaced forward in time.

These observations show that before one attempts to interpret and categorise these electro-cardiograms a standardisation of the equipments with regard to frequency response is required especially since at the present time only empirical interpretations of electro-cardiograms as a whole (including those of adults) are made by cardiologists, who might be misled by such variations in the appearance

of the signals.

In view of the foregoing it is concluded that differences in the shapes of the complexes categorised under A and A<sup>1</sup> are due to orientation of the foetus, distance from the foetus from the detecting electrode or could be produced artificially by the detecting system and may not be due to any functional differences in the foetal ventricles.

#### Complexes in Category B (Fig.56)

In this group, there is a slight "slowing" down at the beginning of the R waves. A tentative explanation is given here that since the electro-cardiogram represents the electrical activity of the heart muscles "en masse", it is quite possible that there is a slight time difference between the depolarisation processes in the two ventricles or that the two ventricles are not operating in identical manner. Adams<sup>(65)</sup> states that "The absolute and relative weights of the two ventricles have been determined during foetal life and at birth. Prior to the 24th week, the left ventricle is usually heavier than the right. After the 28th week the right ventricle increases in weight more than the left ventricle". This might explain the difference in performance, for at birth the two ventricular outputs (working in series with the lung as will be explained later) must be the same to ensure efficient heart pumping function. The numbers on the complexes shown correspond to period of gestation and although the numbers involved in this work (for testing the system) was small there is a trend that it occurred in younger foetuses. It might be just a sign of foetal immaturity rather than abnormality.

If this view is found to be correct with further and more detailed studies, then one could say that those identified under A, A<sup>1</sup> and B (Fig.56) can be regarded as having normal ventricular function.

Complexes in Category C (Fig.56)

In this case the "slowing" down in the complexes occurred later in the rising part of the R-wave. It could be tentatively assumed that the asynchrony of the actions in the two ventricles had been so developed that this might represent some disturbance in heart function.

Most of the foetuses in category C had foetal distress during labour. The letters FBS printed against the complexes indicate that there was some difficulty during labour necessitating foetal blood sampling (FBS). In this procedure blood samples are taken from the presenting part (mainly the scalp) and acidity or  $P^H$  of the blood is estimated as a parameter for judging foetal heart function. The index after FBS indicates the number of such sampling undertaken. It can be seen that in two of the cases numbered 13 and 26 or 4 (same foetus) there were three calls for foetal blood sampling during labour.

The mother of the foetus whose complex is marked 13 had a history of inter uterine death in her first pregnancy and placental insufficiency in her second. However, the Apgar score recorded at birth was 9 in the first minute which is normal. The Apgar score for the foetus numbered 26 was also 9 in the first minute.

In the case of the foetus whose complex is numbered 21 there was also foetal distress with episodes of foetal bradycardia. At birth it had a low Apgar score in the group. The score was 3 in the first minute and 6 in the first 5 minutes of birth. It had to be resuscitated before breathing commenced.

An averaged electro-cardiogram taken from the baby seven months after birth showing a 'slowing' down in the lead II. Fig.59 shows the 'slowing' down after the peak of the R-wave.

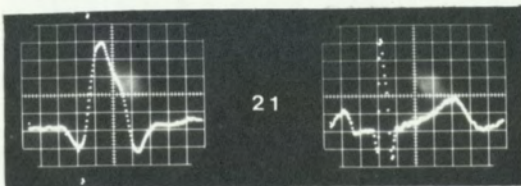


Fig.59.

Shows the transposition of the 'slowing' down in the averaged complex after birth. The prenatal average is numbered 21 in Fig.56.

In the case of the complex marked 8 there was Vasa Praevia one month after the record was taken and the baby had to be delivered prematurely at 34 weeks of gestation. Its Apgar score was the lowest in the group, being 3 in the first minute and 3 at 5 minutes.

In the case of the foetus whose complex is marked 7 in this category, however, there was normal delivery and the baby's Apgar score was 9 in the first minute. The placenta was delivered by fundal pressure.

#### Complexes in Category D

In this case the 'slowing' down occurred after the peak of the R-wave.

In the case of the foetus whose complex is numbered 22 there was foetal distress and one foetal blood sampling (FBS<sup>x1</sup>) was performed. The baby had an Apgar score of 5 in the first minute and 9 in 5 minutes.

In the case of the foetal complex numbered 20 there was no difficulty during labour and the Apgar score of 9 in the first minute is normal. An electro-cardiogram taken seven months after birth showed a 'slowing' down in lead III. In this case as was in the case illustrated in Fig.59, the position of the 'slowing' down was reversed.

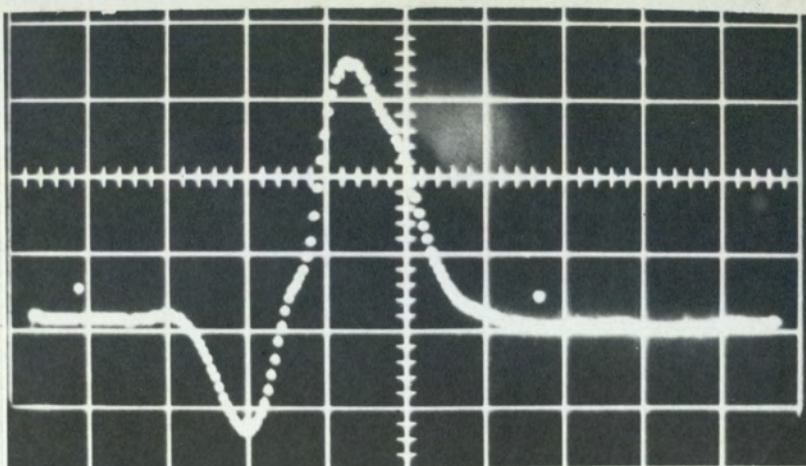


Fig.60.: Showing the post-natal average QRS complex in Lead III. The foetal average is numbered 20 in Fig.56 (see text).

The shift might be due to the order of functioning of the two ventricles after birth. Fig.61 illustrates the many changes which take place in the heart after birth when the lungs begin to function.

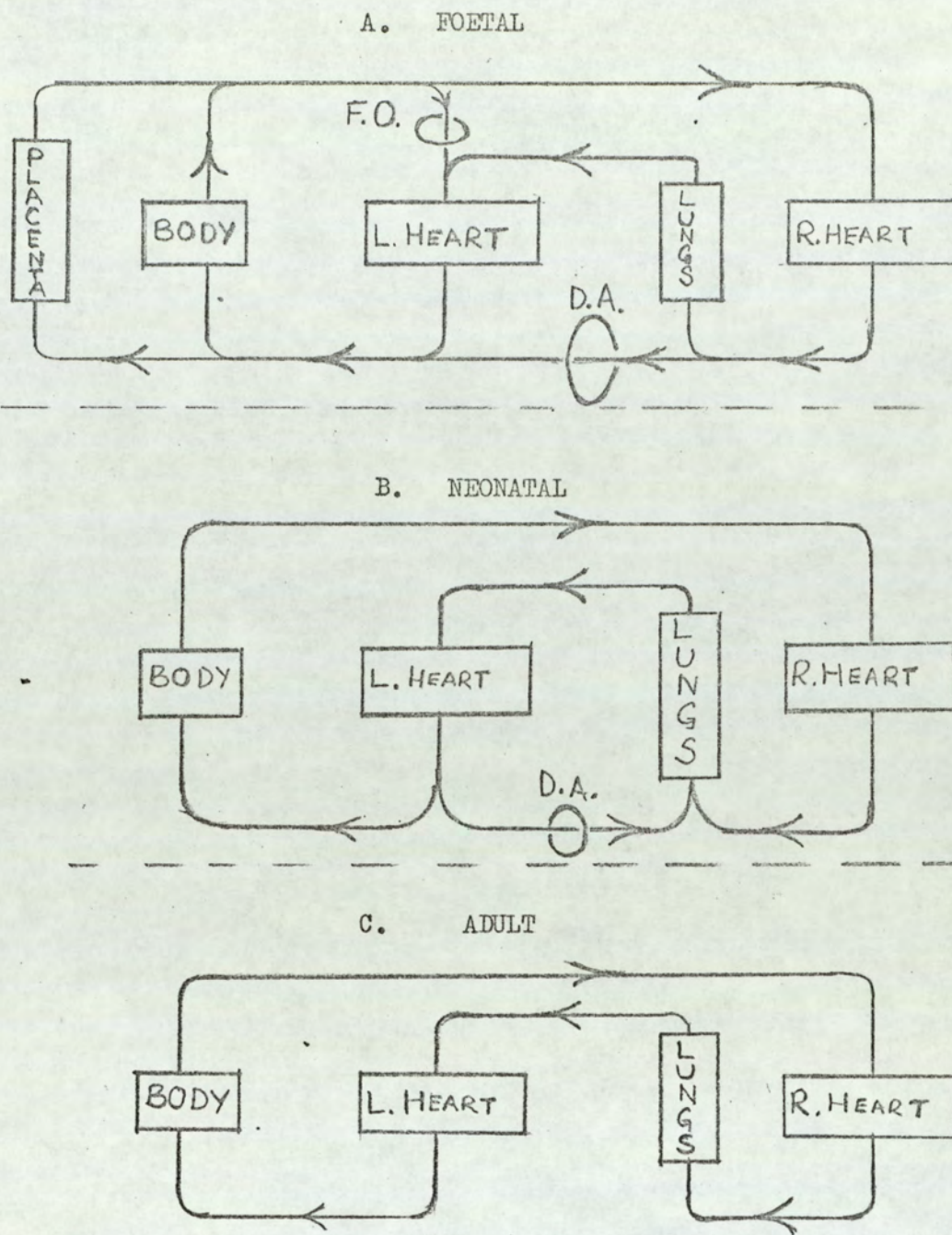


Fig.61.

Simplified diagrams illustrating the changes in the circulation at birth. In A the two ventricles are working in parallel to drive blood from the great veins to the arteries. B is the condition reached a few minutes after birth when the cord is tied and the foramen ovale, F.O. closes. When the ductus arteriosus, D.A. finally closes the adult circulation C is established with the two ventricles working in series. ( G.V. Born, G.S. Dawes, J.C.Mott & J.G.Widdcombe 1954 Cold Spr. Harb. Symp. Quant. Biol. 19. 106 )

In the cases numbered 19, 12 categories A and A' respectively, there was also a call for one foetal blood sampling but there was normal delivery.

In the case of the complex numbered 10 there was one foetal blood sampling performed, and the baby was delivered by forceps. There is a 'slowing' down occurring at the apex of the R-wave as well as the early slowing down. It might be that this indicates that it should have had a category of its own.

It is concluded here that abnormality in the QRS complex might be an indication of some disturbance in the cardiac system which might arise either from the foetal heart itself or from the environment in the uterus, and that larger samples are needed to check whether these abnormalities as shown in categories C and D, could predict the behaviour of the foetus during labour and after.

Lee and Hon<sup>(67)</sup> using scalp electrodes during labour recorded that distortion of the QRS complex could be produced by manipulating the umbilical cord, such manipulation altering the foetal haemodynamics. They concluded that some of these changes may represent organic conduction defects associated with some form of congenital heart disease.

When there is a 'slowing' down or a 'kink' in the waveform near the top of the R-wave, which is used as the fiducial point for triggering the computer, there can be errors of triggering due to "jitter". In other words, the fiducial point is not definite and starting time for sampling might be varying during the averaging process. In such circumstances, such as for complexes obtained in categories C & D, use was made of the fact that differentiation increases the

amplitude of the S wave. With further differentiation the S wave was used as the fiducial point and allowance was made in the value for the delay made in the programming.

Fig.62(a), which shows the timing or sweep summary used to obtain the complex marked 8, can be compared with the computer summary for the rest (Fig. ).

Fig. 62(b) shows the differentiated S wave used for triggering.

The duration of the complex is still 74.62 milliseconds.

```

SWEEP SUMMARY
BEGINS-AT RATE-ENDS
-37.87M 375 U 36.75M
-114.0M 1.125M 109.8M

```

```

AVERAGES
CHAN RATE TYPE SORT
1 L 1 0
1 H 1 0

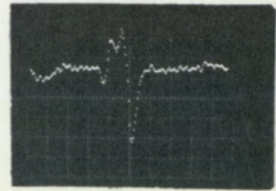
```

```

SYNC ON CHANNEL: S1
64 SWEEPS AT 300.0MS
(VBP,0,230 -6277)
!
[
TIMING...R
TRIGGER...
!
[ <

```

(a)



(b)

Fig.62.

Showing changes in timing,(a), when using the differentiated S-wave instead of the usual R-wave, (b), for triggering.

#### Effect of high cut-off frequency on averaged waveform.

Fig.63(a) and (b) were obtained from the same complex. In Fig.63(b) the bandwidth was cut from 130 Hz to 100 Hz. It can be seen that the "slowing" down seen in Fig.63(a) has been rounded off by this process. This shows that when the bandwidth is too small such features of the electro-cardiogram which need higher frequency components to make them manifest will be lost. In this work the high frequency point was set at 130 Hz only because of the interference of the demodulation in the F.M. tape recorder. This could be increased if a recorder using

an F.M. system having higher intermediate carrier frequencies were available.

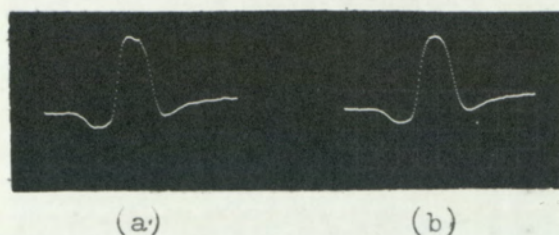


Fig.63. The effect of Bandwidth on the Waveform. The 'slowing' at R in (a) is smoothed off when the High cut-off frequency is reduced.

Effect of changes in foetal heart rate on the averaged complex.

Fig.64(a) and (b) were obtained from the same foetus during labour. Fig.64(a) was obtained when the heart rate was about 130 beats/minute and Fig.64(b) obtained when the rate dropped to 110 beats/min. It can be seen that the rise to the isoelectric line (zero line) from the trough of the S-wave is quicker for the complex in 64(b). One could say that the heart is responding to the fall in heart rate by prolonging the S-T segment. This can better be shown if the whole complex had been produced faithfully without the interference of the maternal complex which affects the extremities of the waveform in the manner discussed earlier. If this were the case, changes in the complex could be used to indicate foetal distress. Here again this was measured in only one case and has not been confirmed.

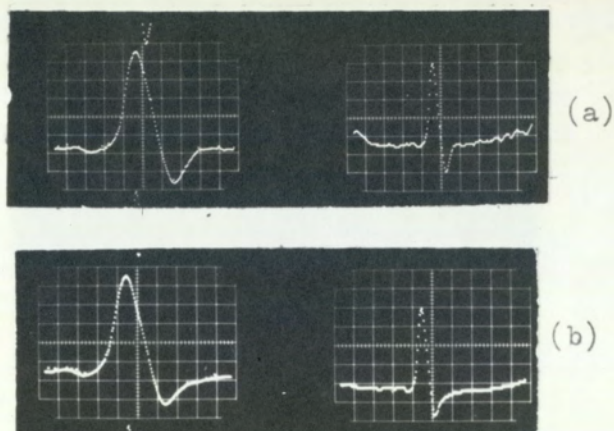


Fig. 64. Change in the averaged complex with change in foetal heart rate (see text above). The averages on the right represent the total electrocardiogram.

TIME MEASUREMENTS ON THE AVERAGED FOETAL Q.R.S. COMPLEXES

Number on Complex	Period of Gestation (MTS)	Duration of QRS(msec)	Duration of QS (msec)	Sex	Rate during averaging beats/minute		
					Minimum	Average	Maximum
				F=Female M=Male			
1	5.00	36.4	19.1	F	143	149	154
2	5.75	47.0	25.4	M	133	133	133
3	5.75	46.4	25.8	M	139	146	154
4	6.00	58.7	26.4	F	146	146	146
5	6.50	49.3	25.4		140	146	152
6	7.00	54.0	28.2	M	150	154	157
7	7.25	49.3	27.0	F	133	145	146
8	7.50	52.4	31.8	M	133	133	133
9	8.00	49.3	24.2	F	140	151	162
10	9.00	52.2	31.4	F	128	141	154
11	9.00	52.0	32.6		128	128	128
12	9.00	53.0	33.0	F	148	154	171
13	9.25	59.5	33.2	M	110	115	120
14	9.25	51.6	33.0	M	143	152	162
15	9.25	63.5	29.4	M	133	133	133
16	10.00	49.2	32.5	F	133	148	164
17	9.75	58.0	31.8	M	122	127	133
18	9.75	55.5	27.0	F	120	130	139
19	9.50	55.5	27.5	M	120	126	133
20	9.50	66.7	38.1	F	139	142	154
21	9.95	55.5	31.5	F	125	131	136
22	10.00	55.5	27.5	F	125	131	136
23	10.00	29.5	34.2	M	86	108	130
24	10.00	58.0	30.6	M	130	133	136
25	10.50	63.5	29.4		130	133	136
26	10.50	58.0	36.5	F	146	146	146

Table (III)

There is a scale on each of the QRS complexes averaged (see Fig.56).

This facilitates accurate measurement of duration.

The duration of each complex is 74.62 milliseconds and using this values of the duration of the QRS were determined.

It was also thought that since it is easier to determine the turning points in the waveforms instead of the rather arbitrary beginnings and endings of the QRS waves, values of the QS segments be determined. The results are tabulated in table (III)

The top graph in Fig.65 shows the relationship between the duration of the QRS complexes with the period of gestation. The lower graph shows the relationship between the duration of the QS segment and the period of gestation.

Although this number used for checking the system was small, the graphs show an increase of durations of both the QRS and QS with period of gestation after 5 months of gestation. The respective regression lines had equations:

$$T_{QRS} = 2.7M + 31.3 \dots\dots\dots (76)$$

$$T_{QS} = 1.8M + 14.6 \dots\dots\dots (77)$$

where T is measured in milliseconds

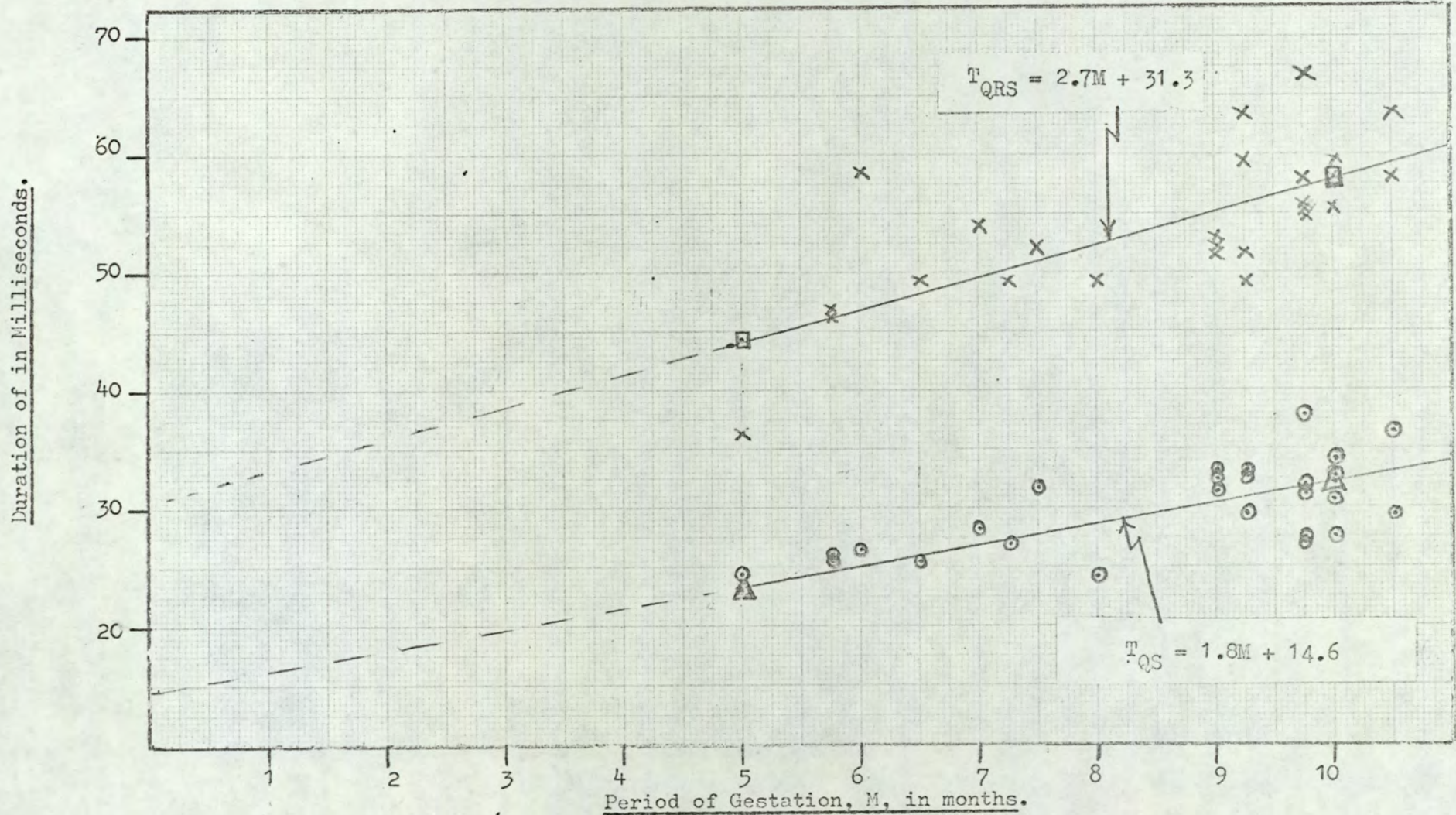
M is the period of gestation measured in months (4wks = 1 month)

The duration of the QRS ranged from 36 to 67 milliseconds with a mean of 54.2 milliseconds at 8.6 months of gestation, after five months of gestation. This result is in agreement with results obtained by Behrer et al<sup>(68)</sup> whose values of the duration of the QRS complex ranged between 30 and 68 milliseconds.

The duration of the QS complex ranged from 19 to 38 milliseconds with a mean of 29.7 milliseconds at 8.6 months of gestation.

If these ranges are considered normal then all the complexes shown in Fig.56 are normal as far as the duration of the QRS complex is concerned.

Fig.65. Duration of QRS Complex v/s Period of Gestation.



The duration of the QS section was measured because it is easier to determine and if it is related to the duration of the QRS then information about QRS complex can be obtained by calculating the mean of the duration of the QRS complex from a raw signal without averaging with a computer. In this case using say a chart recorder or oscilloscope of known speed or sweep one can take the mean of the duration of say 30 complexes.

There was no obvious relationship between the duration of the QRS complexes and the sex of the patient or the foetal heart rate.

The foetal heart rate varied from 120 b/m to 162 b/m with a mean of 138.5 (S.D.± 4.1) for males and 136 b/m to 171 b/m with a mean of 150.9 (S.D.± 3.7) for females.

CHAPTER III

USE OF THE DIGITAL COMPUTER FOR ELIMINATING

THE MATERNAL COMPLEX

CHAPTER IIIUSE OF THE DIGITAL COMPUTER FOR ELIMINATING THE  
MATERNAL COMPLEX

It has been stated earlier that confidence can be put only on the average of the QRS complex when using the method of maternal "blanking". This is because the maternal complex is always influencing the periods in the signal from which the foetal complexes are chosen for averaging as explained under the section on results of averaging using the present system.

The conclusion had been already reached by other workers as well, that it is not possible or very difficult to obtain a maternal complex having exact waveform to that obtained from the abdomen, from any other part of the body where there is no foetal signal to use in eliminating the maternal complex totally from the signal.

The only other method of approach is to average the maternal complex (say 100 complexes) and subsequently subtract the averaged complex from a delayed form of the signal whenever a maternal signal occurs. This should theoretically leave a signal containing the foetal signal and noise including residue of the maternal complex as a result of the subtraction. One could then average this latter signal to obtain the average of the foetal complex with much reduced risk of contaminating the foetal signal with correlated maternal signal.

The added advantage of such a method is that provided a good foetal signal is detected, one can trigger a ratemeter with the signal minus the averaged maternal complex to obtain very directly the foetal heart rate, which is at the moment needed by obstetricians during foetal distress.

This scheme was not tried out in the present experiments for lack of time available.

It has been found, however, that other workers have proposed and tried similar schemes. Favret<sup>(69)</sup> had proposed such a scheme using

two consecutive stages of processing. This is the method that Behrer et al<sup>(68)</sup> used in their work.

A variation has been proposed and tried recently by Van Bommel et al.<sup>(70)</sup> Their main objections to Favret's method are based on the following considerations:-

1. The maternal complex is often not constant in amplitude due to modulating disturbance (e.g. respiration). Consequently, after subtraction of an averaged maternal complex, part of the maternal signal remains. This hampers the exact determination of foetal R peaks in the recording. Further, it is rather difficult to detect very accurately foetal R waves which coincide with maternal QRS complexes without a digital computer because the waveforms of both complexes are statistically not orthogonal.
2. Since both maternal and foetal ECG complexes occur almost periodically, a statistical dependence between these two ECG is noticeable, certainly during finite time. This dependence becomes artificially enormously large when only the foetal ECG complexes are averaged which do not coincide with maternal QRS complexes. In this way the probability of influencing the averaged result of the foetal QRS complex by maternal P and T waves, but not by maternal QRS complexes, is increased. Owing to this dependence between maternal ECG's an averaged PQRST complex arises in which the maternal ECG is not averaged out. Their scheme can be described briefly as follows:-

- (a) Only those foetal complexes for which no coincidence exists between the foetal R-wave and the maternal QRS complex are averaged.
- (b) An artificial maternal average is obtained (free from foetal complexes) and run synchronously with the signal

(b) containing the foetal complexes. A foetal R-wave such as in (a) triggers the parallel averaging of foetal signal in the main signal and the maternal complex in the same temporal period in between the QRS complexes of the artificially produced maternal average.

(c) The result of the average of the artificial maternal complex is then subtracted from the result of the averaged foetal complex.

The results of Van Bommel et al are good and show the beginnings of the P and T waves which are needed for measurements including temporal ones on the averaged foetal complex.

In principle, however, it is felt that the two schemes are nearly the same as far as eliminating the maternal complex is concerned. Both techniques involve the production of a fixed artificial signal.

The difficulty in both methods is that this averaged signal must not be statistically different from any subsequent individual maternal complex. In the case of the method used by Van Bommel et al, once the artificial complex is produced it is the interval between the same artificial complex in time that is selected for producing the maternal averaged residue which is used for subtracting as outlined in (c) above. If the shape of an individual subsequent maternal complex changes, although the part of this complex on which the foetal signal is chosen for averaging might change, the contribution to the maternal averaged residue chosen for the same foetal period would be obtained from the fixed artificial maternal interval. So that what is subtracted might not exactly be what would have been ideally subtracted.

Looking at the results of the subtraction of the averaged maternal waveform obtained by Behrer et al,<sup>(68)</sup> a good example being their Fig.3 reproduced here as Fig.66, one feels that only the maternal QRS complex had been averaged and subtracted leaving the slow maternal P and T waves.

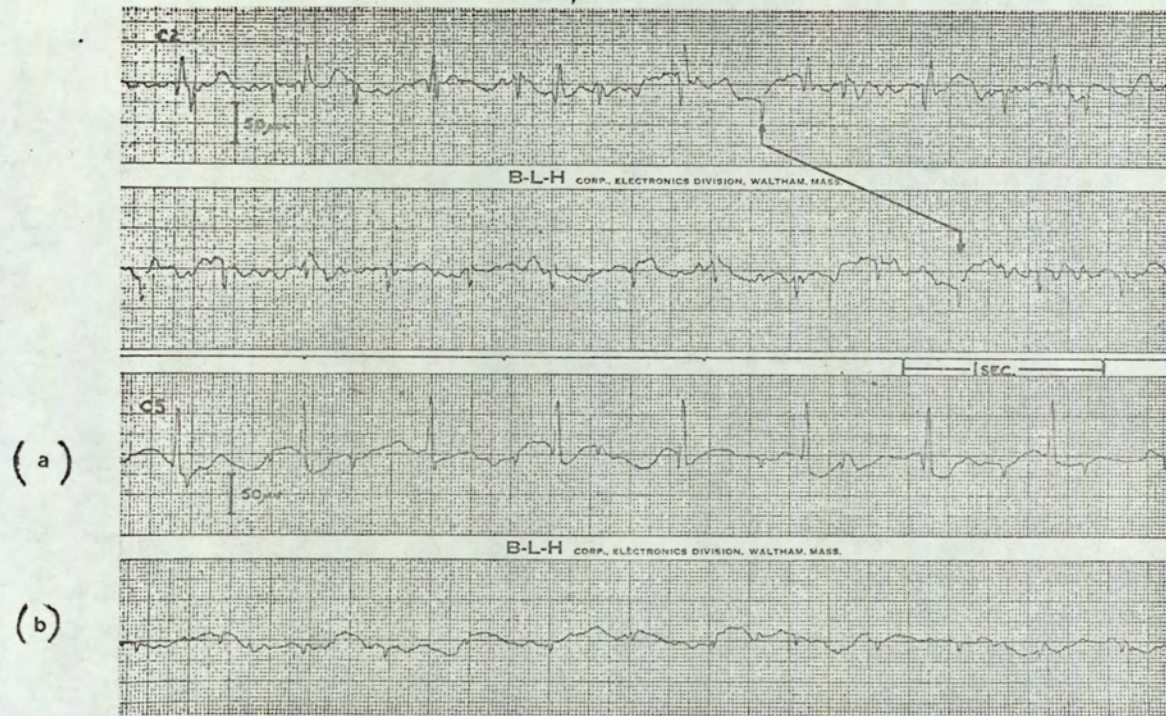


Fig.66. Example of Elimination of Maternal QRS complex in (a) leaving the slow maternal waves in (b) (see text) Reproduced from Behrer et al(68). Fig.3

As a result of using the maternal 'blanking' scheme in the present system, one finds that the statement 2 of Van Bommel et al quoted above is correct and that it is the influence of the maternal P and T waves which must be eliminated.

It is proposed therefore that in using Favret's method the total PQRS of the maternal complex should be averaged out and used to subtract from a subsequent maternal complex. This difference must be re-recorded and computer averaging of the foetal signal carried out subsequently.

It is felt that in the short time that it would take to average say 50 of such foetal complexes (occurring on average 2 beats/min) the maternal complex would not have altered too much. Although the result might not be much different from that produced by the system used by Van Bommel et al, it will have the advantage that a rate meter or pulse interval meter can display continuously (when using occasional updating of the maternal average) the rate which obstetricians need during labour.

This scheme is being justified by the fact that for studies carried out during early periods of gestation (before actual labour) there is no rush for time and the actual period on the tape record from which the maternal average was obtained can be replayed for the maternal subtraction process before foetal complex averaging. During labour the foetal heart rate which is at present important to the obstetrician can be monitored continuously. The foetal averaged waveform can then be computed with the method after the labour period and the findings correlated with corresponding changes in foetal rate.

The scheme which is not essentially different from Favret's with the added precaution that the whole maternal PQRS complex should be averaged and subtracted, would be as shown in Fig.67.

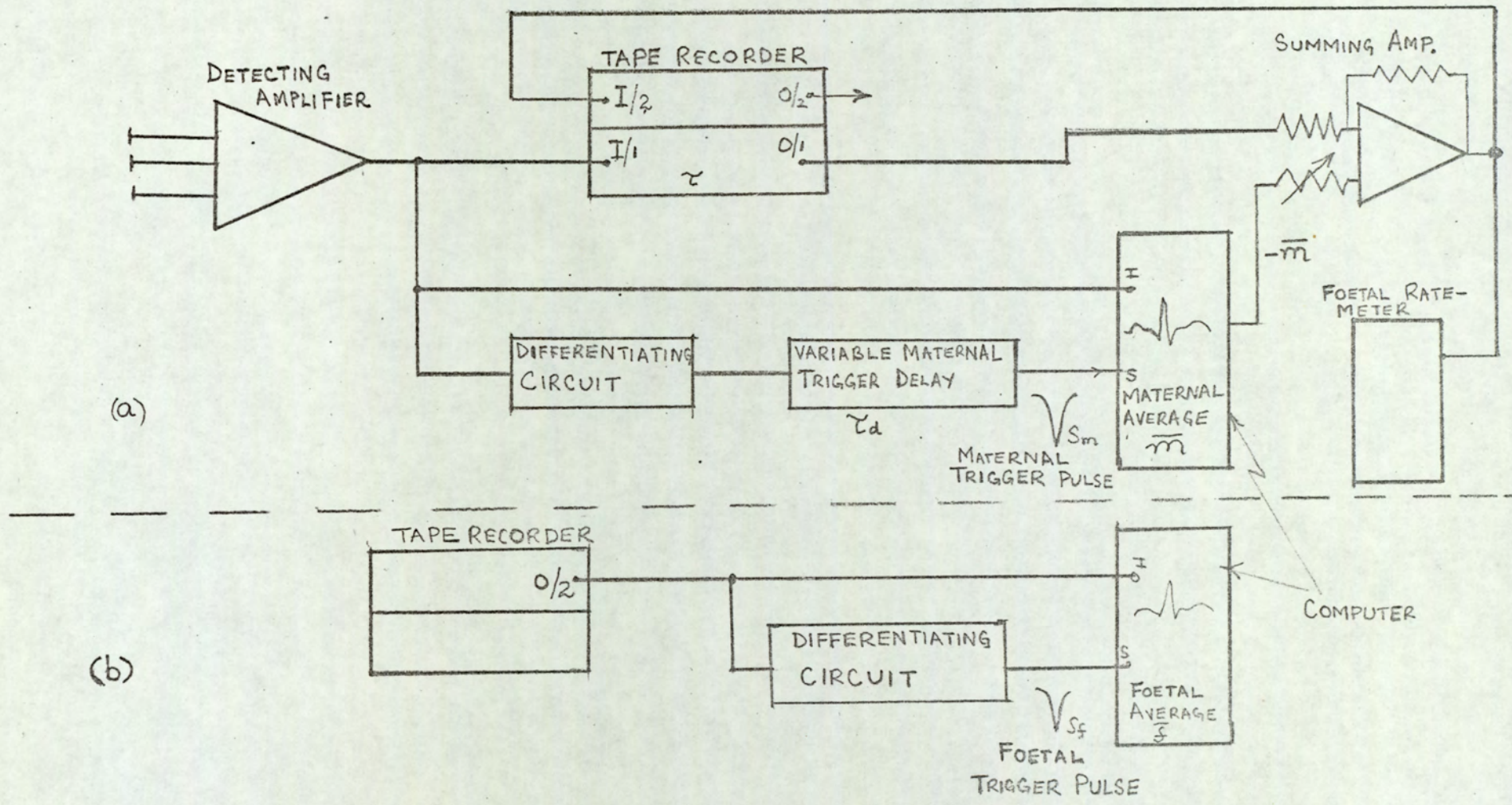


FIG. 67. SCHEME FOR ELIMINATING THE MATERNAL COMPLEX, (a), AND SUBSEQUENT AVERAGING OF FOETAL COMPLEX, (b)

In this scheme the delay

$$\tau^1 = \tau - \tau_d$$

where  $\tau$  is the fixed tape recorder delay

$\tau_d$  is the variable delay for triggering out the averaged maternal PQRSST.

should be such as to ensure synchronous subtraction of the maternal complex.

The differentiating circuits have been included to reduce the wandering of the baseline to ensure dependable triggering.

It might be necessary to make simultaneous measurements from fixed locations on the maternal abdomen to establish the orientation of the foetal heart and the transmission path of the foetal signal. In such cases the best foetal signal from any of the leads (say 3 pairs of leads) could be used to trigger the averaging of the foetal complexes in all the leads. The same can be done with the best maternal signal.

For such work three identical amplifiers would be needed for recording and multiple channels will be needed in the tape recorders and the computers.

Such studies will throw more light on the mechanism of the transmission of the foetal signal and the much needed knowledge gained could be used to produce much simpler measuring systems for routine foetal electro-cardiography.

Schemes of this kind have always been criticised on the grounds that:-

1. They are too elaborate and complicated.
2. The poorer hospital organisations cannot afford to buy computers.

The first criticism can be met by hospital physicists and engineers if they collaborate well with obstetricians.

Computers are now becoming quite readily available and cheaper, and the second difficulty will not remain indefinitely.

There is a need, as many workers including Van Bommel et al<sup>(70)</sup> have pointed out, for a method which computes from the simple, safe and potentially more useful abdominal foetal electro-cardiogram, the foetal P.Q.R.S.T. complex, free from noise. Only then will accurate classification and correlation with clinical experience be possible.

In this present work a general review of the subject has been carried out and some experimental procedures and results presented.

It is felt that most of the difficulties are in instrumentation for detecting a reasonable foetal signal from the maternal abdomen. To this end the thesis has presented plausible lines for developing amplifiers suitable for detecting the foetal signal and also has introduced the use of graphite cloth electrodes which it is felt can improve the detecting process.

For processing the signal, it is felt that the best method is to pursue further the methods using computers discussed and suggested in this chapter.

At the present time obstetricians pay attention only to the foetal heart rate, especially at the very end of pregnancy during foetal distress. This is because this is the only parameter that is understood.

When computers have been used to obtain sufficient knowledge about the shapes and orientations of the foetal electro-cardiogram as a result of studies of the conducting properties of the foetal, uterine and maternal tissues it is probable that foetal electro-cardiography using abdominal electrodes can be developed to become an important and less empirical method for use during pregnancy and labour.

## REFERENCES

1. Von Max Cremer - "Über die direkte Ableitung der Aktionströme des menschlichen Herzens vom Oesophagus und über das Elektrokardiogramm des Fötus" - MUENCHENER MEDIZISCHE WOCHENSCHRIFT No.17 pp 881-813 April 1906.
2. Foa, C. - "Lelectrocardiogramme foetal" - Archive Haliennes de Biologie - Tome LV1 pp 145-147 1911.
3. Krumbhaar, E.B. - "Electrocardiographic studies in normal infants" - Proceedings, American Journal of Physiology Vol.40 pp 133 1916.
4. Maekawa, M. Toyoshima J.  
- Acta Scholae Med.Univ.Imp.Icioto  
12 p 519 1930.
5. Bell, G.H. - J.Obstet & Gynec. Brit.Smp. 45 p 802 1938.
6. Smyth, C.N. - "Experimental Electrocardiography"  
- Lancet 1, pp 1124-1126, 1953.
7. Southern, E.M. - "Foetal Anoxia and its possible relation to changes in the prenatal foetal electrocardiogram."  
- Amer.J.Obstet. & Gynec. 73 pp 233-247 1957.
8. Larks, S.D. - "Fetal Electrocardiography" - Charles C. Thomas, Springfield, Illinois, 1961.
9. Bernstein, R.L. - "Fetal electrocardiography and electro encephalography. Charles C. Thomas, Springfield, Illinois 1961.
10. Caughey, A.F. Jr. - "Electronic detection of fetal life - A review" - Obstet and Gynec. Vol.17. No.3 1961.
11. Shubeck, F. - "Fetal electrocardiography - A survey" - Univ. Mich-Med. Cent.Journal, 30, 19, 1964.
12. <sup>Sureau</sup> Gureu, C. - "Electronic and Medicine" - Documenta Geigy" pp 5-6, 1965.
13. Sheu<sup>n</sup>ker, Lewis - "Fetal electrocardiography" Obstet and Gynec. Review 1966.
14. Caldeyro - Barcia *et al.* Proc. 4<sup>th</sup> International Conference on <sup>1961</sup> medical electronics. N. Y. 1961.
15. Hon, E.H. - "The electronic evaluation of fetal heart rate" -Amer. J. Obstet.Gynec. 75, pp 1215-1230, 1958.
16. Shelley, T. - "Foetal heart rate measurement in pregnancy and Labour" - Ph.D. Thesis Sheffield University, 1967.

\* Title: "Effects of uterine contractions on the heart rate of the human foetus."

17. Sureau, C, Trocellier, R. - "A technical problem of fetal electrocardiography - Note on the elimination of the maternal electrocardiograph"  
- Gynec. Obst. (Paris) 60, 43, 1961.
18. Sureau, C, Trocellier, R. - "Etude de Quelques problemes techniques en electrocardiographic foetal"  
- Med.Elec. Biol.Eng. Vol.1. pp 181-188, 1963.
19. Walden, W.D. and Birnbaum, S.J.  
- "Fotel electrocardiology with cancellation of maternal complexes" - Amer.J.Obstet. & Gynec. 94, pp 596-598 (1966).
20. Goddard, B.A., Newell, J.A., Edwards, R.L., Farr, R.F.  
- "A clinical foetal Electrocardiograph"  
- Med.& Biol.Eng. Vol.4. pp 159-167 (1966).
21. Einthoven, W. - Nobel Prize Lectures - Physiology or Medicine 1922-1941 - Elsevier Publishing Company pp 88.
22. Matthews, B.H.C. - "A new electrical recording system"  
- The moving-iron oscilloscope.
23. Adrian, E.D. and Matthews, B.H.C. - "Otential waves in the Cortex" - J.Physiology 81, 440 (1934)
24. Matthews, B.H.C. - "A special purpose amplifier" - J.Physiology 81, 28 p - 29p.
25. Middlebrook, R.D. - "Differential Amplifiers - Their analysis and their applications in Transistor d-c amplifiers"- John Wiley & Sons (1963)
26. Offner, F.F. - "Push-pull Resistance coupled Amplifiers"  
- Rev.Sci. Inst. Vol.8. pp 20-21 (1937)
27. Blumlein, A.D. - "Long tail pair"  
- British patent No.482740, (4.7.36)
28. Matthews, B.H.C. - "Compressor input stage" - J.Physiology 93 pp25 (1938)
29. — *Tönnies* - Rev.Sci.Inst. 9, p 95 (1938)
30. Goldberg, H. - "Bioelectric Research Apparatus"  
Proc. IRE. Vol.32 pp330-336 (1944)
31. Goldberg, H. - "A high gain amplifier for bioelectric recording"  
Trans. AIEE Vol.59 pp60-64 (1940)
32. Parnum, D.H. - "Biological Amplifiers" - Wireless World Vol.51 pp337-340 (Nov.1945)
33. Klein, G. - "Rejection Factors of Differential Amplifiers"  
- Phillips Research Report, Vol.10 pp241-259 (Aug.1955)
34. Parnum, D.H. - "Biological Amplifiers" Wireless World Vol.51 pp337-340, Nov.1945, pp373-376, (Dec.1945)

35. Birt, D.R. "Self-balancing push-pull circuits"  
Wireless World, Vol.66 pp223-227 (May 1960)  
pp283-285 (June 1960)
36. Angelo, E.J. - "Electronic Circuits" McGraw-Hill Book Co.  
New York pp283-287 (1958)
37. Andrew, A.M. - "Differential Amplifier Design"  
Wireless Eng. Vol.33 pp73-79 (March 1955)
38. Shea, R.F. - Amplifier Handbook - Chapter 18  
McGraw-Hill Book Company.
39. Middlebrook, R.D. and Taylor, A.D. - "Differential Amplifier  
with regulator achieves High stability, Low  
Drift" - Electronics 34, 56, July 1961.
40. Emmons, S.P., Spence, H.W. - "Very low-drift, complementary  
semiconductor network d-c amplifier" IEEE  
Journal of solid state circuits, Vol.Sc.1.  
No.1 pp13-18 (1966)
41. Nyquist, H. - "Thermal agitation of electronic charge in  
conductor" - Physical Review Vol.32, p110 (1928)
42. Bull, C.S. - "Fluctuations of Stationary and Non-stationary electron  
currents" - Butterworths pp76-79 (1966)
43. Schottky, W. - Ann. der Phys. 57, (1918) 541; 68(1922) 157.
44. Johnson, J.B. - "The Schottky effect in Low-frequency circuits"  
- Phys.Review 26 July 1925.
45. Schottky, W. - "Small-shot effect and Flicker-effect"  
- Phys.Review 28, 74, (1926)
46. Bull, C.S. - "Space charge as a source of Flicker Effect"  
Proc.Inst.Elec.Eng. 105, part B,  
No.20 pp 193-194 (1958)
47. Bull, C.S. and Bozic, S.M. - "Excess noise in semiconducting  
devices due to fluctuations in their characteristics  
when signals are applied" - British Journal of  
Applied Physics 1967, Vol.18, pp 883-885.
48. Roy, O.Z. and Nehmert, R.N. - "Keeping the heart alive with a  
biological battery" - Electronics 39, 6 pp 105-107  
March 1966.
49. Flasterstein, A.H. - "Voltage fluctuations of metal-electrolyte  
interfaces in electrophysiology" and "A general  
analysis of voltage fluctuations of metal-electrolyte  
interfaces" - Medical and Biological Engineering,  
Vol.4 pp 583-588 and pp 589-594 (1966)
50. Van Bommel J.H. - "Detection of weak foetal electro-cardiograms by  
Auto correlation and Cross correlation of envelopes"  
I.E.E.E. Tran. on Biomedical Eng., Vol.BME-15 No.1  
pp 17-23 (1968).
51. From "Instrumentation in Medicine" Ed. J.M.A. Lenihan,  
Morgan - Grampion, London 1968.

52. Kendall, B., Farrell, D.M. and Kane, H.A. -  
American Journal of Obstet. & Gynec.  
83, 1629 (1962)
53. Larks, S.D. - Fetal Electrocardiography  
Proc - 3rd International Conference on  
Medical Electronics 1960.
54. Green, J.R. - "Transistor sub units for biological stimulation" -  
Third International Convention on Medical  
Electronics, July 1960.
55. Katzman, R.  
N.Y.Acad.Sci. 112, 3 1964.
56. Cox, Jerome R. Jr. - "Computers in Biomedical Research"  
Vol.II Chap.3 - Academic Press, New York, London.
57. Macy Josiah, Jr. - "Analogue - Digital Conversion Systems"  
Computers in Biomedical Research, Vol.II Chap.I,  
Academic Press, New York, London.
58. Burch, G.E. and Windsor, T. - "A primer of electrocardiography"  
Publisher - Henry Kimpton, London 1960.
59. Kahn, A.R., Koller, S - "Effects of the foetal-maternal interface  
on the foetal electrocardiogram" Proc. 19th  
Conf. on Engineering in Medicine and Biology,  
p 136, 1966.
60. Wimmer, P. - "Ergebnisse der Abdominal - Elektrokardiographie" -  
Geburtsch.U.Frauenh 1954:14:115.
61. Bolte, A. - "Albeitung und Bewertung fetoler Herzaktion potentiale  
bei Schwangenen Frauen" - Archiv. J.Gynäk -  
1961, 194, 594.
62. Bell, G.H., Davidson, J.N. and Scarborough, H. - Text book of  
Physiology and Biochemistry - E. & S. Livingstone Ltd.  
Sixth ed. page 1036.
63. Roche, J.B., Hon, E.H. - "The foetal Electrocardiogram -  $\bar{V}$  comparison  
of lead systems" - Amer.J.Obstet. and Gynec.  
92, pp 1149-1159, 1965.
64. Larks, S.D. - "Electrical axis of the fetal heart" -  
Amer.J.Obstet. and Gynec. 91, 46, 1965.
65. Einthoven, W., Fahr, G. and de Waart, A. -  
Arch. f. physiol. 150:275:1913 (quoted by Larks  
but was not available for reading.
66. Adams, F.H. - "Foetal and Neonatal Cardiovascular and Pulmonary  
function" - Ann.Rev.Physiology 27:257-84, 1965.
67. Lee, S.T. and Hon, E.H. - "The foetal electrocardiogram  $\bar{IV}$  Unusual  
variations in the ORS during labour" -  
Amer.J.Obstet. and Gynec. 92 1965.

68. Behrer, M.R., Glaeser, D.H., Cox, J., Woolf, R.B. -  
"Quantification of the fetal electrocardiogram  
through LINC Computer processing" -  
Amer.J.Obstet. and Gynec. 102, pp 537-548,  
Oct.1968.
69. Favret, A.G. - Proc. XIV Ann. Conf. Engineering  
Med. & Biology 5: 128, 1963.
70. Van Bommel, J.H., Peeters, L., Hengeveld, S.J. -  
"Influence of the maternal ECG on the abdominal  
fetal ECG complex" - Amer.J. Obstet. and Gynec.  
Vol.102, No.4, pp 556 - 562, Oct.1968.

Appendix I

continued from page 30

$e_1, e_2, e_3$  and  $e_4$  are the interaction voltage generators defined as follows:-

$$\begin{aligned} e_1 &= \delta r_{p1} i_{1co} \\ e_2 &= \delta \mu_1 V_{g1co} \\ e_3 &= \delta \mu_2 V_{g2co} \\ e_4 &= \delta r_{p2} i_{2co} \end{aligned} \quad \text{A-1}$$

The subscript "o" denotes the values when there is no unbalance.  $i_{1co}$  can be obtained from equation 30 by putting  $e_1=0$ ,  $e_2=0$  and writing  $V = V_c$ ;

$$i_{1co} = \frac{\beta' \mu_1 V_c}{\beta' \alpha - \beta \alpha'} \quad \text{A-2}$$

similarly from equation (31)

$$i_{2co} = - \frac{\alpha' \mu_1 V_c}{\beta' \alpha - \beta \alpha'} \quad \text{A-3}$$

from equation (18)

$$V_{1gco} = V_c - \left[ i_{1co} (R_1 + 2r_{p3} + 2R_4) + i_{2co} \cdot 2R_4 - \mu_3 V_{g3co} \right]$$

from equation (19)

$$V_{g3co} = - (i_{1co} + i_{2co}) \cdot 2R_4$$

$$\begin{aligned} V_{1gco} &= V_c - \left[ i_{1co} (R_1 + 2r_{p3} + 2R_4) + i_{2co} \cdot 2R_4 + \right. \\ &\quad \left. i_{1co} \cdot 2R_4 \mu_3 + i_{2co} \cdot 2R_4 \mu_3 \right] \\ &= V_c - \left\{ i_{1co} \left[ R_1 + 2r_{p3} + 2R_4 (1 + \mu_3) \right] + i_{2co} (1 + \mu_3) \cdot 2R_4 \right\} \end{aligned} \quad \text{A-4}$$

from equation (22)

$$V_{g2c} = - i_{1co} R_{L1} + (2R_{i5} + R_2) i_{2co} \quad \text{A-5}$$

Substituting from A-2 in the expression for  $e_1$

$$e_1 = \frac{\delta r_{p1} \beta' \mu_1 V_c}{\beta' \alpha - \beta \alpha'} \quad \text{A-6}$$

and  $e_2 = \delta\mu_1 V_{g1c}$  ; from A-2, A-3 and A-5

$$e_2 = \delta\mu_1 \left\{ V_c - \left[ R_1 + 2r_{p3} + 2R_4(1 + \mu_3) \right] \frac{\beta' \mu_1 V_c}{\beta' \alpha - \beta \alpha'} + \frac{2R_4(1 + \mu_3) \alpha' \mu_1 V_c}{\beta' \alpha - \beta \alpha'} \right\} \quad A-7$$

From A-6 and A-7

$$e_2 - e_1 = \delta\mu_1 V_c \left\{ 1 - \left[ R_1 + 2r_{p3} + 2R_4(1 + \mu_3) \right] \frac{\beta' \mu_1}{\beta' \alpha - \beta \alpha'} + \frac{2R_4(1 + \mu_3) \alpha' \mu_1}{\beta' \alpha - \beta \alpha'} \right\} - \frac{\beta' \mu_1 V_c}{\beta' \alpha - \beta \alpha'} \delta r_{p1} \quad A-8$$

From equation (24)

$$\left[ R_1 + 2r_{p3} + 2R_4(1 + \mu_3) \right] \mu_1 = \alpha - \left[ R_{L1} + r_{p1} + R_1 + 2r_{p3} + 2R_4(1 + \mu_3) \right] \quad A-9$$

From equation (25)

$$2R_4(1 + \mu_3) \mu_1 = \beta - 2R_4(1 + \mu_3) \quad A-10$$

Substituting in A-8

$$e_2 - e_1 = \frac{V_c}{\beta' \alpha - \beta \alpha'} \left\{ \beta' \left[ R_{L1} + r_{p1} + R_1 + 2r_{p3} + 2R_4(1 + \mu_3) \right] - 2R_4(1 + \mu_3) \alpha' \delta\mu_1 - \beta' \mu_1 \delta r_{p1} \right\}$$

If we write

$$R = R_{L1} + r_{p1} + R_1 + 2r_{p3} + 2R_4(1 + \mu_3), \text{ we get}$$

$$e_2 - e_1 = \frac{V_c}{\beta' \alpha - \beta \alpha'} \left[ \beta' R \delta\mu_1 - \beta' \mu_1 \delta r_{p1} - 2R_4(1 + \mu_3) \alpha' \delta u_1 \right]$$

$$= \frac{\mu_1 V_c}{\beta' \alpha - \beta \alpha'} \beta' R \left\{ \left( \frac{\delta\mu_1}{\mu_1} - \frac{\delta r_{p1}}{R} \right) - \frac{2R_4(1 + \mu_3) \alpha'}{R \beta'} \cdot \frac{\delta\mu_1}{\mu_1} \right\} \quad A-11$$

$$= \frac{\mu_1 V_c}{\beta' \alpha - \beta \alpha'} \beta' R \left\{ \left( \frac{\delta\mu_1}{\mu_1} - \frac{r_{p1}}{R} \cdot \frac{\delta r_{p1}}{r_{p1}} \right) - \frac{2R_4(1 + \mu_3) \alpha'}{R \beta'} \cdot \frac{\delta\mu_1}{\mu_1} \right\} \quad A-12$$

This equation A-12 expresses  $(e_2 - e_1)$  in terms of fractional unbalances of  $u_1$  and  $r_{p1}$  in the first stage.

In a similar manner using A-2, A-3 and A-5, we get

$$e_4 - e_3 = -\frac{\alpha' \mu_1 V_c}{\beta' \alpha - \beta \alpha'} \cdot \delta r_{p2} + \frac{R_{L1} \beta' \mu_1 V_c}{\beta' \alpha - \beta \alpha'} \cdot \delta \mu_2 + \frac{\alpha' \mu_1 V_c (2R_5 + R_2)}{\beta' \alpha - \beta \alpha'} \cdot \delta \mu_2$$

Substituting for  $\alpha'$  and  $\beta'$  from equations (26) and (27)

$$e_4 - e_3 = \frac{\mu_1 V_c}{\beta' \alpha - \beta \alpha'} \left[ \left\{ R_{L1} \left[ R_{L2} + r_{p2} + (R_2 + 2R_5)(1 + \mu_2) + 2R_4 \right] + (2R_4 - \mu_2 R_{L1})(2R_5 + R_2) \right\} \delta \mu_2 - (2R_4 - \mu_2 R_{L1}) \cdot \delta r_{p2} \right]$$

$$= \frac{\mu_1 V_c}{\beta' \alpha - \beta \alpha'} \left[ \left\{ R_{L1} \left[ R_{L2} + r_{p2} + 2R_5 + 2R_4 \right] + 2R_4 (2R_5 + R_2) \right\} \delta \mu_2 - (2R_4 - \mu_2 R_{L1}) \delta r_{p2} \right]$$

Substituting

$$R_s = R_{L2} + r_{p2} + R_2 + 2R_5 + 2R_4, \text{ we get}$$

$$e_4 - e_3 = \frac{\mu_1 V_c}{\beta' \alpha - \beta \alpha'} \cdot \mu_2 R_{L1} R_s \left\{ \left( \frac{\delta \mu_2}{\mu_2} + \frac{r_{p2}}{R_s} \cdot \frac{\delta r_{p2}}{r_{p2}} \right) + \frac{2R_4 (2R_5 + R_2)}{R_{L1} \cdot R_s} \left( \frac{\delta \mu_2}{\mu_2} - \frac{r_{p2}}{\mu_2 (2R_5 + R_2)} \cdot \frac{\delta r_{p2}}{r_{p2}} \right) \right\}$$

..... A-13

Substituting A-12 and A-13 in equation (37), we get

$$V_{2d} = A_{d10} \cdot A_{d20} \left\{ V_d + \frac{V_c \beta' R}{\beta' \alpha - \beta \alpha'} \left[ \left( \frac{\delta \mu_1}{\mu_1} - \frac{r_{p1}}{R} \cdot \frac{\delta r_{p1}}{r_{p1}} \right) - \frac{2R_4 (1 + \mu_3) \alpha'}{R_s \beta'} \cdot \frac{\delta \mu_1}{\mu_1} \right] + \frac{V_c \left[ R_{L1} + r_{p1} + (1 + \mu_1) R_1 \right]}{\beta' \alpha - \beta \alpha'} R_s \left[ \left( \frac{\delta \mu_2}{\mu_2} + \frac{r_{p2}}{R_s} \cdot \frac{\delta r_{p2}}{r_{p2}} \right) + \frac{2R_4 (2R_5 + R_2)}{R_{L1} \cdot R_s} \left( \frac{\delta \mu_2}{\mu_2} - \frac{r_{p2}}{\mu_2 (2R_5 + R_2)} \cdot \frac{\delta r_{p2}}{r_{p2}} \right) \right] \right\}$$

A-14

From equation (38) and A-14 the common mode rejection ratio  $H_c$  is given by

$$\frac{1}{H_{cf}} = \frac{\beta'R}{\beta'\alpha - \beta\alpha'} \left\{ \left( \frac{\delta\mu_1}{\mu_1} - \frac{r_{p1}}{R} \cdot \frac{\delta r_{p1}}{r_{p1}} \right) - \frac{2R_4(1+\mu_3)(2R_4 - \mu_2 R_{L1})}{R \cdot [R_s + \mu_2(2R_5 + R_2)]} \cdot \frac{\delta\mu_1}{\mu_1} + \right. \\ \left. \frac{R_{L1} + r_{p1} + (1+\mu_1)R_1}{R} \cdot \frac{R_s}{R_s + \mu_2(2R_5 + R_2)} \left( \frac{\delta\mu_2}{\mu_2} + \frac{r_{p2}}{R_s} \cdot \frac{\delta r_{p2}}{r_{p2}} \right) + \right. \\ \left. \frac{2R_4(2R_5 + R_2)}{R_{L1} \cdot R_s} \left( \frac{\delta\mu_2}{\mu_2} - \frac{r_{p2}}{\mu_2(2R_5 + R_2)} \cdot \frac{\delta r_{p2}}{r_{p2}} \right) \right\} \dots\dots A-15$$

From equations (24), (25), (26) and (27) it can be seen that  $\beta'\alpha$  is for ordinary values of the circuit constants about 100 times larger than  $\beta\alpha'$ , therefore

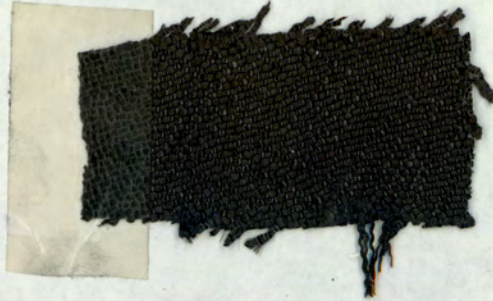
$$\frac{\beta'}{\beta'\alpha - \beta\alpha'} \approx \frac{1}{\alpha} \quad A-16$$

Substituting A-16 in A-15 we find

$$\frac{1}{H_{cf}} \approx \frac{R}{R + \mu_1 [R_1 + 2r_{p3} + 2R_4(1+\mu_3)]} \left\{ \left( \frac{\delta\mu_1}{\mu_1} - \frac{r_{p1}}{R} \cdot \frac{\delta r_{p1}}{r_{p1}} \right) - \right. \\ \left. \frac{2R_4(1+\mu_3)(2R_4 - \mu_2 R_{L1})}{R [R_s + \mu_2(2R_5 + R_2)]} \cdot \frac{\delta\mu_1}{\mu_1} + \right. \\ \left. \frac{R_{L1} + r_{p1} + (1+\mu_1)R_1}{R} \cdot \frac{R_s}{R_s + \mu_2(2R_5 + R_2)} \left( \frac{\delta\mu_2}{\mu_2} + \frac{r_{p2}}{R_s} \cdot \frac{\delta r_{p2}}{r_{p2}} \right) + \right. \\ \left. \frac{2R_4(2R_5 + R_2)}{R_{L1} [R_s + \mu_2(2R_5 + R_2)]} \left( \frac{\delta\mu_2}{\mu_2} - \frac{r_{p2}}{\mu_2(2R_5 + R_2)} \cdot \frac{\delta r_{p2}}{r_{p2}} \right) \right\} \quad A-17$$

## Appendix II

Attached to this page is a sample of the graphite cloth which has been used for making electrodes.



Brief notes on the formation of <sup>ra</sup>graphite cloths:-

Among the organic materials that when heated to 2,700°C leave a graphite carbon residue are certain fibres, both natural and synthetic.

Textile forms, such as yarns, felts and woven and knitted fabrics composed of high purity flexible graphite became available in 1959. Individual fibres are 3 to 12 microns in diameter and have tensile strengths of 50,000 to 100,000 psi at ambient temperatures, and higher at elevated temperatures.

Graphite can be re-crystallised to increase its density from about 1.7 to as high as 2.18, while commercially re-crystallised graphite has a density from 1.92 to 1.97.

The permeability of re-crystallised graphite to water is comparable with that of brass, and is some  $10^5$  to  $10^7$  smaller than that of electrode grade graphite. Graphite has been used in the nozzles of rocket motors.



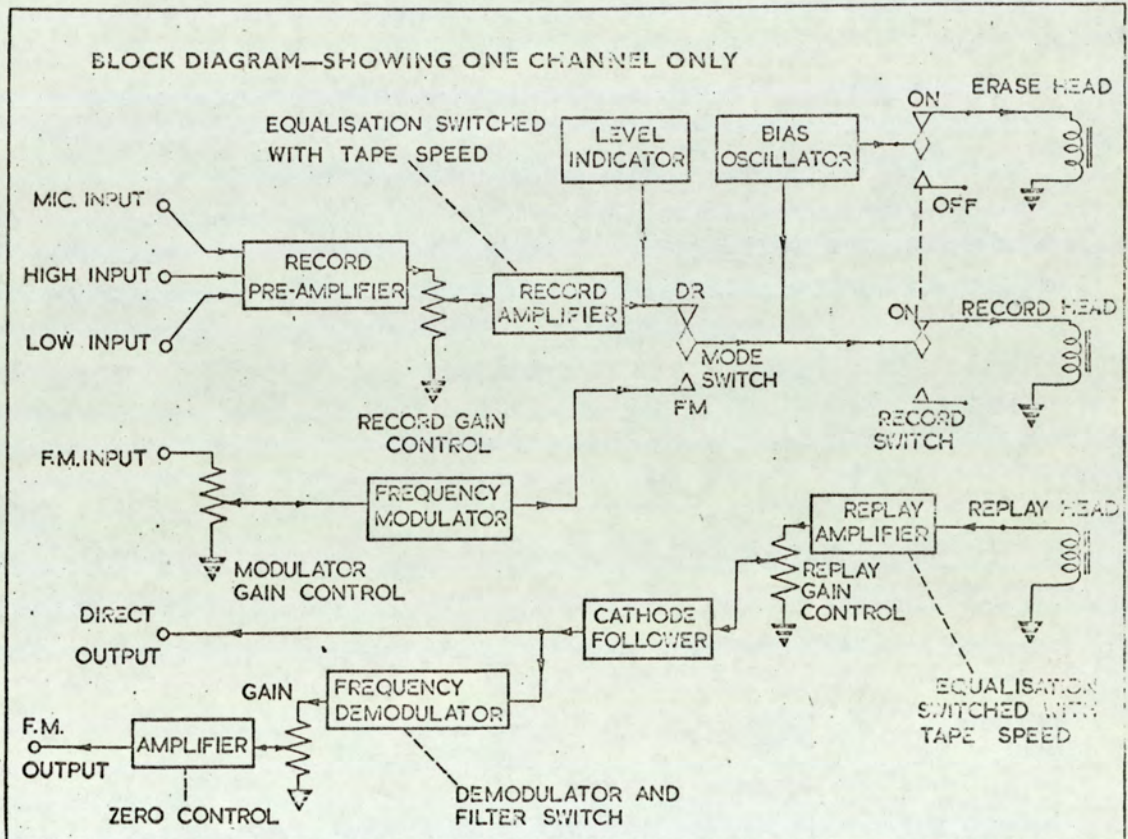
# DESCRIPTION

The Elliott-Tandberg system combines the Tandberg tape deck with the transistorized frequency modulation channels used in the Elliott range of magnetic tape instrumentation equipment. The Tandberg deck was chosen for its excellent performance and reliability; the combination has been engineered to the high standards expected from instrumentation systems.

The audio amplifiers used in the Tandberg recorder have been retained, only minor alterations being made. These are employed when using Direct recording/reproducing techniques and are selected by means of the push-button mode switch associated with each channel. When either or both "Mode Switches" are in the F.M. position the frequency modulation channels are brought into use in order to handle data with greater accuracy and extend the overall response down to d.c.

The bandwidth obtained when using either mode depends upon the tape speed used. The frequency conscious elements of both systems can be switched to suit the selected tape speed, the choice being determined by the incoming data.

The correct direct recording level is indicated by the 'magic eyes'. When the twin light beams touch, the maximum permissible input is being applied. Exceeding this value will increase the harmonic distortion as will a gross mis-match of impedance at the input and output terminals. Please read the Performance Specification carefully and ensure that the conditions specified are not abused.



Before dispatch the equipment is adjusted so that the overall performance conforms to the Specification in all respects under normal laboratory conditions. Adjustments should not be made without consulting the Servicing and Maintenance manual, which also includes details of the periodic preventive maintenance instructions necessary to maintain the original excellent performance.

# P E R F O R M A N C E   S P E C I F I C A T I O N

**Tape Speeds:** 7½, 3¾, 1⅞ in/sec.  
**Tape Capacity:** 1,800 feet.  
**Tape Speed Accuracy:** ±0.2% relative. ±1% absolute.  
**Number of Tracks:** 2/4 on ½ in. wide tape.  
**Spooling Time:** 3 minutes in either direction.  
**Wow and Flutter:** 0.15% at 7½ in/sec., 0.2% at 3¾ in/sec., 0.3% at 1⅞ in/sec.  
**Magnetic Heads:** Record, Replay and Erase.  
**Level Indicator:** Twin light beams.  
**Position Indicator:** 4 digit mechanical counter.

## Direct Record/Reproduce System

Tape Speed in/sec.	Frequency Response
7½	40 c/s - 16 Kc/s
3¾	40 c/s - 10 Kc/s
1⅞	55 c/s - 5 Kc/s

**Erase & Bias frequency:** 80 Kcs/  
**Total Harmonic Distortion:** 3% r.m.s.  
**Equalisation** Conforms to N.A.R.T.B. Standards.  
**Inputs:** 5mV into 100 Kilohm  
           50mV into 1 Megohm  
           1.5V into 5 Megohm.  
**Output:** 1.5V into 2 Kilohm.  
**Signal: Noise Ratio:** 48 dB at all tape speeds.  
**Crosstalk:** 45 dB (measured at 1 Kc/s.)

## Frequency Modulation System

Tape Speed in/sec.	Carrier Frequency	Frequency Response ±1 dB.
7½	12 Kc/s	d.c. - 2.4 Kc/s
3¾	6 Kc/s	d.c. - 1.2 Kc/s
1⅞	3 Kc/s	d.c. - 600 c/s

**Deviation:** ±40%.  
**Overall Accuracy:** ±1%.  
**Input:** 500mV into 20 Kilohm.  
**Output:** 1 V into 1 Kilohm.  
**Signal : Noise Ratio:** 35 dB at all tape speeds.  
                                   40 dB with reduced band-width.  
**Crosstalk:** 45 dB (measured with carrier recorded on  
                                   both tracks.)

**Power Supplies:** 200 - 250V 50 c/s  
                       100 - 125V 60 c/s  
                       24V d.c. Invertors available.  
**Power Consumption:** 100W.  
**Weight:** 45 lbs.  
**Dimensions:** 16 in. x 12 in. x 10 in. high.